THE UNIVERSITY OF KANSAS CENTER FOR RESEARCH, INC.
2291 Irving Hill Drive—Campus West
Lawrence, Kansas 66045

Progress Report

for

A RESEARCH PROGRAM TO REDUCE INTERIOR NOISE IN GENERAL AVIATION AIRPLANES

KU-FRL-317-4

NASA Grant NSG 1301

GENERAL AVIATION INTERIOR NOISE STUDY

Jan Roskam
Principal Investigator

Vincent U. Muirhead
Co-Investigator

Howard W. Smith
Co-Investigator

Prepared by Tonnis D. Peschier

University of Kansas
Lawrence, Kansas

August 1977

GENERAL AVIATION INTERIOR

NOISE STUDY

by

Tonnis D. Peschier

Abstract of Report Submitted to
The University of Kansas
in partial fulfillment of the
requirements for the degree of
Doctor of Engineering

August 1977

Presented in this report are the organization of and work completed for an ongoing general aviation interior noise research project focusing on the transmission of sound through aircraft type panels. Described are typical noise source, sound transmission path and acoustic cabin properties and their effect on interior noise. Based on both annoyance and physiological damage criteria, it is concluded that typical in-cabin noise levels of around 90 dB(A) or greater are undesirably high. Some theoretical and empirical methods are discussed that are intended for prediction and analysis of the transmission of sound through panels. Included is a description of the construction, calibration and properties of an acoustic panel test facility. Some preliminary experimental results obtained in this facility are presented. These results show an average sound transmission loss in the mass controlled frequency region comparable to theoretical predictions. The results also verify that transmission losses in the stiffness controlled region directly depend on the fundamental frequency of the panel. Experimental and theoretical results indicate that increases in this frequency, and consequently in transmission loss, can be achieved by applying pressure differentials across the specimen. The significance of this and other ways to reduce panel sound transmission will be determined through future research work as outlined in this report.

TABLE OF CONTENTS

TABLE OF CONTENTS (continued)

TABLE OF CONTENTS (continued)

LIST OF FIGURES

LIST OF FIGURES (continued)

LIST OF TABLES

LIST OF SYMBOLS

Symbol	Definition	Dimension
A	Total absorption	m^2
a	Panel dimension	m
b	Panel dimension	m
C	Constant (see Appendix C)	
D	Flexural rigidity	Nm
E	Young's modulus	N/m^2
f	Frequency	Hz
G	Shear modulus	N/m^2
g	Panel surface weight	N/m^2
h	Panel thickness	m
I	Moment of inertia	m^4
I	Acoustic intensity	$Watt/m^2$
K	Correction factor	dB
K	System stiffness	N/m
K	Constant (see Appendix D)	
M	System mass	kg
m	Positive integer	
$\overline{m}$	Panel surface mass	kg/m^2
N	Internal membrane force per unit length	N/m
n	Positive integer	
NR	Noise Reduction, $SPL_S - SPL_R$	dB
P	Amplitude of harmonic excitation	N/m^2
p	Sound pressure	N/m^2
PSD	Power Spectral Density	

LIST OF SYMBOLS (continued)

Symbol	Definition	Dimension
PSIL	Preferred Frequency Speech Interference Level	dB
$R_{12}(x_1, x_2, \tau)$	Space time correlation coefficient	
S	Panel area	m^2
s	Fraction of surface mass fully participating in panel motion at resonance	
SPL	Sound Pressure Level	dB, dB(A)
T	Time period	sec
t	Time	sec
TL	Transmission Loss	dB
V	Volume of a cavity	m^3
v	Velocity component of a panel perpendicular to its surface	m/sec
w	Displacement component of a panel perpendicular to its surface	m
W_A	Acoustic power	Watt
$W_{m,n}$	Coefficients of expansion in Fourier expression for panel deflecton	m
x, y, z	Cartesian coordinates	m
z_K	Distance from k^{th} layer to surface of laminate	m

Greek Symbols

α	Sound absorption coefficient	
ζ	Damping ratio	
η	Damping factor	
λ	Wave length	m

Greek Symbols (cont'd.)	Definition	Dimension
λ	Poisson's ratio	
ν	Normal stress	N/m^2
ρ	Mass density per unit area	kg/m^2
τ	Sound transmission coefficient $\frac{I_{trans}}{I_{inc}}$	
τ	Time difference	sec
ω	Frequency	rad/sec
∇^2	Laplace operator $\frac{\partial^2}{\partial x^2} + \frac{\partial^2}{\partial y^2} + \frac{\partial^2}{\partial z^2}$	

Subscripts

f	Face
i	Positive integer
inc	Incident
h	Hysteretic
k	kth layer of a laminate
m	Positive integer
max	Maximum
min	Minimum
n	Positive integer
R	Receiver side
r	Resonance
rms	Root mean square
S	Source side
t	Torsional
trans	Transmitted
x, y, z	Directions relative to which properties are defined

LIST OF ABBREVIATIONS

AE	Aerospace Engineering
ASTM	American Society for Testing and Materials
CPM	Critical Path Method
CRINC	(KU) Center for Research, Inc.
FRL	Flight Research Laboratory (at KU)
KU	University of Kansas
LaRC	(NASA) Langley Research Center
NASA	National Aeronautics and Space Administration
OSHA	Occupational Safety and Health Administration
TH	Technische Hogeschool (University of Technology, Delft, Holland)
TL	Transmission Loss

CHAPTER 1

INTRODUCTION

This report presents the organization and work completed under a National Aeronautics and Space Administration-funded research project to study the transmission of sound through general aviation airplane structures. Also reported are descriptions and discussions of the testing equipment and procedures of the project and of relevant analysis and prediction methods. In addition, a description is included of the exposure of general aviation passengers to noise and of important noise sources and receiving space (i.e., cabin) effects.

The project is the second of two consecutive phases of a research program, the broad goal of which is to reduce interior noise in general aviation airplanes. The objective of the first program phase was to develop an effective and competent noise research team at the University of Kansas. This phase was intended as one of the preparations for the second phase, a long range follow-up research project. During the last part of phase one and the first part of phase two, many other preparations were made including the design, construction and calibration of a test facility, purchasing of equipment, development of testing and data reduction procedures and the study of pertinent literature. It is this period of preparation that is covered in this report (February 1977 through the middle of August 1977).

Project phase one officially started on April 15, 1976, when the Flight Research Laboratory (FRL) of the University of Kansas (KU) began work on a grant for the National Aeronautics and Space Administration (NASA), Langley Research Center (LaRC) entitled "A Research Program to Reduce Interior Noise in General Aviation Airplanes," NASA Grant No.

NSG 1301. The activities of this program phase were intended as preparations for a follow-up project as can be concluded from the statement of work outlined in the original proposal to NASA (Reference 1):

1. Familiarization with interior noise state-of-the-art;
2. Detail design of an on-board interior noise measuring and recording system;
3. Development of in-flight procedures for utilizing measured data and of ground procedures for analyzing and interpreting the data; and
4. Definition of a long range follow-up research program in interior and exterior noise.

On April 30, 1977, the ending date of the preparation phase, NASA Grant No. NSG 1301 was extended to carry out the continuing work which was defined and partially prepared during the initial phase. The proposal for this second project (Reference 2) detailed the program objectives as follows:

1. To determine the sound transmission loss characteristics of various structural panels and panel treatments (experimentally);
2. To compare test results with predictions from pertinent analytical methods;
3. To provide a systematic collection of panel and panel treatment sound attenuation characteristics, based on both experimental and analytical considerations; and
4. To use these results to extend or develop prediction methods.

These research objectives were the results of a study of the factors that affect interior noise, the exposure of passengers to noise, and of many exchanges of views with personnel of both NASA and general aviation

industry (Beech and Cessna Aircraft Corporations). It was concluded that in-cabin noise levels are generally very high, despite the use of acoustical treatments. It was also found that the available information (generally consisting of theories or product specifications by manufacturers of sound proofing materials), is quite limited. These considerations have resulted in a (for general aviation industry) need to expand usable knowledge in the areas of noise transmission mechanisms and control.

Considering the present and possible future regulations concerning general aviation interior and fly-over noise, a program of research has been planned and is being conducted at the NASA Langley Research Center. As one of many subcontractors, KU was given a NASA grant to do research in the area of noise reduction. The work to be conducted by KU-FRL will augment the Langley General Aviation Noise Program goal to investigate structural transmission phenomena and prediction. It will also provide information more directly applicable in design and modification of general aviation aircraft. The latter results were the reason for general aviation manufacturers to stimulate the KU-FRL research program with valuable information as well as test specimens.

In addition to general aviation industry, the following individuals, supporting the project directly and this report indirectly, are acknowledged:

Mr. D. G. Stephens, NASA LaRC: project technical monitor and KU ad-hoc professor

Dr. J. Roskam, KU-FRL: principal investigator and director of KU-FRL

Dr. R. Ross, KU-FRL: interim principal investigator

Prof. H. Wittenberg, Delft University of Technology (Netherlands): Dean of the Department of Aerospace Engineering

Mr. D. Andrews, KU-FRL: graduate research assistant, in-flight noise measurements; contacts with industry

Mr. D. Carlson, KU-FRL: technical electronic adviser

Mr. D. Durenberger, KU-FRL: graduate research assistant, theoretical analysis; design special test sections

Mr. T. Henderson, KU-FRL: graduate research assistant, design, construction and calibration of test facility

Mr. E. Shu, KU-FRL: graduate research assistant, theoretical analysis.

The project organization is shown in Figure 1.1 on the next page.

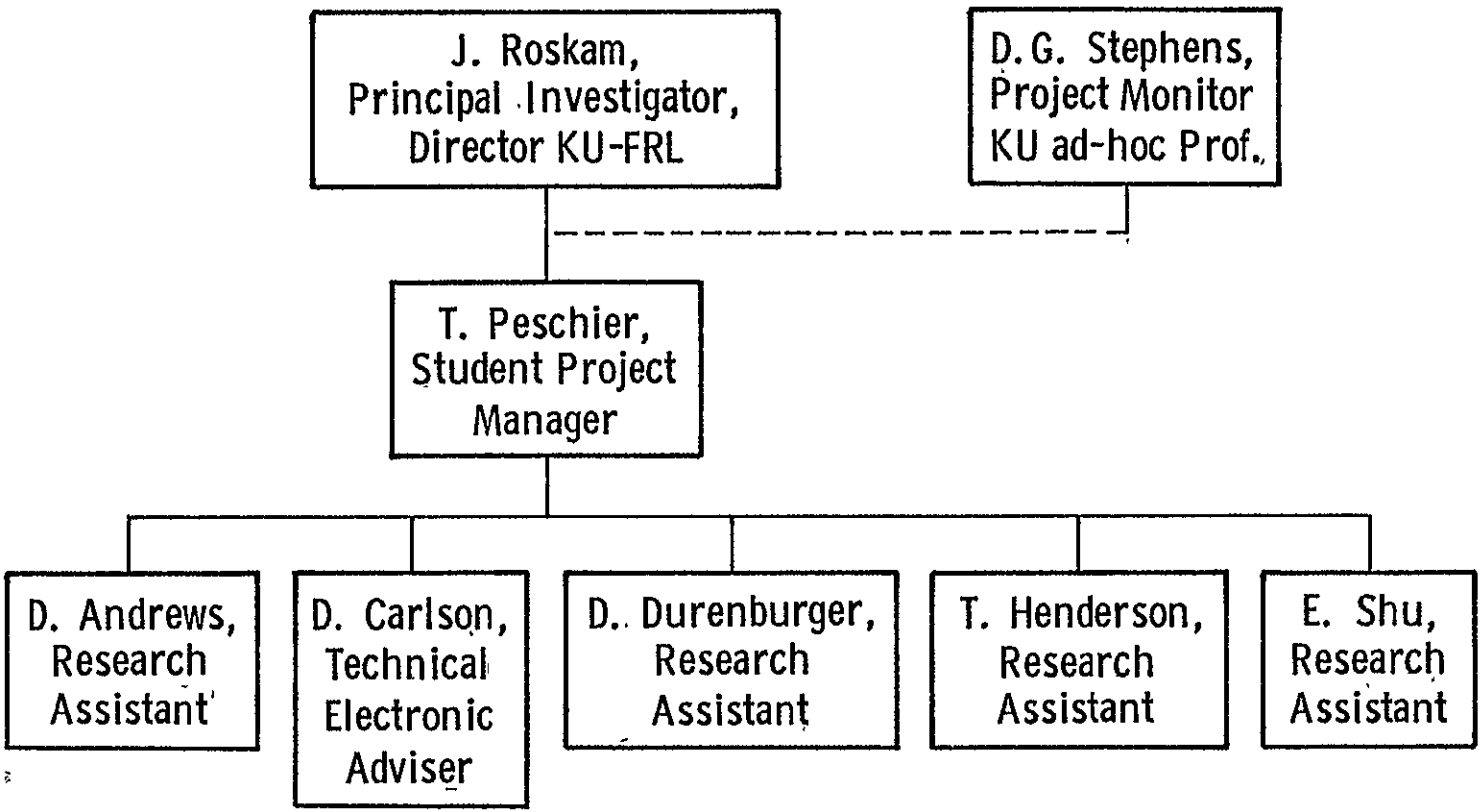

Figure 1.1. Project Organization Chart.

CHAPTER 2

PROJECT CHRONOLOGY AND MANAGEMENT

This chapter presents a chronological history of the project, an outline of the organizations and individuals involved, the project budget, and the project schedule.

2.1 Project History

In February 1976 a proposal for "A Research Program to Reduce Interior Noise in General Aviation Airplanes" was submitted to NASA LaRC. This proposal was the result of a time of exploring necessities for and possibilities of doing general aviation oriented noise research at the University of Kansas Flight Research Laboratory. In the fall of 1975, several KU professors and students discussed the need for noise research with the Beech and Cessna Aircraft Corporations (Wichita, Kansas). Industry indicated an interest in this type of research, so a group from the KU-FRL went to NASA LaRC to discuss the needs and possibilities of getting NASA grants with D. G. Stephens (Noise Effects Branch) and D. J. Maglieri (Noise Control Branch). As the likelihood of a grant for an interior noise university research program was high and interested KU personnel were available, preparations were made for a possible (interior) noise research program. The KU Department of Aerospace Engineering included a course, AE790: Sound Generation of General Aviation Aircraft, in its spring 1976 curriculum to educate interested people in the basics of pertinent acoustics. Also, the Delft University of Technology in Holland (involved in general aviation fly-over noise) had expressed a willingness to cooperate with such a program and was contacted about further educating two or three KU students in noise research. The Delft University was in favor of such cooperation.

Finally, a proposal for a NASA-Industry-TH Delft-KU program was prepared and submitted to NASA LaRC (Reference 1).

The primary goal of this program was to develop an effective and competent research team at the University of Kansas in the area of general aviation interior noise. This would be a preparation for a long range follow-up research program in both interior and exterior noise. The definition of this follow-up program was to be one of the major tasks along with the other activities mentioned in Chapter 1.

In April 1976 the request for a grant was approved and the development of a noise research team at KU was intensified. In the summer of that year Messrs. D. Durenberger and T. Henderson worked for the Beech Aircraft Corporation in the Structural Dynamics Department. Mr. D. Andrews went to Holland for six months to work as a research assistant at the Delft University of Technology, and Mr. T. Peschier worked for the Cessna Aircraft Company for six months as a test engineer. In January 1977 Mr. D. Durenberger started working for the Delft University. During the fall of 1976, the noise research team at KU prepared a follow-up program in the area of general aviation noise. Discussions with NASA LaRC and the Beech and Cessna Aircraft Corporations finally resulted in a $225,000 interior noise research proposal to NASA LaRC in December 1976. The emphasis of this proposal was on both laboratory and in-flight research, as, during the fall of 1976, it became apparent that this was an area having the greatest likelihood of NASA support. The request for this grant was denied and in the spring of 1977 a new proposal was prepared (Reference 2). This proposal, suggesting financial support for interior noise related research of sound transmission through general aviation type structural panels, was accepted

by NASA LaRC. Consequently, in May 1977, the educational type noise research program was continued with a laboratory type sound transmission research project.

As it became clear during the Spring of 1977 that this follow-up program had a high likelihood of getting NASA support, the design and construction of the test facility was initiated before this starting date. On June 15, 1977, the construction was completed and a month later the calibration. At the time of writing this project report the first tests are being conducted. Figure 2.1 presents some of the milestones during the interior noise research projects.

2.2 Project Support Organization

The groups involved in the various aspects of the interior noise research program are indicated in Figure 2.2.

The Noise Effects Branch in the Acoustics and Noise Reduction Division at NASA LaRC has had responsibility in funding the general aviation interior noise work done under NASA Grants NSG 1301. Mr. D. G. Stephens (LaRC) has been the project technical monitor of this grant.

The noise research is being conducted by University of Kansas students and faculty in the Space Technology Center, Nichols Hall. Dr. Jan Roskam is the principal investigator of the project. Mr. T. D. Peschier (KU-Doctor of Engineering degree candidate) has been the student project manager.

The Delft University of Technology (Holland) has participated in the project by educating two KU research assistants in the area of noise measurement and analysis. The coordinator in Delft was Prof. H. Wittenberg.

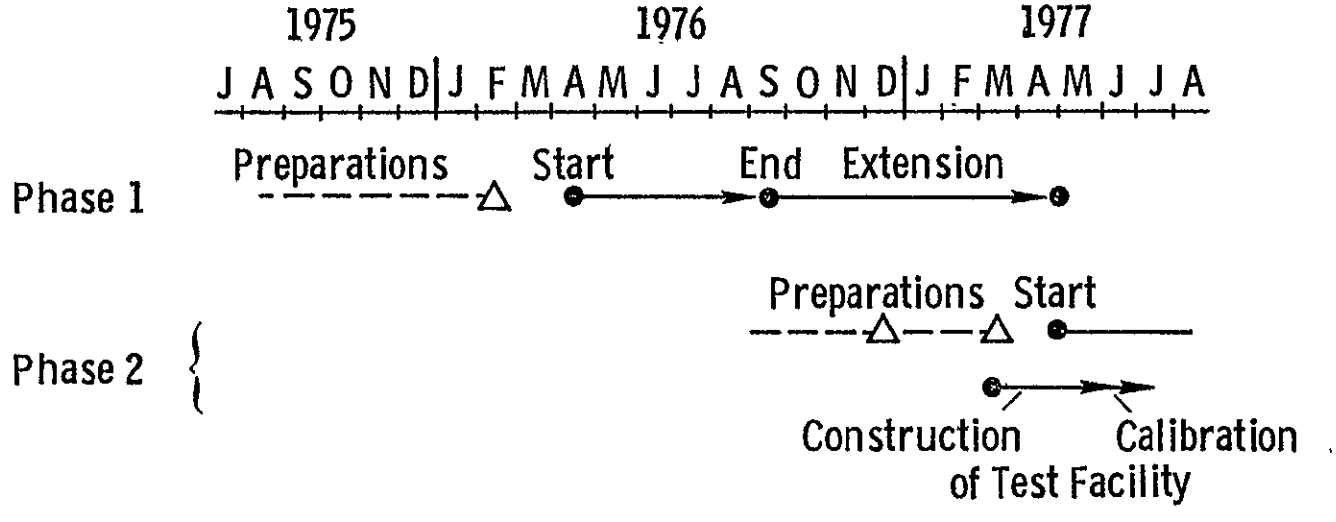

Note: △ = Submission of Proposal to NASA LaRC

Figure 2.1. Milestones in General Aviation Interior Noise Research at the University of Kansas.

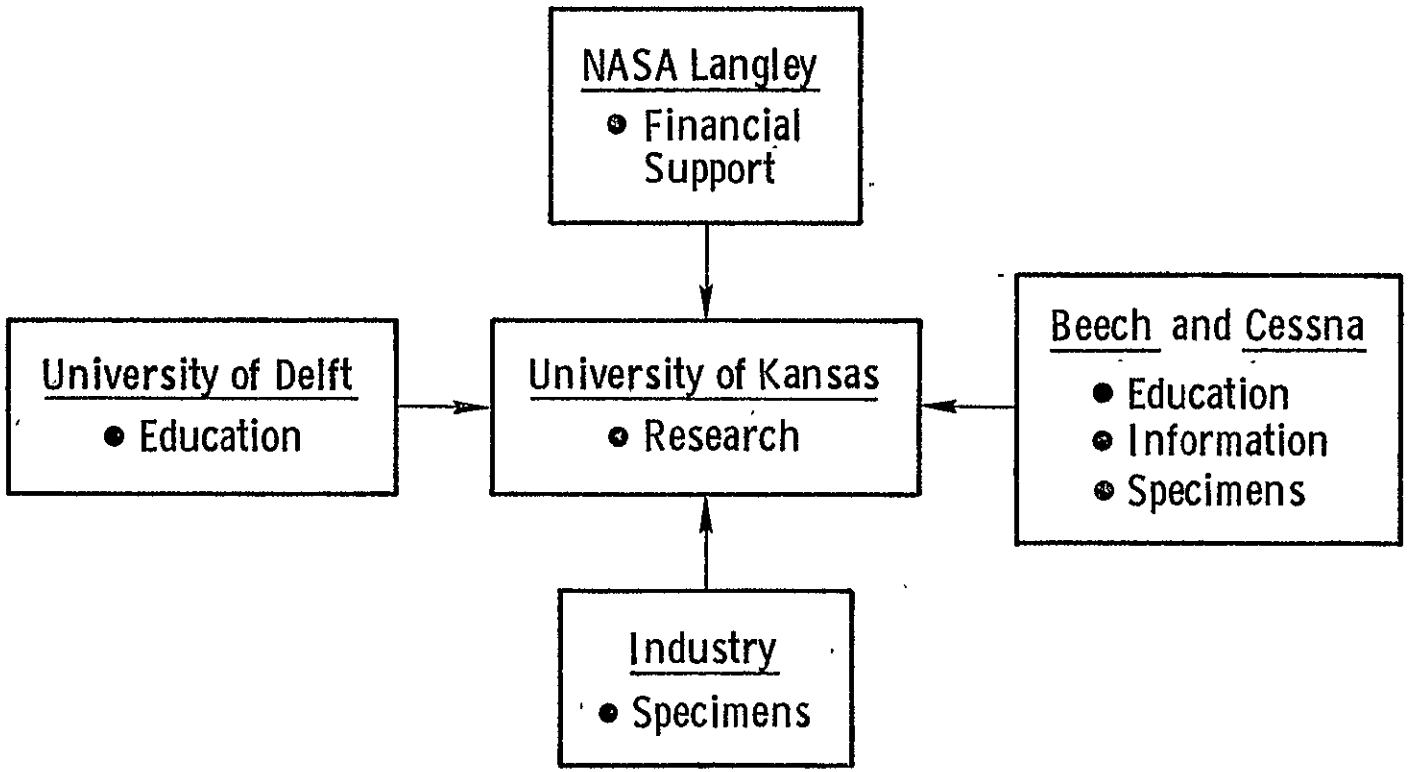

Figure 2.2. Interior Noise Project Support Organization.

The Cessna and Beech Aircraft Companies have provided valuable information. By employing three research assistants in their acoustics and vibration branches, these companies helped developing a competent research team. Their support also included the supply of many test specimens.

Specimens were and will continue to be provided by manufacturers of sound proofing materials and of aircraft.

2.3 Project Budget

The total funding for the Interior Noise Research Project is outlined in this section. Funding was obtained from the National Aeronautics and Space Administration, Langley Research Center, Hampton, Virginia, and the University of Kansas on a cost-sharing basis. All income and outflow of project funds were handled through the business office of the University of Kansas Center for Research, Inc. (CRINC), by the principal investigator of the project, Prof. J. Roskam, the interim principal investigator Prof. R. Ross and the student project manager Mr. T. Peschier. Table 2.1 outlines the budgets and actual expenditures of the first (educative) program phase (April 15, 1976 - April 30, 1977) and of the second (panel sound transmission) phase (May 1, 1977 - April 30, 1978). The amounts of cost-shared funding provided by KU are excluded from the table. These amounts generally consisted of matching funds from the University for the principal investigator's salary during the academic year.

Each item in the breakdown of expenditures in Table 2.1 is underlined and explained below.

The actual amount paid for salaries and wages during the first project phase, was lower than projected. This was a result of having

Table 2.1 Projected and Actual Expenditures in the Interior Noise Research Project

Phase I (April 15, 1976 - April 30, 1977)	Projected	Actual
Salaries and wages (including fringe benefits and overhead)	27,114	23,020
Other expenditures	2,971	6,304
Total	29,915	29,324

Phase 2 (May 1, 1977 - April 30, 1978)	Projected	Actual (8/77)
Salaries and wages (including fringe benefits and overhead)	42,009	14,476
Electronic equipment	22,115	19,764
Test specimens	1,000	25
Acoustic materials	1,000	107
Construction of plane-wave tube	1,500	804
Other expenditures	2,500	450
Total	70,124	35,626

two noise research assistants employed at the Beech Aircraft Corporation, one at the Cessna Aircraft Company and two at the Technological University of Delft (Holland) during the course of the project (see section 2.1). This effectively resulted in the training of a KU noise research team at no cost to NASA.

The actual amount paid for other purposes was higher than projected. Besides expenditures for supplies, travel and telephone, the cost of some preparations for the second project phase are included in this item. These preparations included (1) the construction of certain items for the test facility (done by subcontractors) and (2) the purchase of some electronic equipment.

After three and a half months of research in the second project phase, a significant portion of the funds outlined in Table 2.1 has been expended.

The funds intended for salaries and wages have been used extensively. This is a direct result of the considerable research effort during these first months. A sizable research team was employed to expedite the completion of the test facilities and measuring and analysis procedures. Also, new research assistants had to be trained, as several will graduate soon. However, the rate of spending funds for salaries and wages will decrease by a factor of 2.5 in the near future.

The funds intended for electronic equipment have also been expended almost completely. However, no further significant expenditures are anticipated as all necessary items have been purchased.

Of the funds intended for the construction of the plane wave tube, approximately half have been used. The total construction cost was higher than the amount shown in Table 2.1 but part of this was financed

with funds of the first project phase. At the time of writing this report, the basic test facility, including accessaries for testing under pressure, have been paid for. The remainder of the available funds will be needed for the construction of the special test sections.

The funds for test specimens have hardly been used as many specimens were obtained from manufacturers at no cost to the project. However, it is likely that costly configurations will have to be constructed in the future.

The expenditures in the category acoustic materials are quite low. Up till the writing of this report only a small quantity has been purchased, to improve the characteristics of the test facility. In the future, similar expenditures will be required for the construction of special test sections.

The last item in the breakdown in Table 2.1, other costs, refers to expenditures for supplies, telephone, travel, etc. At the present rate of expenditure, barring any unforeseen difficulties, the available funds should be sufficient to complete the project within the budget.

2.4 Project Schedule

The period to be covered by the first phase of "A Research Program to Reduce Interior Noise in General Aviation Airplanes" was originally intended to be between April 15, 1976, and September 15, 1976. The objective of this phase was to develop an effective and competent research team at KU in the area of general aviation noise. This was partly accomplished by employing two research assistants at the Beech Aircraft Company, one at Cessna and two at the Technological University of Delft (Holland). This effectively resulted in the training of a KU noise research team at no cost to the project. The consequent savings

in salaries and wages made it possible to extend the first project phase to April 30, 1977. The extended period was used to expand the knowledge of research assistants and to prepare the follow-up noise research project.

This second project phase started on May 1, 1977, and will cover a period of one year. The time phasing of research activities was strongly influenced by one of the requirements defined by Mr. T. Peschier's comprehensive examination committee on April 8, 1977. This requirement was in the form of an interim deadline before which certain activities should be completed. This deadline is indicated on a flowchart of program activities (Figure 2.3). After applying an elementary form of the critical path method (CPM) certain conclusions were reached with respect to the number of research assistants that should be employed in order to meet this and the final deadline of the project. These conclusions are shown in Figure 2.4. It is expected that implementing this schedule will result in meeting the interim and final deadline at the projected cost. Based on the flowchart (Figure 2.3) and the projected involvement of research personnel (Figure 2.4) a time-phase diagram of project activities was constructed. This is depicted in Figure 2.5. Also shown is the actual progress that has been made between the starting date and the time of writing. The actual progress will now be discussed.

The test facility was completed two weeks after the projected date. This was mainly caused by some construction problems. As a result the calibration of the facility was also delayed. As this checkout took a week shorter than projected, the first testing could be done just one week after the intended date. The data reduction and analysis was started at the same time. This was done to check the usefulness and

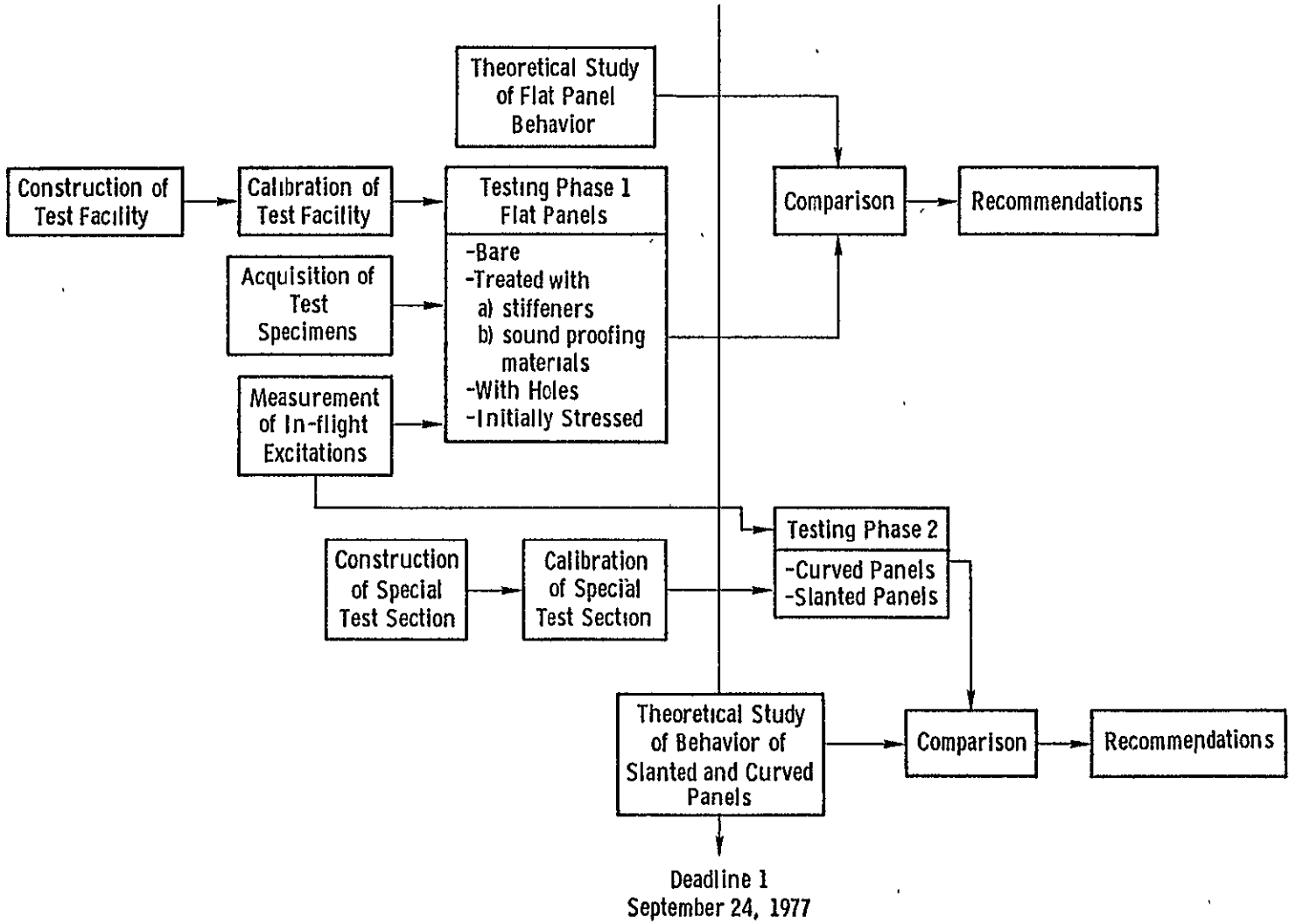

Figure 2.3. Flowchart of Research Activities (Phase 2).

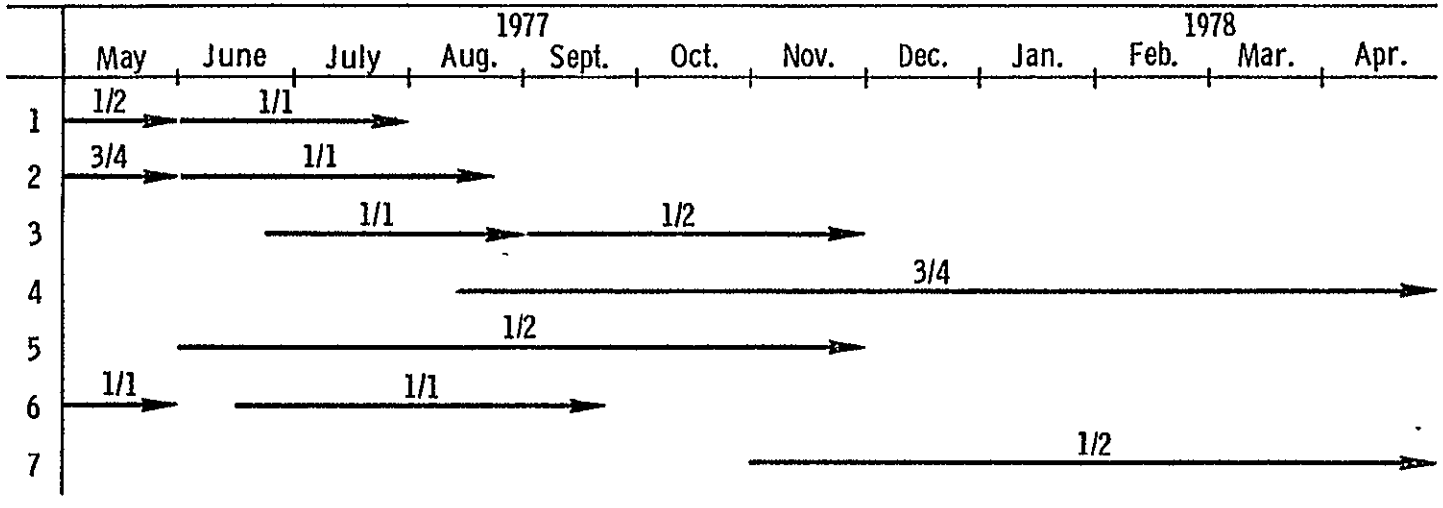

Figure 2.4. Projected Employment of Research Assistants.

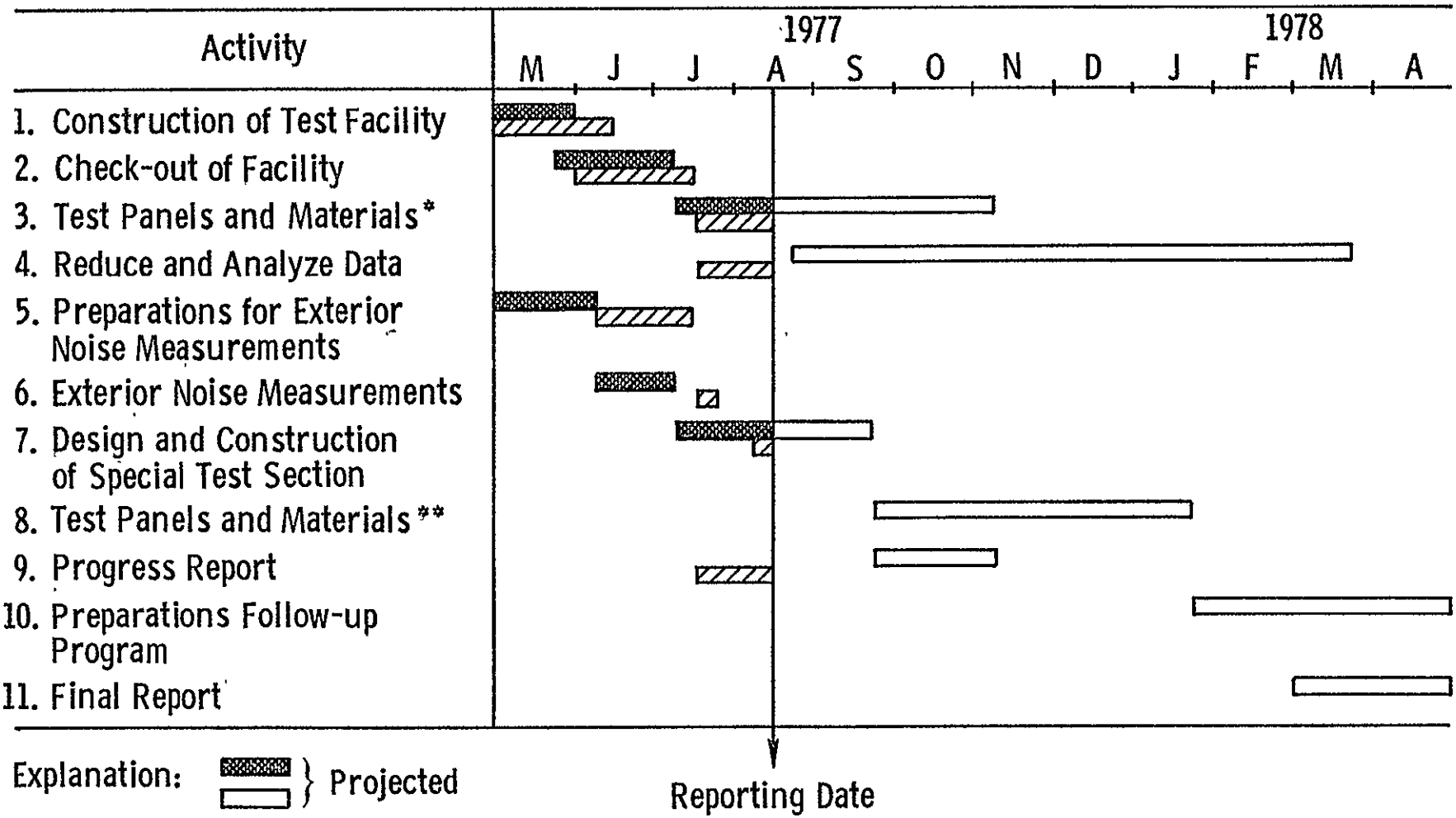

Figure 2.5. Projected and Actual Progress of Second Program Phase.

validity of all procedures before the size of the research team will get significantly smaller (end of September 1977). The measurements of in-flight panel excitations were delayed but completed before the recorded data could be used in the test facility. The design of the special section for testing of curved and slanted specimens was started one month late due to the time needed to complete other (more urgent) activities. No further delay is anticipated at this time.

CHAPTER 3

NOISE EXPOSURE IN GENERAL AVIATION AIRCRAFT

This chapter presents some typical general aviation in-cabin noise levels. The magnitudes of these levels will be discussed in the light of generalized effects on people and pertinent regulations.

3.1 Noise Exposure Criteria

There are several reasons for concern with cabin noise levels in an airplane. Noise may cause annoyance and make communications difficult. Sometimes noise can cause fatigue resulting in performance degradation of certain tasks. If those tasks are related to efficient functioning of the pilot, noise becomes a safety factor. In severe cases, humans may experience physiological damage. Thus from a marketing standpoint as well as for reasons of safety, health hazards and comfort, noise must be controlled. To exercise such control, noise criteria must be available. In the design stage, all noise criteria have the same basic objectives; that is, to serve as a guide in deciding whether or not the noise radiation of a system will be acceptable with respect to the purposes for which it is intended. Noise criteria are sometimes classified in accordance with the purposes they serve (Reference 3).

1. To prevent the risk of physiological damage to humans,
2. To minimize the degree of interference with speech communication,
3. To minimize noise induced psychological disturbances.

Reliable criteria are difficult to develop as they are actually a measure of the effect of noise on people. Satisfactory criteria to judge damage-risk to hearing and to annoyance can only be based on a vast amount of empirical information. Even then, no simple

straightforward statement will completely cover all aspects of noise performance for any specific purpose.

In some cases noise criteria have been established in the form of enforceable regulations. At this moment, there are no regulations with respect to aircraft interior noise levels. However, there is a specification to meet when the customer is the military (MIL-A-8806 A). The Occupational Safety and Health Administration (OSHA) regulations cover employees (crew). The OSHA standards are intended to protect ninety percent of the people over long periods of time from hearing-damage risk. Table 3.1 presents an abstract from these standards (Reference 3).

Table 3.1 OSHA Permissible Noise Exposures (Reference 3).

Duration per Day - hours	Sound Level (slow response) - dB(A)
8	90
6	92
4	95
3	97
2	100
1.5	102
1	105
0.5	110
0.25 or less	115

Note: OSHA regulations cover the crew of aircraft.

The noise levels that can cause interference with speech communication have been thoroughly investigated. A relationship among the variables of distance from speaker to listener, voice levels and a measure for background noise level is shown in Figure 3.1. In this graph, the required voice effort is expressed in terms of the preferred frequency speech-interference level (PSIL), a commonly used criterion

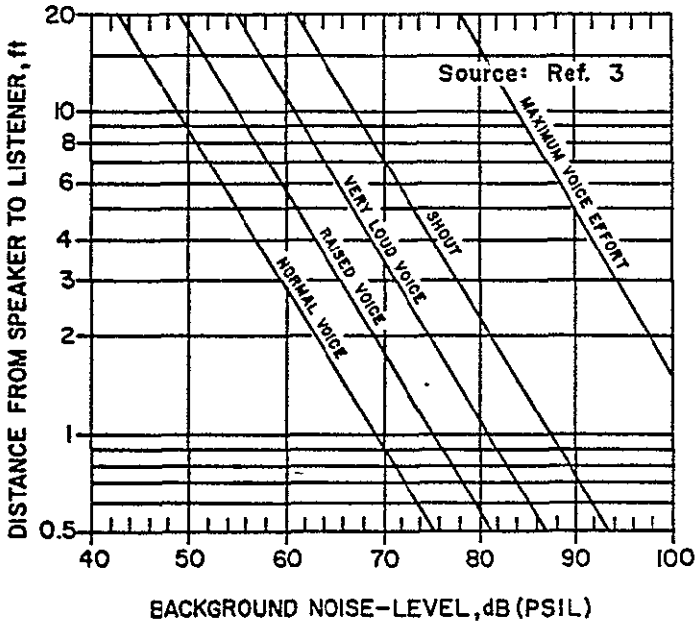

Figure 3.1. Relation of Required Voice Effort for Communication in Terms of PSIL and Distance between Speaker and Listener.

(Reference 3). This variable is computed by taking the average of the background noise, measured for the 500, 1000 and 2000 Hz octave bands.

The annoyance-type criteria are based on subjective experiences more so than the other criteria. The annoyance caused by noise can depend on many different parameters. Through extensive studies, however, some of the physical characteristics of noise were related to its acceptability. To compare the acceptability of one environment with that of another the noise level is usually expressed in a numerical scale which depends on several human and acoustic properties. The outcome can then be compared with empirically established acceptance levels. Reference 4 presents an excellent example of such an acceptability study for the case of general aviation aircraft passengers.

3.2 Noise Exposure in General Aviation Aircraft

Figure 3.2 shows a linear and A-weighted* version of a general aviation interior noise spectrum (KU-FRL test data). Spectra like these are typical for propeller driven aircraft. Characteristic are (1) the large number of peaks occurring at the fundamental and successive harmonics of the propeller blade passage and engine firing frequencies, and (2) the concentration of the acoustic energy below 2000 Hz. It can also be seen that the region between 50 and 800 Hz virtually determines the overall sound pressure level (both linear and A-weighted).

Interior noise levels like these have been measured in many aircraft. In Figure 3.3 (from References 4 and 5) these levels are compared with levels found in other vehicles. In this graph, the noise environment is expressed dB(A) (i.e., actual noise level corrected for frequency

---

* A-weighting: frequency dependent attenuation of signal to simulate frequency dependent sensitivity of human ear.

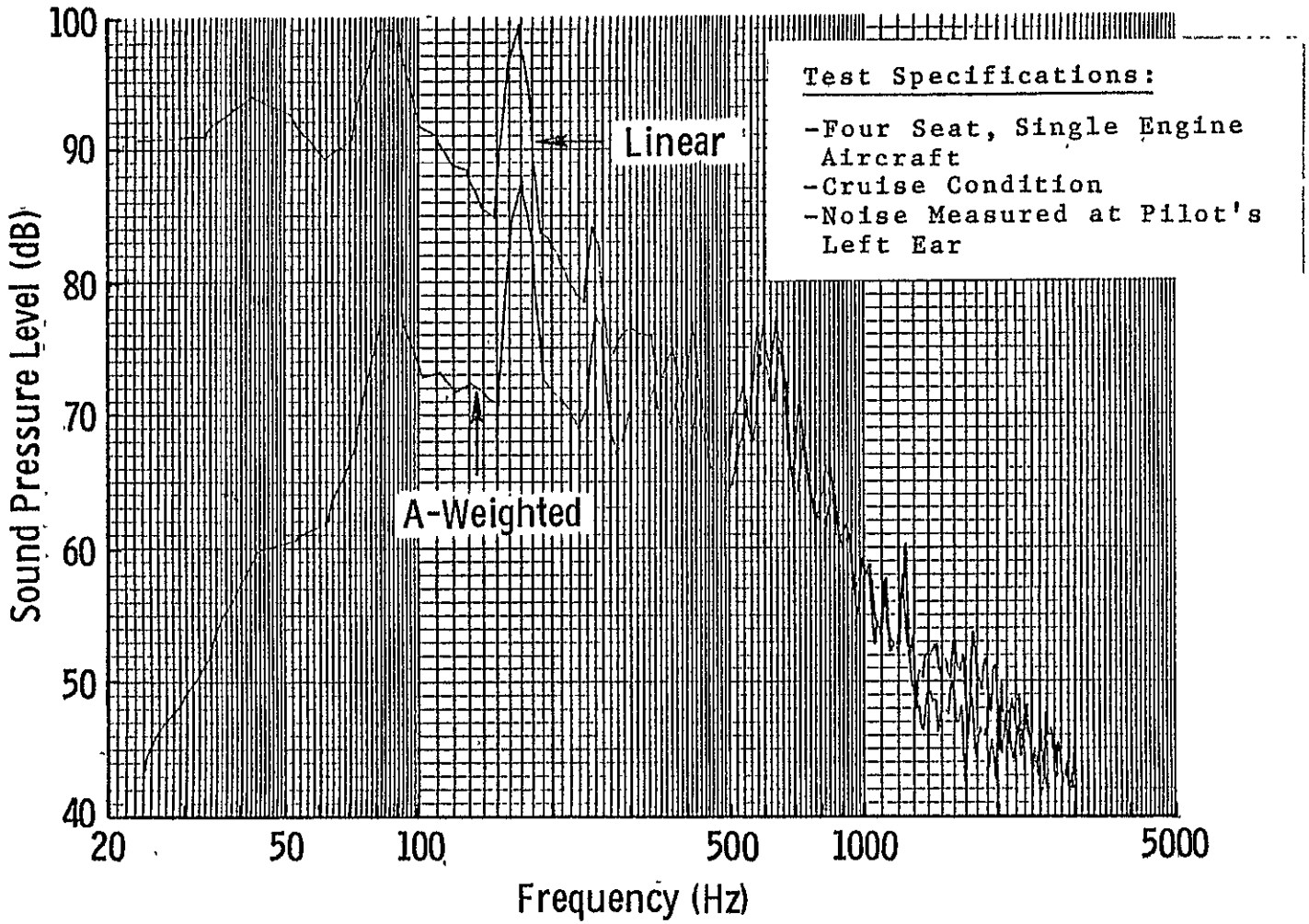

Figure 3.2. Typical General Aviation Interior Noise Spectra (Data on File at the KU-FRL).

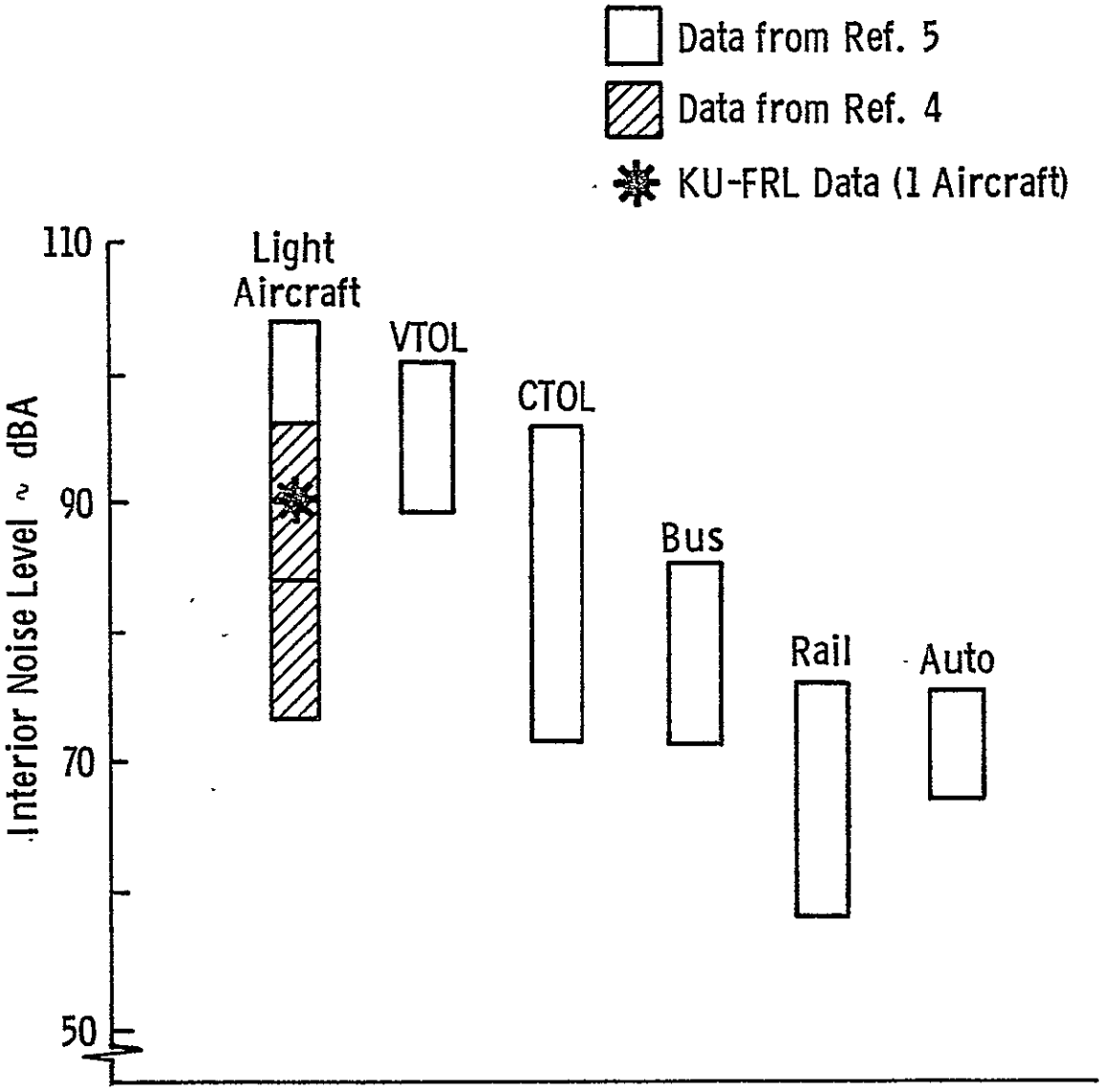

Figure 3.3. Comparison of Interior Noise Levels of Current Transportation Systems (Cruise Conditions).

dependent sensitivity of the human ear). The use of this scale implies that the graph gives a first indication of low (light aircraft) interior noise acceptability as compared with, for example, automotive vehicles. The passengers' environment being different, an absolute acceptability of light aircraft in-cabin noise cannot be determined from such a graph.

OSHA's Permissible Noise Exposures (Table 3.1) can be used to estimate the maximum flight time within which the risk of hearing damage is small. Based on the "usual levels" from Reference 4 (Figure 3.3), it can be concluded that one should not fly in "noisy" aircraft for more than three and one half hours a day. Obviously this type of criterion establishes an absolute maximum flight time. In many "less noisy" aircraft the instantaneous noise level can be high enough to interfere with speech. The preferred frequency speech interference level for the noise environment depicted in Figure 3.2 is 72 dB. This low value is a result of the concentration of noise below the 500 Hz octave band. From Figure 3.1 it can be seen that speech is thus only possible with a "raised" or "very loud" voice. It should be noted that this is not a particularly noisy airplane (see Figure 3.3).

The relation between the criteria described above and passenger acceptance of the noise environment is being studied extensively. Figures 3.4 and 3.5 show some of the results reported in Reference 4. These results indicate that (1) of the environmental variables affecting comfort, noise is the second most important factor (Figure 3.2) and (2) over sixty-five percent of the passengers (of regularly-scheduled commercial light aircraft) find aircraft interior noise uncomfortable (Figure 3.3).

Based on comparisons of general aviation interior noise data with

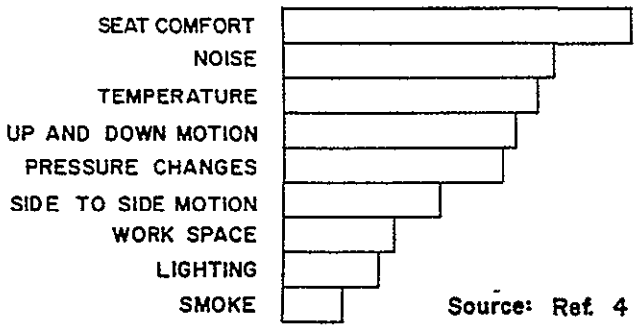

Figure 3.4. Relative Importance of Environmental Variables in General Aviation Aircraft (Results of Flight Experiments).

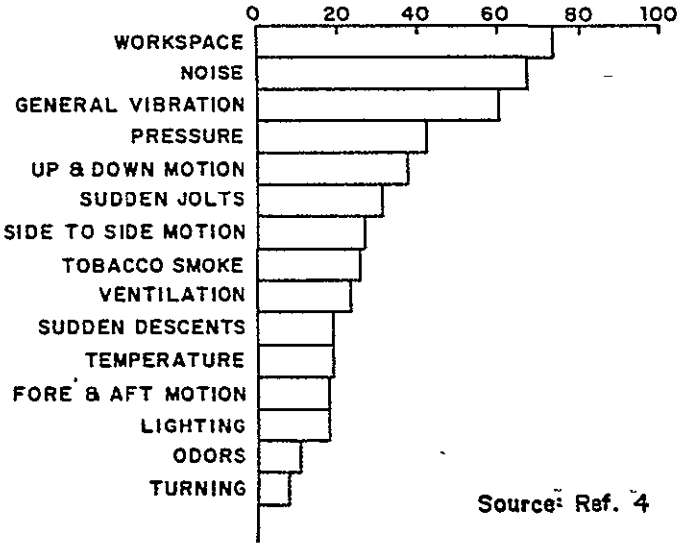

Figure 3.5. Percentage of General Aviation Passengers Finding Environmental Variable Very or Somewhat Uncomfortable (Results of Flight Experiments).

several pertinent criteria, it can thus be concluded that the current noise situation is a subject of concern.

CHAPTER 4

SOURCES OF INTERIOR NOISE

This chapter presents a description of sources of interior noise in general aviation aircraft. The transmission paths from possible sources to the cabin interior will be discussed and indications will be given of the relative importance of these sources.

4.1 Introduction

Control of general aviation in-cabin noise requires knowledge with respect to the noise sources and transmission paths. Sources include propellers, engines, auxiliary equipment and the flow of air over the fuselage. Noise can enter through the light weight fuselage structure, windows or through acoustic "leaks" (for example, holes in the fire wall). Noise can also be transmitted directly by structural vibrations induced by the engine (see Figure 4.1), or by other sources of vibrations.

Past research has proven that it is extremely hard to establish the relative importance of the various noise sources and transmission paths. In the far field (more than approximately a wingspan away from the aircraft) engine exhaust and propeller noise have proven to be predominant, but in the near field their importance is questionable. Interior noise, though definitely influenced by the nearfield of the aircraft, also depends on the direct noise radiation by the engine (causing structural vibrations), its vibrations (transmitted through the engine mounts) and noise caused by leaks and vents. This complexity is the reason that no general rules exist to predict the relative importance of every source on the in-cabin noise level. To evaluate the possible merits of control of panel sound transmission, it is important

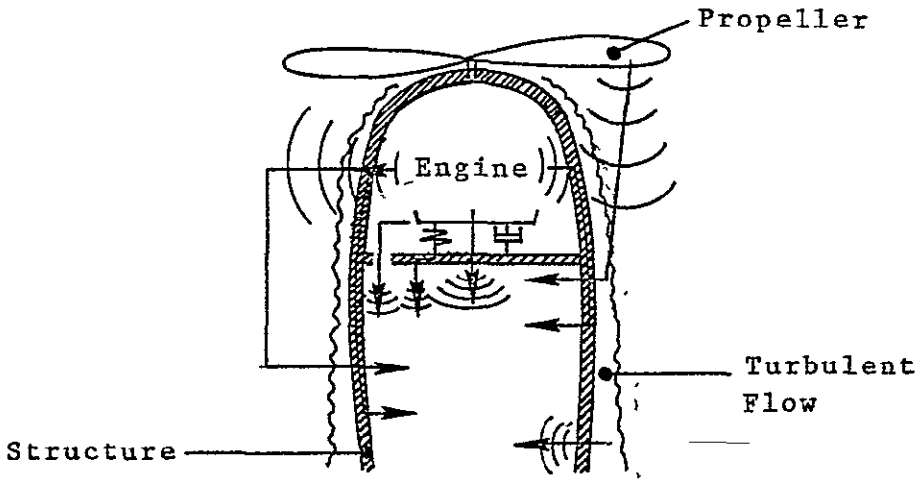

Figure 4.1. Typical Sound Transmission Paths.

to have an idea of source and transmission characteristics. In the following sections these characteristics will be discussed briefly.

4.2 Propeller Noise

The noise spectrum of a propeller exhibits a large number of peaks, which occur at the fundamental and successive harmonics of the blade passage frequency. At a given location the magnitudes of these peaks are dependent on operational variables (power consumed and tip Mach number). The total sound energy (sum of all peaks) and the relative magnitude of the peaks will change with location as well as operational variables. Figure 4.2 shows an example of such a near field spectrum (from Reference 6). It can be concluded that most of the sound energy is concentrated below 1000 Hz.

Both theoretical (for example, Reference 7) and empirical (Reference 8) methods exist to predict near field propeller noise distributions. These methods, however, assume a free field (i.e., no reflecting or scattering surfaces present) and can thus result in distributions quite different than the actual one. In addition, these methods are not valid in the propeller slipstream, where both aerodynamic and acoustic pressure fluctuations occur. Since no information could be found with respect to the relative magnitudes of both types of pressure fluctuations, the KU-FRL research team did some measurements in a propeller slipstream. These measurements and their results will be reported in detail in a future KU-FRL publication. A few typical examples are shown in Figure 4.3. Note the broad band characteristics of the excitations measured on the windshield. Such a spectrum suggests that pronounced propeller noise peaks in a slipstream can be of lower magnitude than broad band pressure fluctuations.

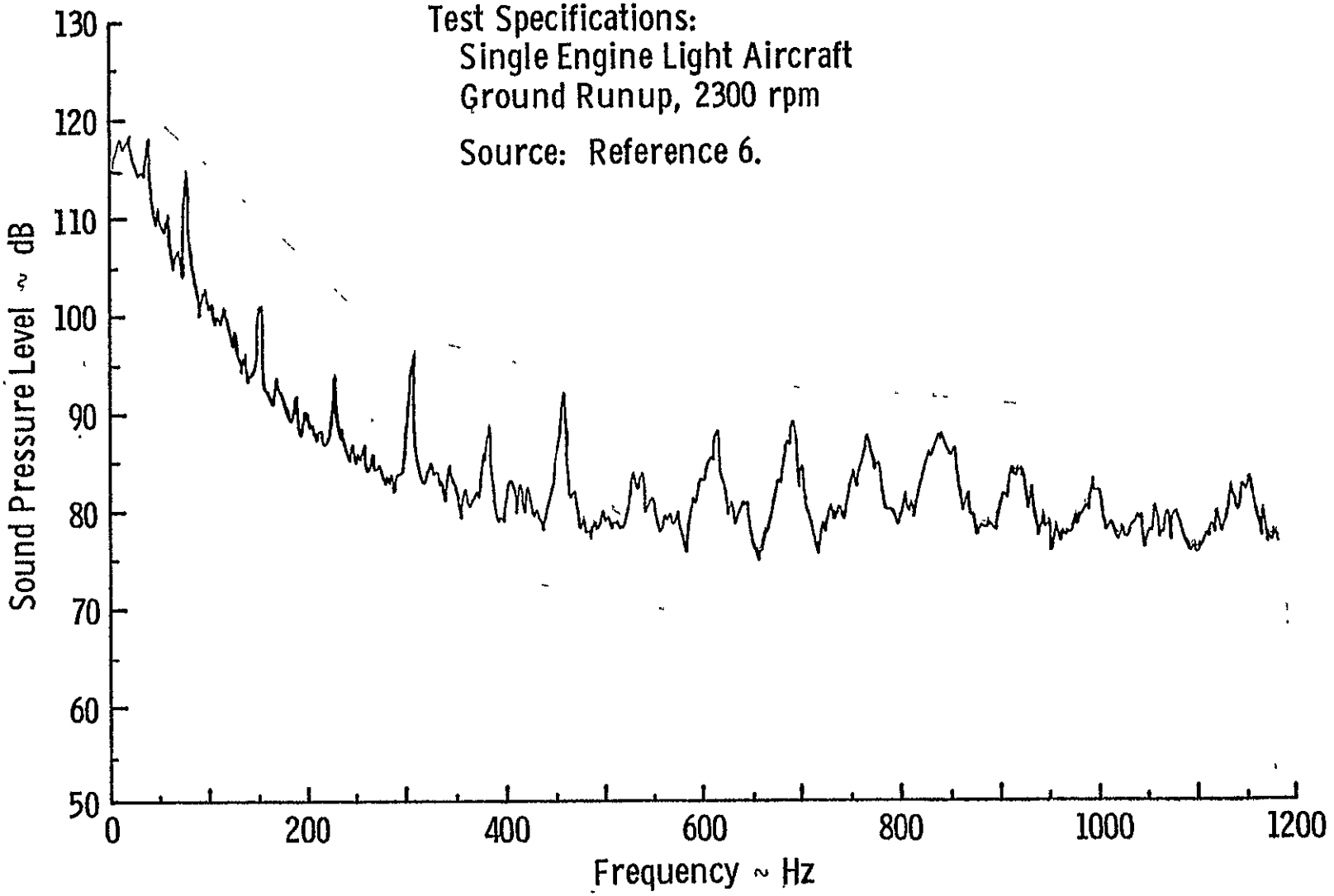

Figure 4.2. Typical Noise Spectrum in the Near Field of a Propeller Driven Light Airplane.

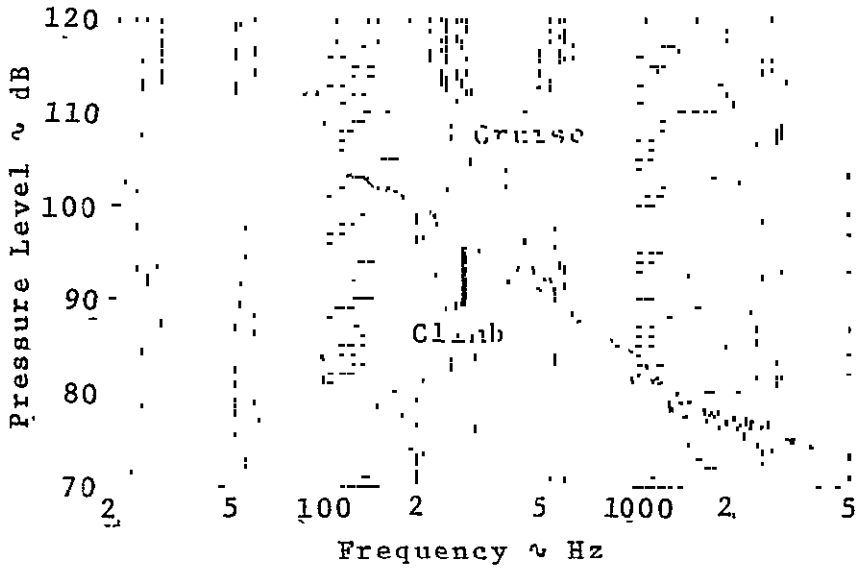

a) Windshield

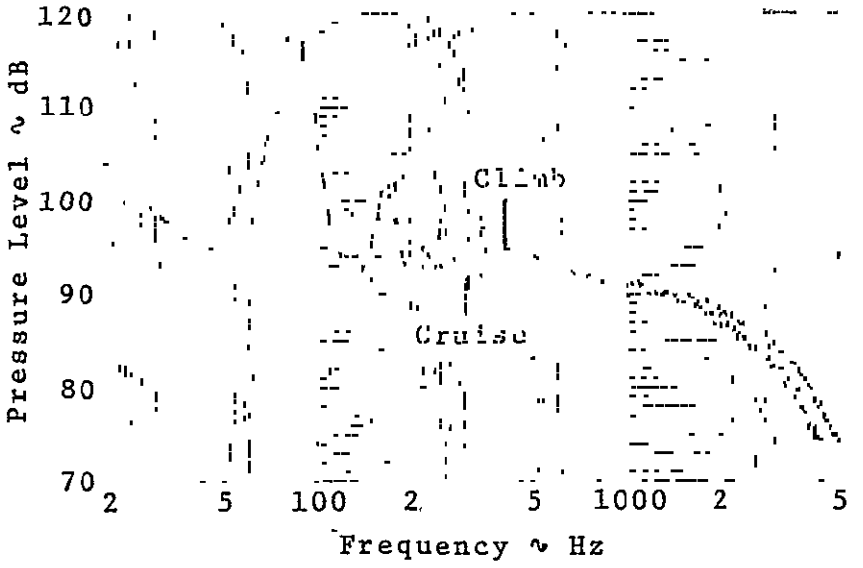

b) Side Window

Figure 4.3. Pressure Fluctuations in the Boundary Layer of the Fuselage of a Single Engine Airplane (KU-FRL Data to be Published).

Both (airborne) types of pressure fluctuations will excite the fuselage structure in a similar way. An acoustic radiation into the interior will thus result from both.

4.3 Engine Noise

Engine noise is partially caused by the periodic release of combustion gasses from the exhaust. The noise spectrum exhibits a large number of discrete peaks at the fundamental and harmonics of the firing frequency. In the far field the levels are generally lower than the propeller noise levels (Reference 9). Generalization, however, is hard to justify since for usual propeller-engine combinations (two blades and a four cylinder-four stroke engine) blade passage frequency and firing frequency coincide. Only from "odd" combinations can the individual contributions of noise be established.

In the nearfield, the magnitude of engine noise strongly depends on the position relative to the exhaust. Figure 4.4 gives an example where the noise level on one side of the test aircraft was completely dominated by the exhaust contribution (from Reference 6). Such exhaust noise will transmit through the fuselage structure, causing a contribution to the interior noise level. It can easily be seen that the fuselage excitation is position dependent.

There are more engine noise generators contributing to the in-cabin noise, e.g., engine intake, local engine resonances and the vibrations of the cabin structure due to the alternating forces applied to the fixing points. Especially engine vibrations transmitted through the mounts can cause a considerable rise of in-cabin noise. To reduce the problem the power unit is usually suspended on soft isolators. However, if the isolators are too soft, very large clearances will be needed

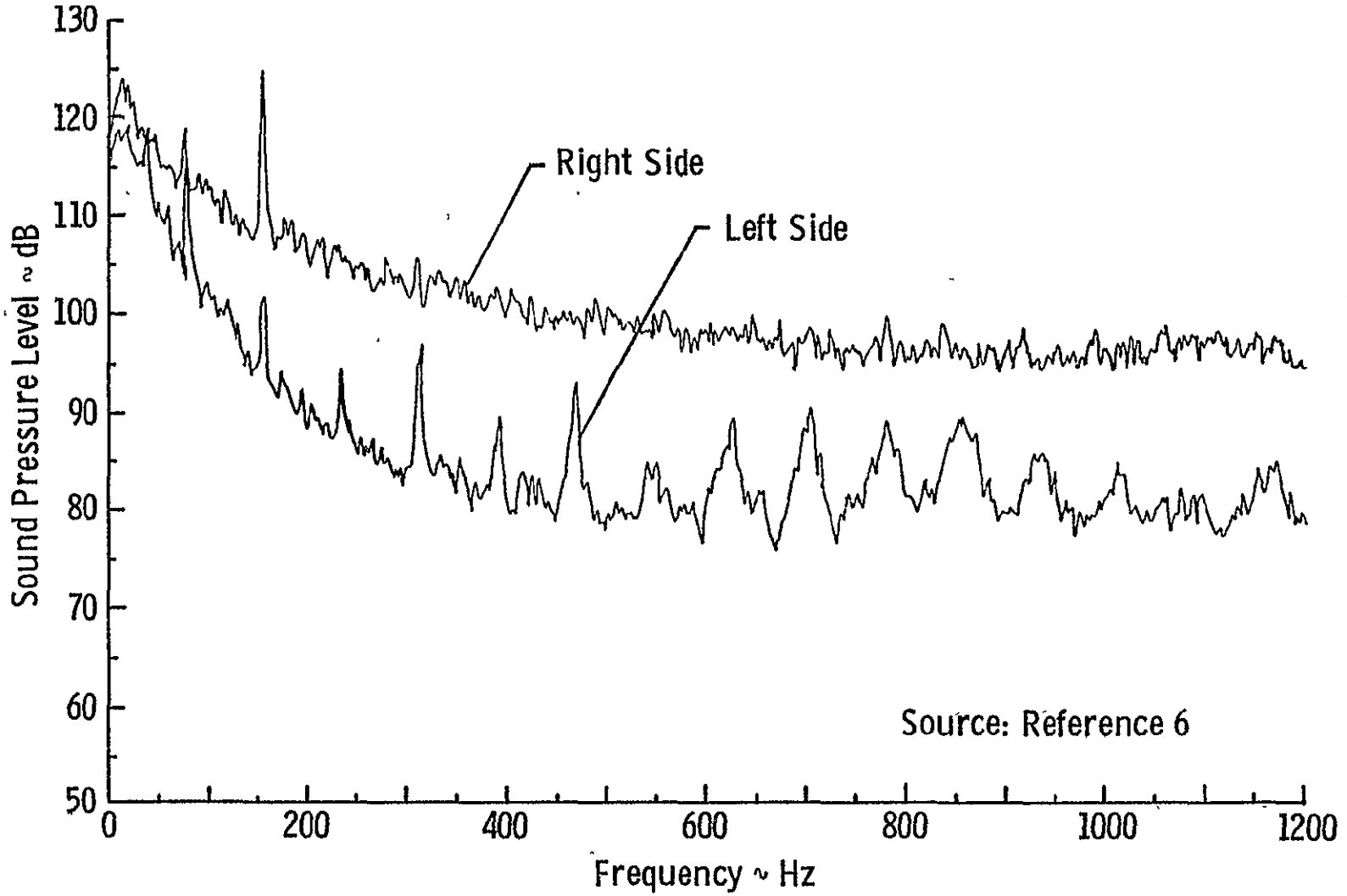

Figure 4.4. Influence of Observer's Position (Relative to Exhaust) on Exterior Noise.

around the engine to accommodate large amplitudes of motion. Another partial solution is to locate the engine mounts at the nodal points of a dominant resonance mode. Unfortunately, it is unknown how much of the vibrational energy of a normal aircraft engine is transmitted into the fuselage structure. It is known that in automotive vehicles the structure borne vibrations are in many cases predominant (Reference 10). In these cases, engines cause an interior noise level of 60 to 100 dB(A). In the case of aircraft, the only thing that has been measured is the influence of such excitations on the in-cabin noise levels. Table 4.1 shows some of the results reported in Reference 11.

Table 4.1 Acoustic Response Inside Cabin Under Mechanical and Acoustical Excitation (Reference 11)

Mechanical Excitation Level (lbf)	Acoustic Excitation Level (dB)	SPL (dB) at Front Head Position
1	0	76
2	0	82
4	0	86
0	97	76
0	103	82
0	106.5	86

Notes: 1. mechanical excitation applied to engine frame
2. acoustical excitation is exterior reverbant field

Noise radiated by engine surfaces can also give rise to interior noise. This airborne type noise will mainly excite the fire wall. Its magnitude depends on engine type and structure as well as the space between the engine and the surrounding structure. Reference 10 reports the possibility of sound build-up in this space. It can be concluded

that both engine noise and vibrations can cause a high interior noise level. However, research has been insufficient to come up with methods to predict its relative importance.

4.4 Airflow Over the Fuselage

In flight, the noise inside a cabin can have its origin in aerodynamic boundary layer noise associated with the flow of air over the fuselage skin. The boundary layer pressure field is aerodynamic and does not have the characteristics of an acoustic field. In the case of relatively slow general aviation aircraft, boundary layer pressure fluctuations are believed to be quite small (see Reference 12). However, fuselages immersed in a propeller slipstream are expected to experience more significant dynamic pressure fluctuations. A result of these fluctuations is the local excitation of the aircraft skin. As mentioned in section 4.2, the KU-FRL research team conducted some pressure measurements in the boundary layer of a fuselage immersed in a propeller slipstream. The results (see Figure 4.3) show a significant broad band contribution especially on the windshield. Only measurements taken at the storm window contain a few discrete peaks. The overall levels at both locations are the same though.

4.5 Leaks and Vents

In many general aviation aircraft, especially the ones in which the major cabin noise problems were solved, leaks and vents can be predominant noise sources. Seal leaks occurring around openings of windows and doors may contribute significantly to the interior noise of light aircraft. The effect of such a leak on the noise spectrum is illustrated in Figure 4.5 (from reference 5). The magnitude of the increase due to hissing air occurs at frequencies above 1000 Hz and is related to the

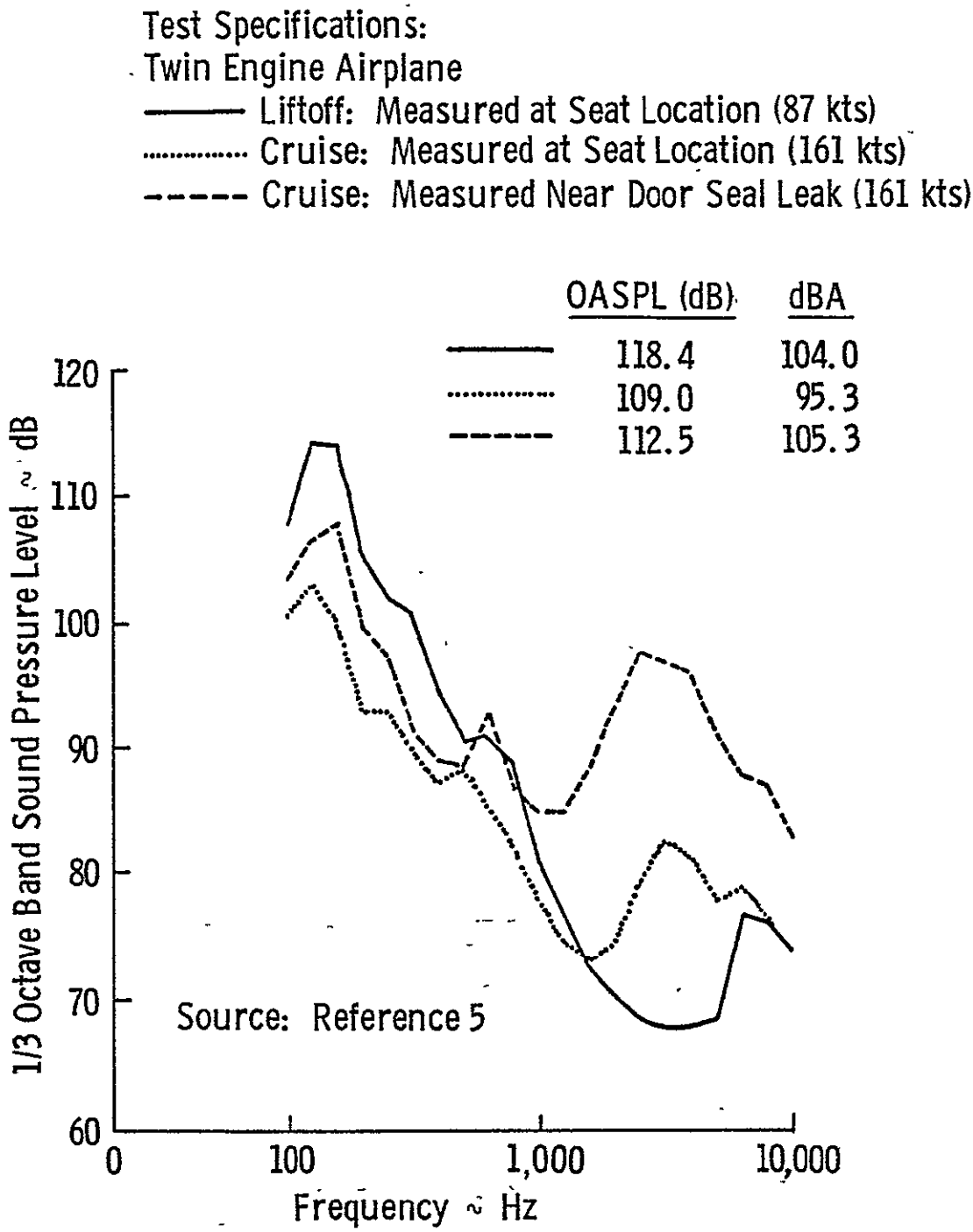

Figure 4.5. Effects of Door Seal Leak on Noise Spectra Measured in a Twin Engine Aircraft.

local air velocity over the fuselage and the extent of the leak. Fortunately, the number of those air leaks in production aircraft have been reduced by quality control procedures.

Ventilating systems can be particularly difficult noise problems, as they are connected directly to the exterior of the airplane and considerable high velocity air may be conducted through the system. The proper use of duct lining may reduce the noise transmitted into the cabin. In addition, the construction of orifices, at the outlet grilles, may need attention.

CHAPTER 5

EFFECTS OF RECEIVING SPACE AND SURROUNDING STRUCTURE

This chapter will present a discussion of the effects of a finite cavity behind a sound transmitting panel on the noise level inside. Also explained will be the influence on the panel sound transmission characteristics of the actual flexible supporting structure as opposed to the ideal laboratory boundary conditions.

The objective of the KU-FRL noise project is to investigate experimentally and analytically the transmission of sound through isolated panels. Panels in aircraft are surrounded and influenced by other panels and backed by a finite cavity with position and frequency dependent absorption properties. This environment has a significant influence on the interior noise level just like the properties of the panels themselves. Thus, to estimate the sound pressure levels in a space behind a panel, the effects of the surrounding structure and the receiving space on the panel motion and the distribution of acoustic energy within the space must be considered. These effects are illustrated in Figure 5.1.

An important effect is that the modes of sound induced vibration of a fuselage structure are influenced by the properties of its supports. If a large plate is supported by stringers that represent simple or clamped edges the local plate behavior will be the same as the one of an isolated panel. When these supports are replaced by flexible stringers which permit deflection perpendicular to the plate and restrain (to some extent) the rotation of the plate, additional "overall" modes will

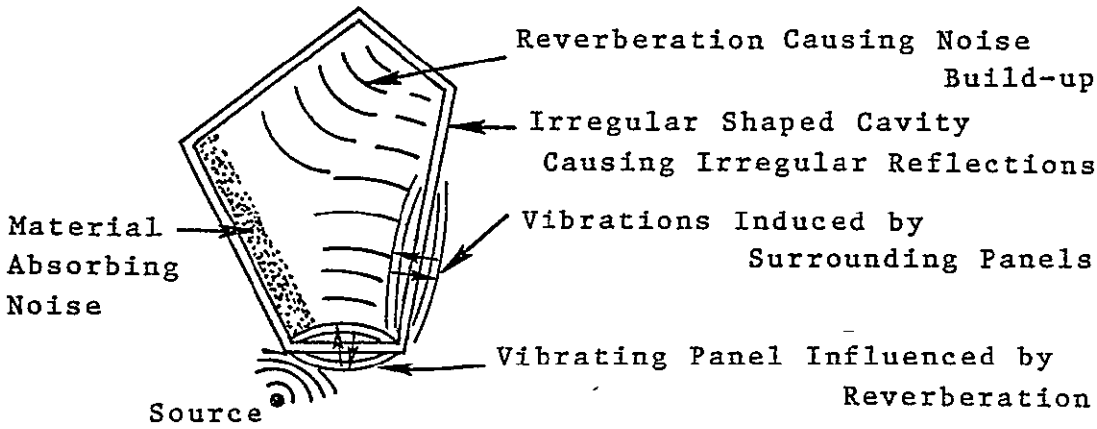

Figure 5.1. Parameters Influencing Interior Noise.

occur. This is illustrated in Figure 5.2. The significance of these overall vibration modes on the sound transmitted into the interior depends on the stringer bending and torsion properties.

Similar to the fuselage structure, the air in the cabin has many modes of oscillation having varying degrees of damping. Consequently, the noise level in the cabin, being a superposition of the contributions from all modes, depends on both fuselage and cavity sound damping properties. According to Reference 14,, the effects of receiving space can be accounted for by a correction factor for the panel transmission loss which depends in the first place on the relative size of the receiving space. An area defined as a "small receiving space" (relative to the wavelength of sound) behaves essentially as a stiffness, and the acoustic pressure is more or less uniform throughout the space. According to Reference 14 this phenomenon occurs when the wavelength of the sound is greater than six times the typical receiving space dimension. In general aviation aircraft with a cabin width of five to ten feet, this would occur at frequencies below approximately 35 Hz. In this frequency region, however, there are no audible excitations.

In a "large" receiving space, the wavelength is smaller than one tenth of a typical receiving space dimension. Under these conditions, reasonably diffuse sound fields may be expected. In general aviation aircraft such a "large" receiving space may be expected at frequencies above approximately 1000 - 2000 Hz. Figure 5.3-a shows the measured distribution of sound in a DC-3 (from Reference 15) at frequencies where the "large" receiving space characteristics may be expected.

In a medium-sized receiving space, discrete resonances with accompanying standing waves will occur. At the maxima in these standing

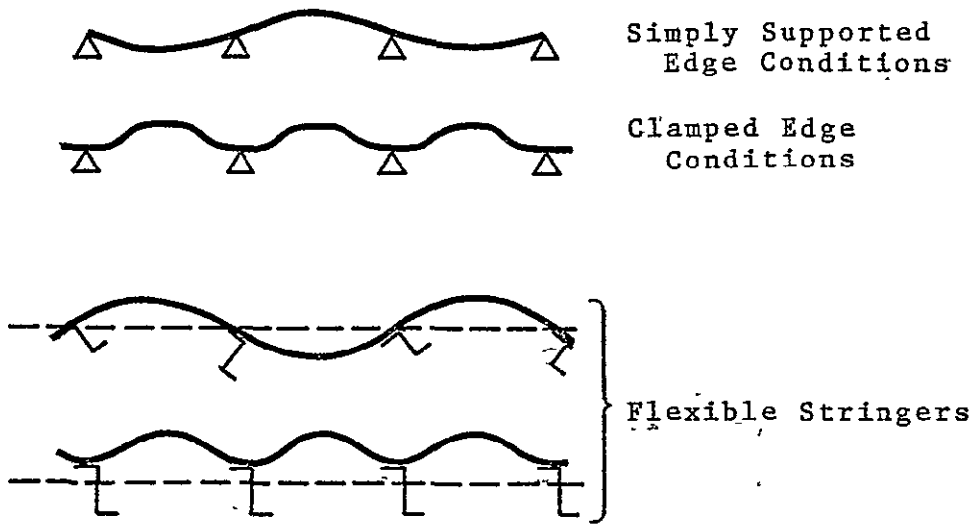

Figure 5.2. Illustration of Modes of Multi-supported Plate (Source Reference 13).

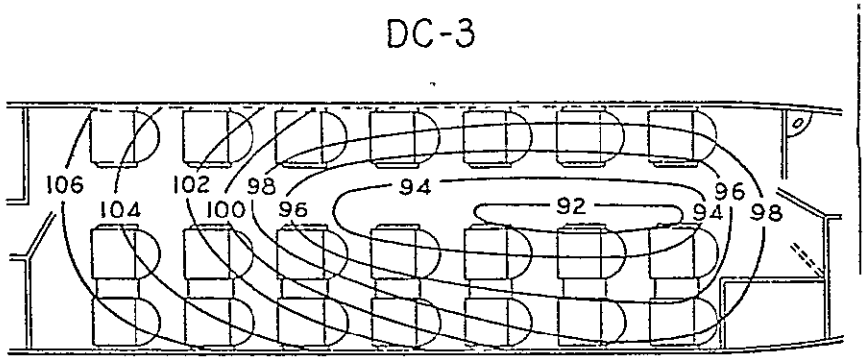

a) 75 - 150 Hz Octave Band

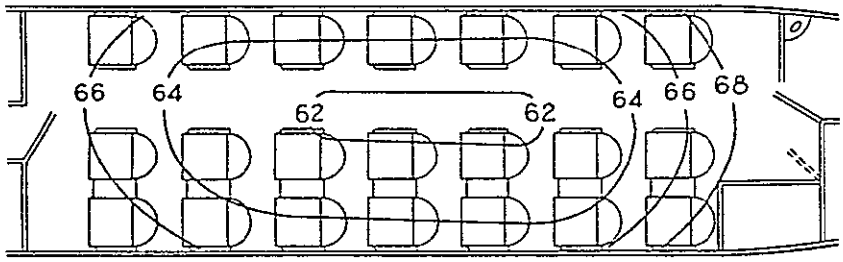

b) 1200 - 2400 Hz Octave Band

Note: Numbers indicate Sound Pressure Level in dB.

Figure 5.3. Distribution of Sound Inside a DC-3 (Source Reference 15).

in these standing waves, the acoustic pressures can build up considerably over those for free-field receiving conditions, while the minima can have sound pressures as low as those for free field conditions. The build-up of standing waves in this frequency region strongly depends on the acoustical absorption as the following table indicates.

Table 5.1 Influence of Absorption on Difference Between Maximum and Minimum Noise Levels in a Standing Wave (Reference 14)

Absorption	Absorption Coefficient	$SPL_{max} - SPL_{min}$ (dB)
High	.4	8 - 18
Medium	.25	15 - 23
Low	.13	23 - 30

The average absorption coefficient in a receiving space depends on the type of surface treatment used, on the fraction of the total surface that is treated, and on the absorbing objects inside. Average absorption coefficients quoted for airliners are in the order of .4 to .5 (References 13 and 16). A typical distribution of sound in such an airplane is shown in Figure 5.3-b (from Reference 15). The enclosed cabins of light aircraft contain large areas of plexiglass and equipment which provide little acoustic absorption. Some absorption is provided by ceilings, floors and seats, but the effectiveness is small as considerable portions of these are shielded. A significant build-up of standing waves may thus be expected in general aviation aircraft. Unfortunately, the major part of typical general aviation noise occurs in the same frequency region as the build-up of standing waves. As a result, the nonuniformity of the sound distribution inside the cabin will be very

pronounced. Consequently, the control of receiving space effects is utterly important, if the acoustic environment of passengers and crew is to be improved. To date, research in this area has been mostly theoretical. Reference 17 presents a discussion of several of such methods designed for the prediction of receiving space effects. The application of many of these methods will result in considerable mathematical complications when used for irregularly shaped cavities surrounded by a nonuniform flexible structure. The only known applications of such methods are in the automotive industry (for example, General Motors Corporation, see Reference 18). Considering the apparent significance of the effects of receiving space and surrounding structure in general aviation aircraft, the use of such methods could also be helpful when trying to improve the in-cabin noise state-of-the-art.

CHAPTER 6

SOUND TRANSMISSION THROUGH PANELS-THEORETICAL

This chapter contains a discussion of the vibrational response of panels to a dynamic (acoustic) load. Analytical and semi-empirical methods are presented to compute panel response and the resulting transmission of sound.

6.1 Introduction

Knowledge with respect to the response of structural and nonstructural aircraft panels to applied time-varying loads is of importance for the development of theoretical and empirical interior noise analysis procedures as well as for the immediate design and modification of general aviation aircraft. The excitations normally encountered in these aircraft have an aerodynamic, mechanical or acoustic nature, but all occur in the frequency region below 2000 Hz (see Figure 3.2). In this region the panel motion and noise transmission are governed by panel stiffness (below resonance region), structural damping and stiffness (resonance region), and surface mass (above region of major resonances). This is illustrated in Figure 6.1. In general aviation aircraft, low order panel resonances occur in the frequency region from 50 to 200 Hz, depending on panel size, material, thickness and boundary conditions. From Figure 3.2 it can be seen that the major portion of the interior noise is concentrated in this region and at slightly higher frequencies. As a result the panel response in and around this resonance region has a significant influence on interior noise levels in general aviation aircraft. This behavior is discussed in the following sections as well as possible ways of controlling panel response.

6.2 Radiation of Sound from a Finite Plate

The radiation of sound from plates with enforced motion is treated in many publications (examples are References 13 and 19), and will, therefore, not be discussed in detail.

The sound radiated from a plate with enforced oscillatory motion depends in a complicated manner on (1) the amplitude of the vibration, (2) the mode shape, and (3) the ratio between the acoustic wavelength and the separation between nodal lines of a mode shape. When a plate is excited by a plane acoustic wave, it will respond with an oscillatory motion. The mode shape at a certain frequency will be the sum of the resonant mode shapes of the panel. The fraction of each of these shapes contributing to the total panel deformation is inversely proportional to the difference between the frequency of the excitation and the frequency of that particular resonance (see Appendix C). This implies that the main contributors to a deformation shape at a certain frequency are the nearest resonance modes. The sound power radiated from an oscillating piston (i.e., a surface all points of which move in-phase and with the same amplitude) is proportional to the mean-square velocity of the plate times its area. A plate exhibiting a complicated oscillating deformation can be considered as a large collection of such piston areas. Each of these small areas displaces the surrounding fluid, and the fluid motion from each area interacts with that from neighboring areas. As a result the radiated power is in general not a simple function of the average panel velocity. The relative phase relations for various areas of the panel for a particular mode ($m = 5$, $n = 4$) are indicated by Figure 6.2 (from Reference 19). For general aviation type structural

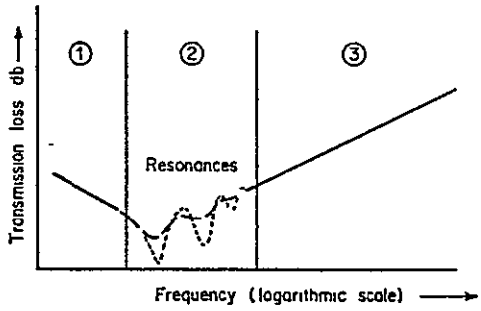

Note: 1) is "stiffness" region
2) is "resonance" region
3) is "mass-law" region

Figure 6.1. General Response of a Panel.

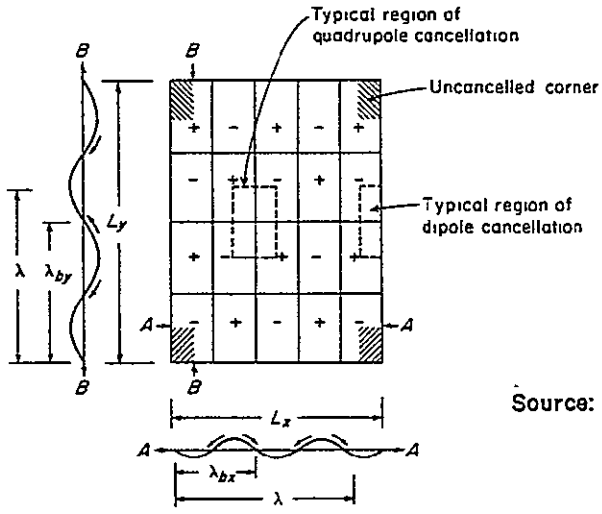

Source: Ref. 19

Figure 6.2. Displacement Pattern for the m = 5, n = 4 Mode on a Panel with Simply Supported Edges. The Relative Phases of the Antinodes Are Indicated by + and -. Arrows Indicate Air Movement during That Half-period of Vibration. The Uncancelled Corner Areas Are Widely Separated Compared to a Wavelength in Air and Do Not Cancel Each Other. This Mode is Called a Corner Mode.

panels, adjacent subsections are separated by much less than half an acoustic wavelength in the surrounding air.

Example: m = 7, n = 7 mode for .032" thick 18" x 18" clamped plate made of 2024-T3 Aluminum: $f_{7,7}$ = 977 Hz (Appendix A)

→ acoustic wavelength: $\lambda \approx 13.5"$

separation between nodal lines ≈ 2.5"

Consequently, the air displaced outward by one subsection moves to occupy the space left by the motion of the adjacent subsections, without being compressed and very little power is radiated. Only at the edges of the panel is the "cancellation" not quite so effective (see Figure 6.2). In a similar way, it can be shown that the fundamental panel mode will be an efficient sound radiating shape. In general, higher order modes transmit less sound. As a result, the transmission of sound above the region of major panel resonances is usually treated as a resonance-free region. Its characteristics are then comparable with those of an infinite plate. The transmission of sound through such infinite plates is discussed in section 6.5. Below the resonance region the transmission of sound is governed by the mean-square velocity of its oscillatory motion, the shape of which is virtually identical to the fundamental resonance mode. The transmission of sound in this region is treated in section 6.3. Section 6.4 presents the transmission of sound at resonance frequencies.

6.3 Sound Transmission Below Resonance Region

At low frequencies (below the fundamental frequency of the panel), the noise transmission is controlled by panel stiffness and the transmission loss decreases at 6 dB per octave to within the neighborhood of

panel fundamental frequency (Reference 13). The problem of stiffness controlled transmission loss of panels has not been completely explored, but estimating schemes and a few experimental results are known. Reference 14 gives the following (unproven) tentative relation at a frequency $f_{1,1}/4$ ($f_{1,1}$ = panel fundamental frequency):

$$TL(f_{1,1}/4, \text{ Stiffness}) = TL(f_{1,1}, 45°, \text{ mass law}) + 10 \log s^2 + 15 \quad \text{(dB)} \qquad (6.1)$$

where

s = fraction of surface mass (= mass/area) fully participating in panel motion at resonance (≈ .2 case investigated in Reference 14)

This relation indicates the requirement for high resonance frequencies to achieve a high transmission loss at a given frequency..

Reference 20 presents the results of an experimental study of the noise attenuation characteristics at low frequencies. It was concluded that for a given panel surface density, at any frequency an octave or more below resonance, the noise reduction will increase with an increase in the fundamental frequency. The test results showed a trend as predicted by equation 6.1; however, quantative transmission loss values were different (on the average 3-5 dB lower). To facilitate prediction and analysis of test results as well as any extrapolations to account for structural changes, the following approximate transmission loss equation has been derived:

$$TL = 20 \log \frac{\bar{m} \left| (f_{1,1}^2 - f^2) \right|}{f} + K \quad \text{(dB)} \qquad (6.2)$$

Appendix B presents the derivation, assumptions and constraints. Again, equation 6.2 indicates the strong dependence on the fundamental plate resonance. To control the stiffness controlled transmission loss as well as to control the location of the (low transmission loss) resonance region, it is thus extremely important to be able to predict the resonance frequencies of panels. Realizing this importance, the KU-FRL noise research team dedicated some of its time to studying the prediction of resonances and influencing parameters. A compilation of useful results is presented in Appendix A.

If stiffness control is to be used to reduce low frequency transmission of characteristic general aviation sound through panels, resonance frequencies have to be raised substantially. Rigidification is generally successful only when it is applied to the extent that all structural resonances are increased beyond the frequency range of major excitations. This can be achieved by decreasing the panel surface density ($\overline{m}$) and size or increasing the bending stiffness (D). As fundamental frequencies of aluminum panels (in general aviation aircraft) are generally between 50 and 150 Hz, $D/\overline{m}$ should be increased significantly (for example, by a factor of 20). Such an increase could be obtained through the use of, for example, stiffeners (or in general: orthotropic panels), curvature, honeycomb-type constructions, or different basic plate materials (like filamentary composites). Applying a pressure differential across a plate also has a stiffening effect. The derivation of an approximate prediction method that accounts for the stiffening due to a pressure differential is presented in Appendix C.

It should be mentioned that the amplitudes of resonant vibrations depend on the structural damping of the system as well as on its

stiffness (see section 6.4). As a result, the sound transmission at a resonance frequency can also be controlled by changing the plate-stiffness.

6.4 Sound Transmission in the Region of Panel Resonances

When a simple linear system is excited, the damping and stiffness are the system characteristics which control the response at its resonance frequency. When the system is excited randomly, the mean square value of the displacement is also dependent on the mass of the system:

Harmonic excitation:

$$\text{resonant amplitude} = P/2K\zeta \qquad \text{(Reference 13)} \qquad (6.3)$$

Random excitation:

$$\text{r.m.s. value of resonant amplitude} = \frac{\pi PSD_P(\omega_r)}{2M^{1/2}K^{3/4}\zeta} \qquad \text{(Reference 13)} \qquad (6.4)$$

Note: ζ = hysteretic damping coefficient

Normally three degrees of damping are specified as follows (Reference 14).

Table 6.1 Damping Categories

Damping Category	Approximate Loss Factor $\eta = 2\zeta_H$
Low	.007
Medium	.03
High	.1

The cyclic energy dissipation of structural materials is frequently very low. Consequently, panels to which no damping materials have been applied usually fall into the category "low damping." For a panel to have "high damping," it must either be of special construction or it must be heavily treated with damping treatments or devices. At this

time a popular method of controlling the resonant panel response is to add damping materials to the structure. From equations 6.3 and 6.4 it can be seen that the most effective materials are those that provide the highest value of K x ζ (or: $K^{3/4}$ x ζ). Since these materials usually come under the category of plastics, their properties are strong functions of temperature. An example of this dependency is shown in Figure 6.3 The material characterized in this graph (LD-400, manufactured by Lord Mfg. Co.) is currently being used in many Cessna and Beechcraft airplanes.

Damping materials added to aircraft panels are in the form of unconstrained or constrained layers. An unconstrained layer has one free surface, and it dissipates energy as it undergoes oscillating bending strains due to flexural vibrations. A constrained layer is sandwiched between the basic plate and another stiff layer. The damping layer dissipates energy by virtue of the shear strain when the plate vibrates. The optimum damping treatment for a vibrating panel depends on properties of the damping material, as well as on the basic plate and excitation characteristics. Equations for the optimization of the damping treatment (for a special case like lightweight aircraft structures) can be found in the literature; for example, Reference 13.

Still another way of reducing resonant amplitudes is to apply a tuned damper. This vibration absorber consists of a mass and a resilient element, and it has its own resonant frequency (see Figure 6.4). By tuning this resonant frequency to the plate's critical frequency, the vibration of the plate at the point of absorber attachment is attenuated. The level of vibration attenuation of a tuned damper depends on the tuning accuracy. As the vibration absorption is only effective in a

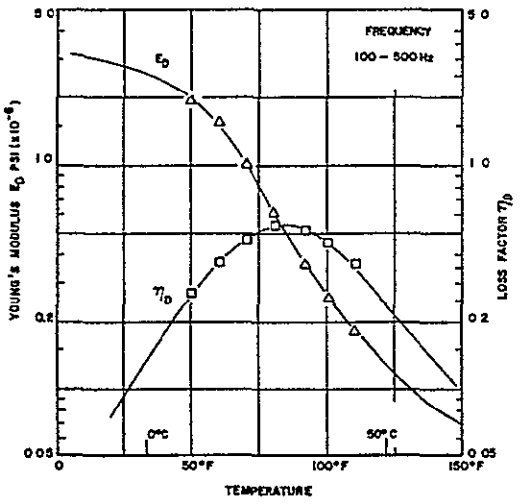

Source: Ref. 21

Figure 6.3. Complex Modulus Data for LD-400 (AFML Data).

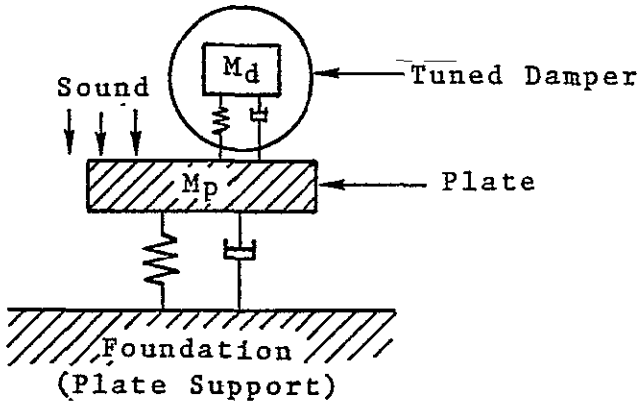

Figure 6.4. Schematic of a Tuned Damper.

narrow frequency band, this tuning is very critical. An advantage over damping materials is the virtual temperature independence, but a disadvantage is that tuned dampers are not readily available commercially since their characteristics must be tailored to meet specific performance requirements for each application.

6.5 Sound Transmission in the Mass Controlled Region

Panels of finite dimensions behave approximately like infinite panels at frequencies above the range containing the lower resonance modes. Consequently, its sound transmission loss obeys the "mass law" which can be stated, in approximate form, as:

$$TL_{400\ Hz} = 21 + 20 \log g \quad (45°) \quad (dB) \quad \text{(Reference 14)} \quad (6.5)$$

where g is the panel surface weight (lb/ft^2).

This expression indicates an increase in transmission loss of 6 dB for each doubling of the surface mass, but experiments give an average value of only 4.4 dB (Reference 22). Equation 6.5 and similar relations indicate that damping and stiffness properties are of no significance. Similarly, it can be proven that the introduction of curvature or modification into a multilayered panel will have no influence on the transmission loss (provided the surface mass remains constant). Such theoretical predictions have been validated with experimental results (for example, Reference 20).

At high frequencies, the transmission loss can be improved (above the mass law results) by adding absorptive materials with or without a resilient skin. The absorption of a porous layer is proportional to its thickness (for given material properties). At high frequencies shear losses due to viscous effects occur when the vibrating air enters and passes through the porous material. To achieve an appreciable

absorption at frequencies as low as 500 Hz, layers of 4 to 5 inches thick are generally required. By adding an impermeable membrane to the porous layer, the transmission loss in the lower frequency region can be improved. It is in this group of absorptive materials that many improvements have been reported (based on information found in product brochures).

CHAPTER 7

KU-FRL PANEL SOUND TRANSMISSION LOSS TEST FACILITY

This chapter will briefly describe the design and construction of the KU-FRL plane wave tube. The properties and limitations of this acoustic test facility will be discussed, and test and data reduction procedures will be recommended to assure reliable and reproducible results. Some preliminary test data will be presented and compared with desired results. Finally, future additions to the facility that are necessary to comply with the research requirements will be discussed.

7.1 History

Early in the fall of 1976, conversations with general aviation industry indicated a definite interest in laboratory testing of bare and treated aircraft structures. At the same time, NASA LaRC expressed an interest in this research and concurred to provide initial funding necessary to conduct such a program. A study of possibilities for laboratory testing of panels and sound proofing materials was then initiated. During a preliminary design stage which lasted through December 1976, financial implications and research objectives were evaluated. This study resulted in the decision to use a plane wave tube, if such a program would be funded by NASA. An interior noise research proposal, submitted to NASA LaRC in December 1976, suggested the use of such a facility for the experimental investigation of sound transmission through aircraft structures. Though the proposed research program was not funded, NASA LaRC confirmed its interest in the proposed laboratory testing project. Consequently, in early 1977, construction drawings were prepared, and a new noise research proposal emphasizing the use of a plane wave tube was submitted to NASA in March 1977. In this proposal

the suggested research starting date was April 15, 1977. At the time of the submittal, the likelihood of funding for such a program was considered to be high. Consequently, construction work was initiated in March 1977 to attempt to reduce time needed for and problems normally encountered during the initial phase of a research program. After three months (on June 15, 1977), the construction of the basic plane wave tube was completed. Because of some unexpected construction problems, this completion was approximately one month after the anticipated date. At the same time, however, the starting date of the (approved) project was shifted to May 1, 1977, and the duration was extended from ten to twelve months by NASA. After the construction, one month was dedicated to familiarization with the test facility, equipment and to calibration of the tube and determination of its properties. On July 15, 1977, the testing phase of the project was started. Concurrently, some refinements were made on test and data reduction procedures. At the time of this writing, the basic research facility is fully operational. Also, the design of special test sections required to comply with some of the research requirements has been initiated.

7.2 Description

The KU-FRL test facility for measurement of sound transmission through panels is described in detail in Reference 23. Consequently, this section will present a brief description only. A sketch of the test facility is shown in Figure 7.1 and a photograph in Figure 7.2. The panel to be tested is mounted between two chambers (A and B in Figure 7.1). The source chamber, consisting of a massive brick wall, concrete collar and steel box, contains nine evenly distributed loudspeakers. This chamber can be considered as a speaker box. Its purpose

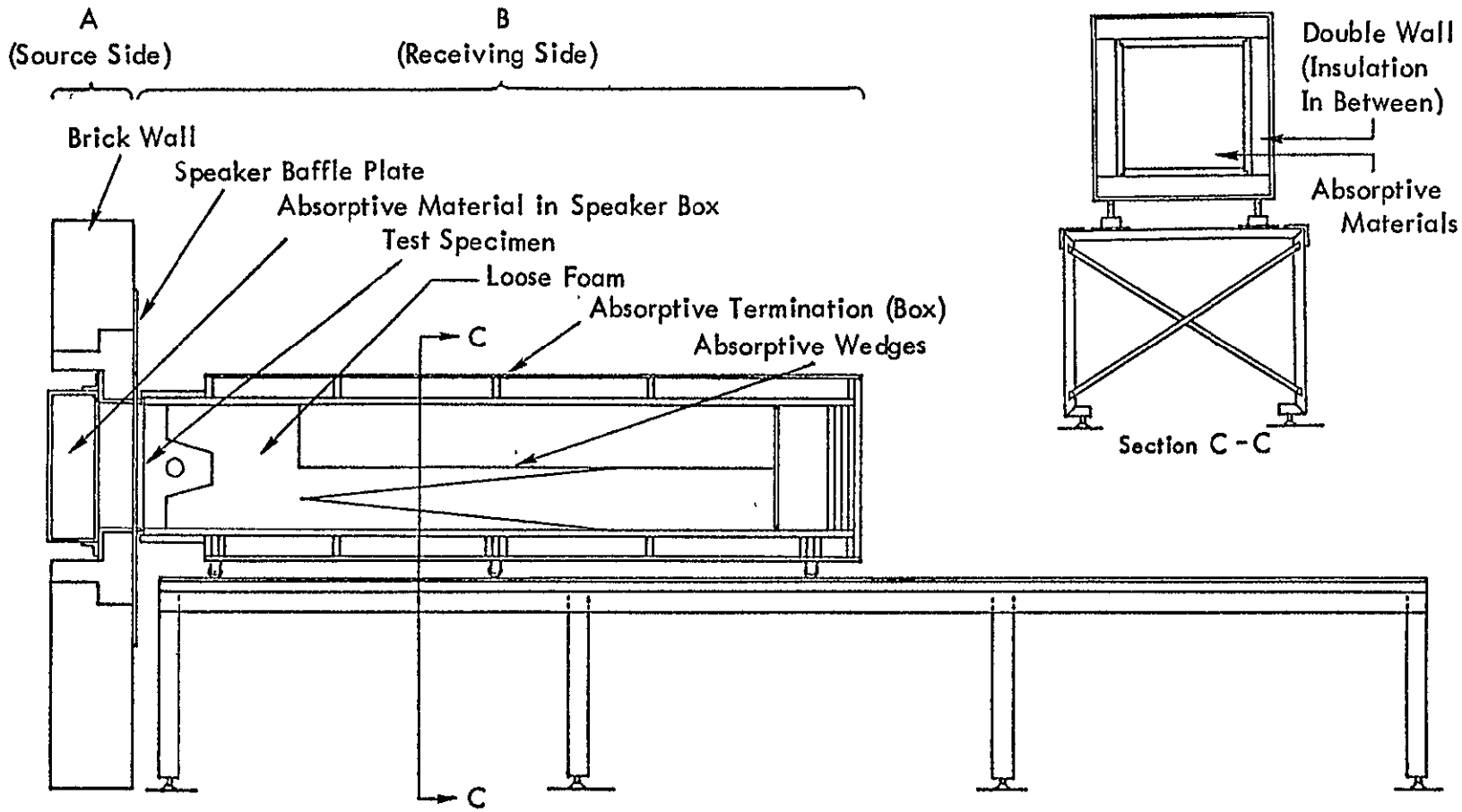

Figure 7.1. Plane Wave Tube.

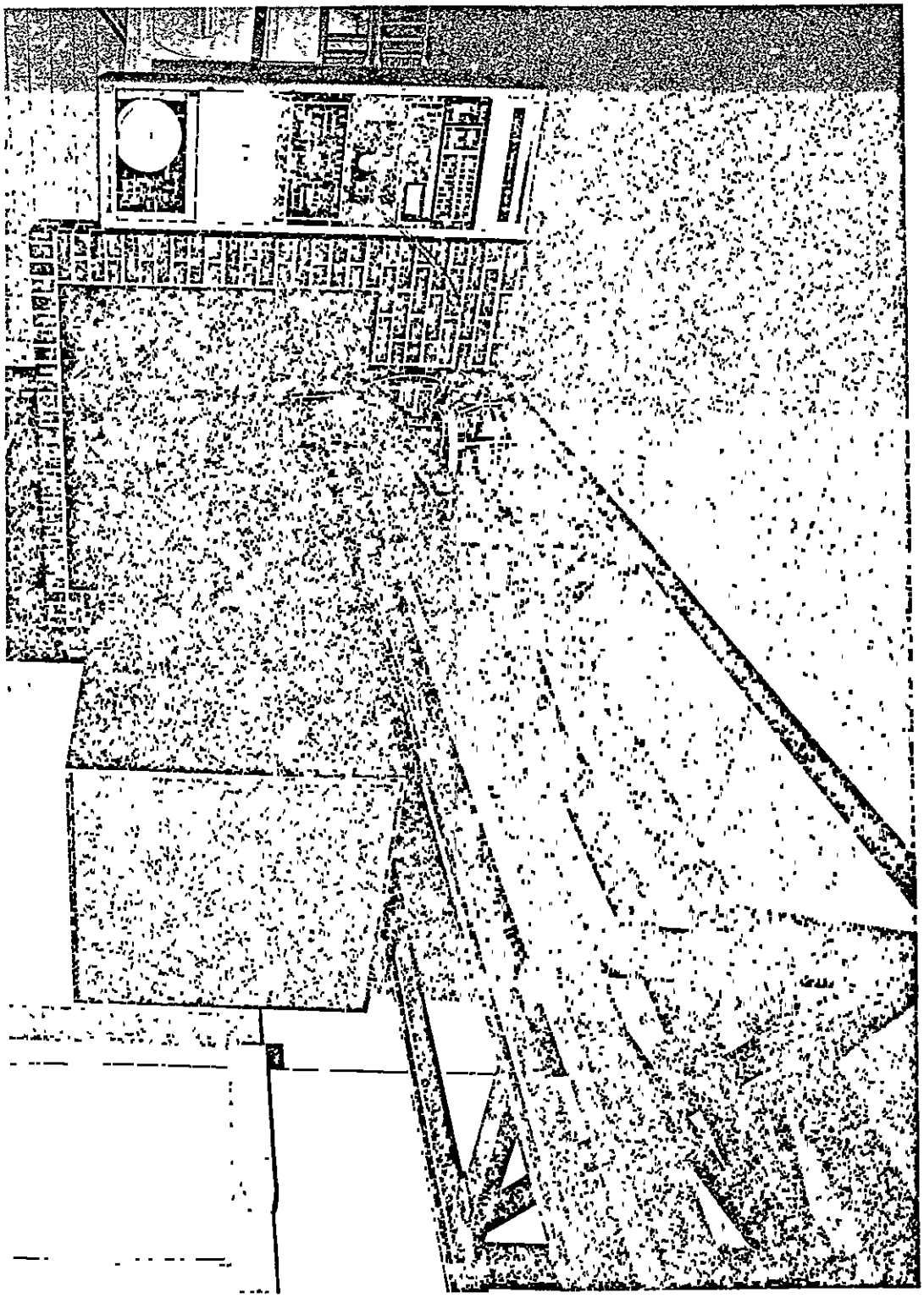

Figure 7.2. The Plane Wave Tube Test Facility

is to (rigidly) support the speakers and to avoid radiation of sound to the rear and side. It contains sound absorbing materials to minimize standing waves that can induce undesired speaker sound radiation characteristics. The panel under test is separated from the front side of the speaker baffle by a small distance. This is to shift possible standing waves between the baffle and test specimen to high frequencies. To reduce the effect of standing waves in this space parallel to the panel and speaker baffle (disturbing the desired uniform excitation of the surface of the panel), sound absorbing material almost fills this space. The receiving chamber (B in Figure 7.1) is a termination which absorbs almost all of the sound passing through the panel. It significantly improves the noise environment in which research personnel have to work, and at the same time, it influences the transmission of sound through the panel in the same way as an infinite space of air. To facilitate the installation of test specimens (between this termination and the speaker box), it is mounted on wheels and rests on a steel table.

The noise generating system and the equipment needed for measuring and analyzing the transmission of sound through a panel are depicted in Figures 7.3 and 7.4. The loudspeakers will normally be driven by the output of a white noise generator, amplified by a common power amplifier. In some cases, the white noise generator will be replaced by a pure tone generator or a tape recorder with recordings of in-flight boundary layer pressure fluctuations. An equalizer is included in this noise generating system to obtain a flat noise spectrum (given a flat noise generator spectrum).

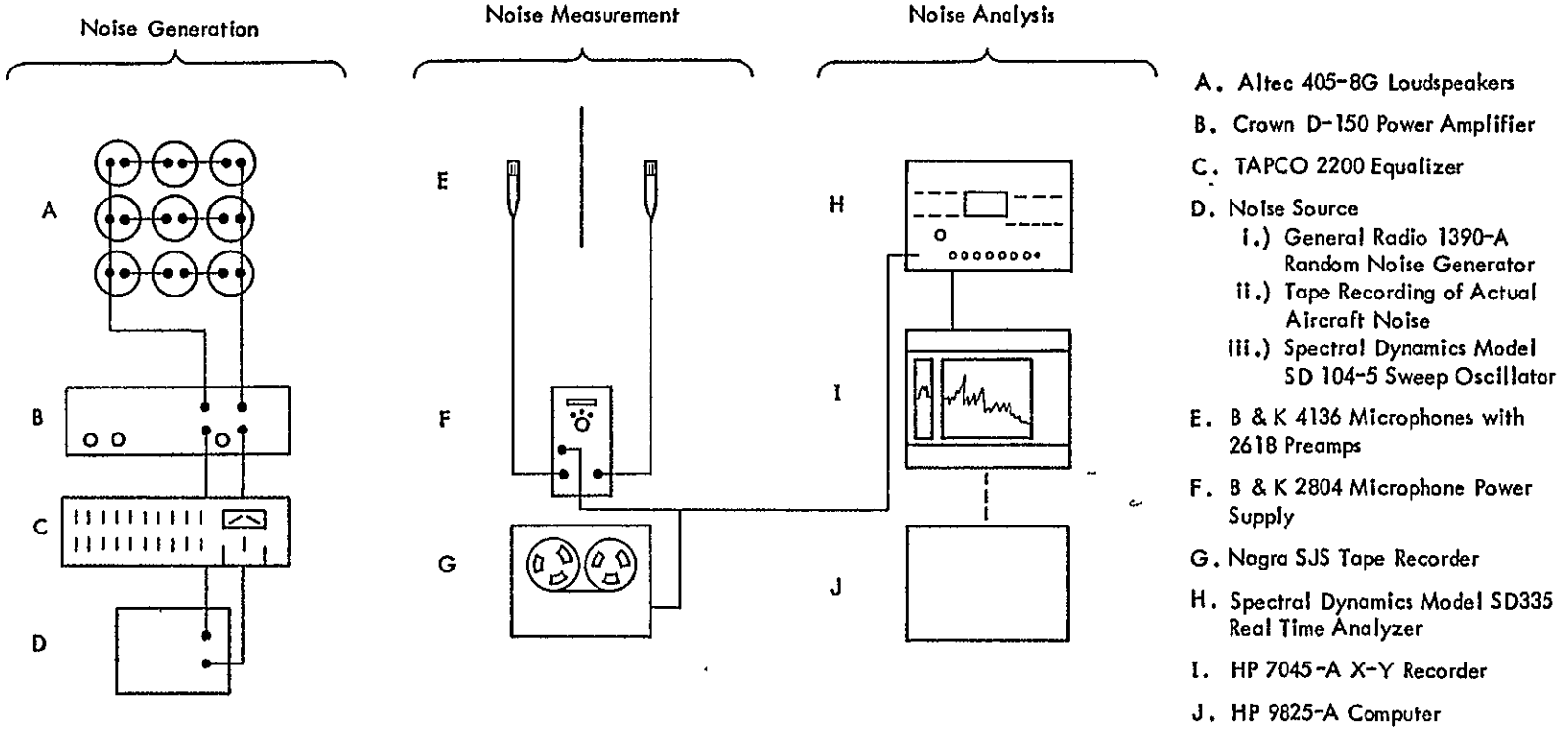

Figure 7.3. General Arrangement of Electronic Equipment.

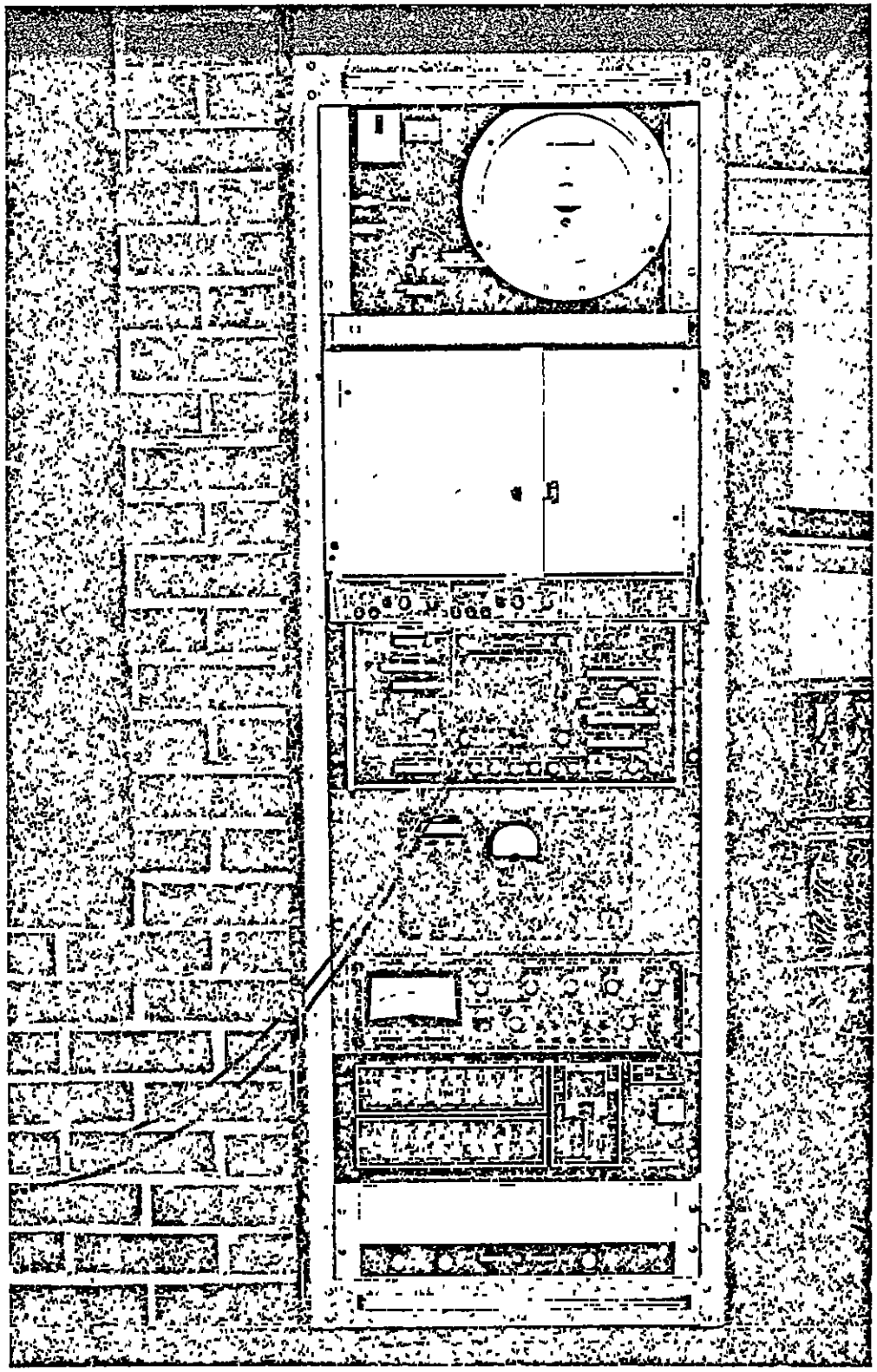

Figure 7.4. Electronic Equipment Associated with the Plane Wave Tube.

The noise measuring system consists of two microphones located at both sides of the panels under test. The output signal of each of these microphones is fed into a real time analyzer. An X-Y recorder is used to plot the two analyzed microphone signals. Next, these curves are read into a computer (with curve digitizing capabilities) which subtracts the two microphone signals, applies all necessary corrections and plots the final test results.

The testing capabilities of this basic test arrangement have been (and will be further) extended for measurements under nonstandard conditions. One extended capability which can already be implemented is testing with a (static) pressure differential across the test specimen. Other extensions not yet finalized will be discussed in section 7.6.

7.3 Properties and Limitations

The purpose of this section is to indicate some of the properties and limitations of the KU-FRL method of measuring the transmission of sound through panels. One important difference between this and other existing test procedures is the type of excitation that is being used. In the KU-FRL plane wave tube, nine identical loudspeakers provide a fluctuating sound pressure field which is theoretically uniform and in-phase over the surface of the panel. Many acoustic test facilities utilize two reverberation rooms between which the specimen is mounted. In these facilities, randomly incident noise is applied over the surface of the panel, resulting in a statistically uniform excitation. However, there are several other test practices (for example, using a reverberant source room and an anechoic termination). All these methods yield a different kind of panel noise reduction. The transmission loss (TL) of the panel, as defined in subsection 7.3.2, can be obtained in all these

cases by correcting for room effects and by selecting the right microphone locations. However, there can still be a difference between the results due to the different types of excitation that are being used. The properties of the KU-FRL plane wave tube will be described in the following subsections. A discussion of differences between this and other test methods due to differences in excitation will be included. Also presented will be some properties of the KU-FRL facility that make testing under nonstandard conditions possible.

7.3.1 Plane Sound Waves Versus Other Types of Excitation

In the case of a plane wave tube, the direction of propagation of sound waves is normal to the panel surface and the pressures are thus, theoretically, in-phase over the panel. The reverberant chamber provides randomly incident noise which is (theoretically) uniform over the panel. To account for such differences, the excitation field can be characterized by space-time correlation coefficients ($R_{12}(x_1, x_2, \tau)$)*. The space-time correlation coefficient of the sound pressure, giving a measure of the phase relationship of the pressures over the panel surface, is important in determining which types of modes of vibration will be excited.

The greatly simplified governing differential equation of undamped motion of plates can be expressed by (Reference 24):

$$D\nabla^2\nabla^2 w(x, y, t) = p_z(x, y, t) - \overline{m}\frac{\partial^2 w(x, y, t)}{\partial t^2} \qquad (7.2)$$

---

* $R_{12}(x_1, x_2, \tau) = \lim_{T\to\infty} \frac{1}{2T} \int_{-T}^{+T} F_1(x_1, t)F_2(x_2, t + \tau)dt$ (Ref. 13) (7.1)

where: F_1 and F_2 are the sound pressures at two points x_1 and x_2 in an acoustic field.

The dynamic parameters of this system are shown in Figure A.1 of Appendix A. The particular solution of this equation is associated with the panel excitations and has been evaluated for many loading conditions (Reference 24). For example, using a Fourier analysis it can be proven quite simply that in the case of a uniform harmonic pressure, even order vibration modes cannot be excited. Since generation of such an acoustic excitation in a plane wave tube is attempted, these modes are not expected to show up in the KU-FRL test results.

If the excitations vary randomly with time (as in the reverberation room methods), a Power Spectral Density analysis can explain the nature of the panel responses. Since the PSD of the panel response equals the PSD of the random excitations divided by the square of the amplitude ratio of the transfer function, most of the energy of vibration will be concentrated in the narrow frequency bands around (all) the resonances of the panel.

It can thus be concluded that the type of excitation can have a significant influence on the behavior of the plate. Consequently, an accurate reproduction of the actual noise environment in an acoustic test appears desirable, but it is normally found that such accuracy cannot be obtained. This is not just a result of the lack of sufficient information with respect to actual in-flight pressure correlation coefficients, but even more of the practical problems encountered when trying to reproduce such an excitation field.

Just like reverberation test methods, the KU-FRL plane wave tube generates its own characteristic excitations which are not identical with the actual aircraft environment. Considering the objectives of the KU-FRL noise research project (to study the effect of flight conditions,

structural changes and sound proofing treatments on the transmission of sound through panels), the difference between actual and laboratory excitations is not important. However, data obtained in the laboratory test facility will not be identical to those obtained in flight.

7.3.2 KU-FRL Test Procedure Versus ASTM Recommended Practice

A test procedure for measurement of sound transmission loss of materials is specified by and described in ASTM Standard E-90-70, "Standard Recommended Practice for Laboratory Measurement of Airborne Sound Transmission Loss of Building Partitions." To measure the transmission loss of a specimen it is mounted in the connecting opening between two reverberation rooms. Care is taken to assure that the only sound path between the two rooms is through the specimen. The rooms should be large enough to support a diffuse sound field at the lower frequencies. This requirement is expressed through the relation: $V > 4 \times \lambda^3$. This means that the volumes should be at least 45,000 ft^3 to maintain such a field at frequencies as low as 50 Hz. To avoid the possibility that the method of clamping the boundaries of the specimen will effect the transmission loss (TL) measurements the minimum dimensions of the specimen should be at least 8 ft. by 8 ft. This transmission loss is defined as follows:

$$TL = 10 \log \frac{1}{\tau} = 10 \log \frac{I_{inc}}{I_{trans}} \quad (dB) \qquad (7.3)$$

where $\tau = \frac{I_{trans}}{I_{inc}}$ is the transmission coefficient, that is, the ratio of the transmitted intensity (I_{trans}) to the incident intensity (I_{inc}). In a test procedure utilizing reverberation rooms, the transmission loss is computed from the relationship:

$$TL = NR + 10 \log S - 10 \log A \quad (dB) \tag{7.4}$$

where

S = area of the panel (m^2)

A = total absorption in receiving room = αS (m^2)

α = absorption coefficient

$$NR = SPL_S - SPL_R \quad (dB) \tag{7.5}$$

Equation 7.4 is used because the noise reduction (NR) is dependent on the total absorption in the receiving room. If noise comes through the plate and bounces around in the receiving room, the level is not what it would be if a free field existed on the receiving side.

The application of the ASTM test procedure has certain implications with regard to the test results. The use of a diffuse sound field can result in a different panel behavior than the use of plane waves (see subsection 7.3.1). The room volumes required for low frequency measurements are enormous, and due to financial constraints, not possible in a KU-FRL noise research project. However, the use of well-chosen absorptive materials in a plane wave tube can result in a highly effective anechoic termination (as opposed to a reverberant receiving room). The use of an effective anechoic termination implies that a free field condition is simulated on the source side. As a result of the large volume of loosely packed absorptive materials and wedges right behind the test specimen, the following relationship can be used for computing transmission loss:

$$TL = NR + K \quad (dB) \tag{7.6}$$

The correction factor K in Equation 7.6 is not a result of receiving space effects. It is necessary to account for the presence of both incident

and reflected sound at the location of the source microphone. If it is assumed that all the incident sound energy is either transmitted or reflected by the panel, the pressure increase due to reflection may be calcualted. The result will be:

$$K = 20 \log\{10^{NR/20} + 10^{-NR/20}\} - 6 - NR \quad (dB) \qquad (7.7)$$

There are important differences between the ASTM test procedure and the KU-FRL method. The large panel size, recommended by ASTM, will in all practical cases eliminate the effects of panel resonances on the transmission loss characteristics. Using smaller (18" x 18") size panels, as in the KU-FRL tube, facilitates studies in this extremely important frequency region.

In an ASTM-type procedure, the output signals of several microphones are commutated. The averaged results are used to compute the transmission loss. In the KU-FRL test facility, the use of one microphone situated close to both source and receiving side of the test panel will, at low frequencies (below approximately 2000 Hz), result in position dependent transmission loss characteristics. The reason for this is that the microphone is in the near field of the specimen at large sound wavelengths ($\lambda > 6$ in).

Another difference between the KU-FRL facility and other existing test facilities is the possibility of testing in the plane wave tube under nonstandard conditions. These conditions include variations of angle of sound incidence and pressure differentials across the specimen. In addition, curved panels and specimens with initial membrane stresses will be included in the intended test series.

7.4 Comparison of Desired and Measured Properties

The properties that are desired of a plane wave tube can be summarized as follows: (1) a uniform sound pressure over the panel surface, (2) the capability of reproducing the frequency spectrum of actual in-flight panel excitations, (3) a receiving chamber with acoustic properties identical to those of free air, and (4) measured panel sound transmission characteristics equal to predicted results at frequencies above the region of major panel resonances. The third requirement (regarding acoustic properties of the termination) is necessary to meet the fourth requirement (regarding the similarity between measured and predicted results) if the receiver microphone is placed at the right location. From Figure 7.5 it can be seen that the fourth requirement has virtually been met. The measured transmission loss curve of this panel is slightly higher than the mass law above approximately 150 Hz. This does not necessarily mean that the acoustic properties of the termination are identical to those of free air. To confirm this, the transmission loss of two specimens were measured both with and without the termination installed. From the preliminary results, it can be concluded that the termination raises the transmission loss of panels by approximately 3 dB (in the frequency region that could be measured). More extensive tests will be carried out in the near future. The excursions of the transmission loss curve around the mass law, as shown in Figure 7.5, are not completely due to anomalies of the test facility. The peaks and valleys occurring in these curves correspond to the resonance modes of the panel under test. Figure 7.6 shows an example of a transmission loss curve exhibiting significant excursions. It is also indicated to which calculated resonance modes these extremes correspond. As expected in a

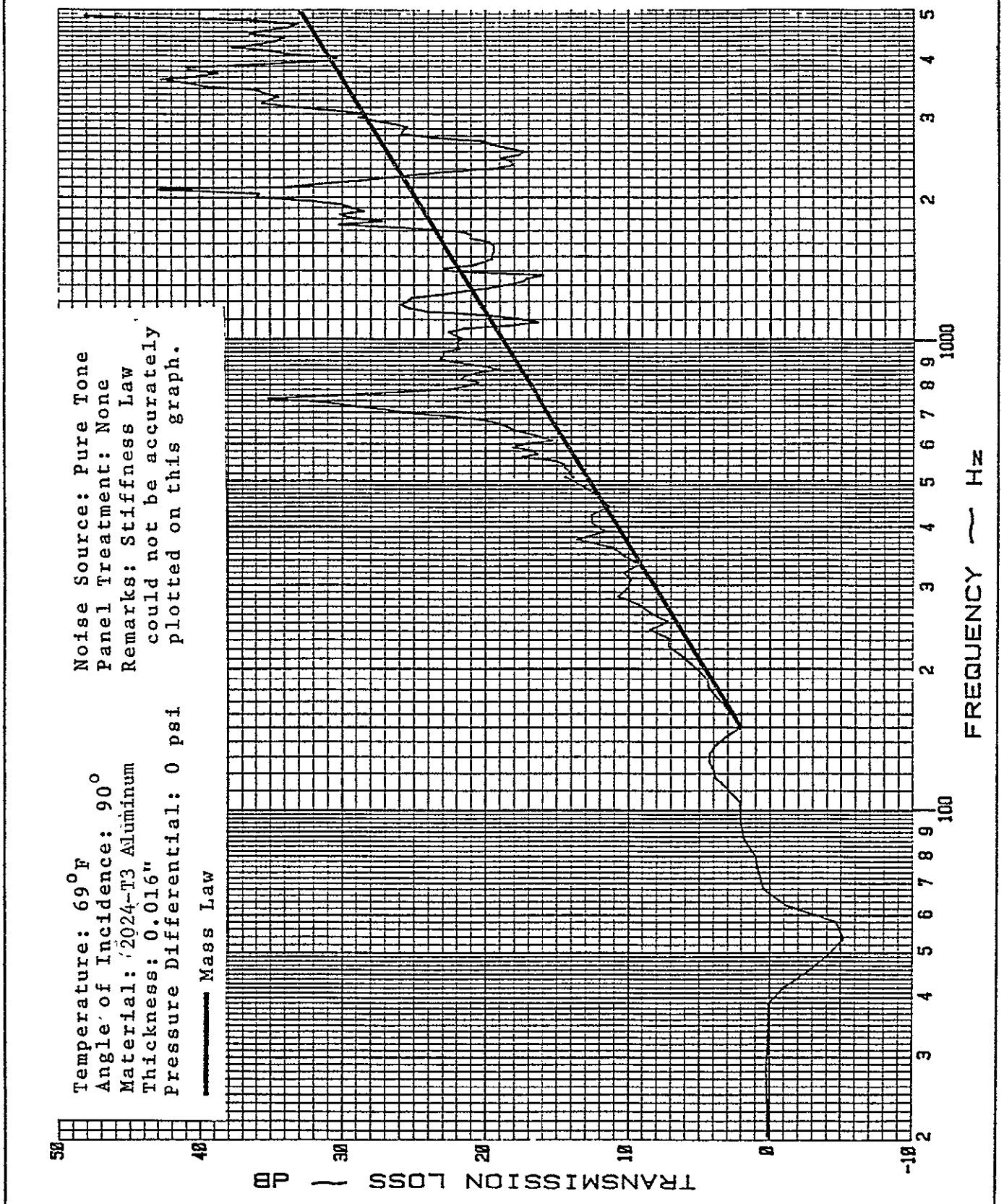

CALC			REVISED	DATE	Figure 7.5. Sound Transmission Loss Characteristics of a 0.016" Thick Aluminum Panel of 18" x 18" under Standard Conditions.	
CHECK						
APPD						
APPD						
					UNIVERSITY OF KANSAS	PAGE 72

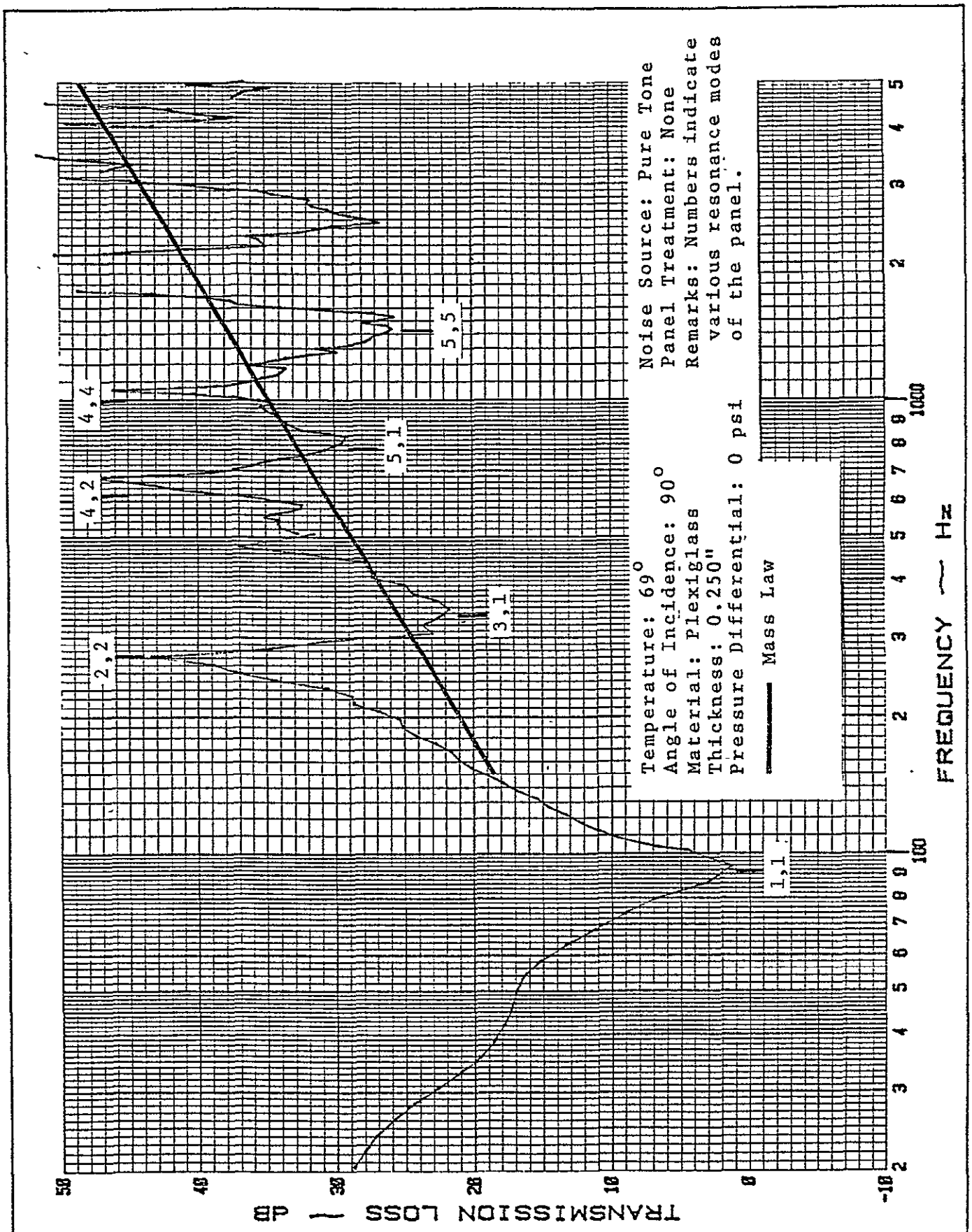

CALC			REVISED	DATE	Figure 7.6. Sound Transmission Loss Characteristics of a 0.250" Thick Plexiglass Panel of 18" x 18" under Standard Conditions.
CHECK					
APPD					
APPD					
					UNIVERSITY OF KANSAS

perfect plane wave tube, only the odd order modes (1-1, 1-3, 3-3, etc.) result in a dip of the transmission loss curve below the mass law. The uniformity of the excitations in the KU-FRL facility seems to be confirmed by the lack of extremes at even-odd modes (1-2, 1-4, 3-2, etc.). However, the even order modes (2-2, 4-4, etc.) show up as peaks. A complete explanation for this phenomenon has not been found yet, but it is likely that it is caused by a not completely uniform excitation.

The reproducibility of measured pressure fluctuations can be judged from Figure 7.7. Shown are the flat spectrum of the noise generator and the spectra of sound radiated by the speakers both with and without the use of the equalizer. It can be concluded that the equalizer significantly improves the reproduction of the measured spectrum, even though the spectrum of the radiated sound is not identical to the input spectrum.

7.5 Recommended Use of the Test Facility

This section will recommend some procedures that can facilitate testing and data reduction, prevent damaging equipment and assure reproducibility of reliable results. These recommendations are based on equipment manuals, conversations with manufacturers of equipment, trials and errors. They are believed to be necessary. The procedures presented are sufficient to cover the type of research being conducted at the time of writing this project report. Any other research will require the design of additional procedures.

Procedures for using the test facility can be divided into calibration and test procedures. Following the recommended calibration steps is the first requirement for obtaining accurate and reliable test results. These steps are presented in Appendix D. It is estimated that the time

Figure 7.7. The Results of Optimizing a Noise Source Using the Equalizer.

	CALC	CHECK	APPD	APPD
REVISED				
DATE				

UNIVERSITY OF KANSAS

required for this daily procedure is approximately half an hour. It should be emphasized that the section about the frequency adjustement of the X-Y plotter is extremely important. Any deviation from the recommended procedure will result in less acceptable accuracies.

Procedures for testing without a pressure differential across the specimen are also presented in Appendix D. There are different procedures for testing with white noise, pure tones or actual aircraft excitations. The differences are a result of the different pieces of equipment being used. When applying white noise, the linear averaging mode of the real time analyzer should be used. The number of samples recommended is a tradeoff between accuracy (within .5 dB) and time required for a test (which depends on the frequency range that is being analyzed). When applying pure tone excitations, the peak averaging mode should be used. The sweep rates specified in Appendix D will result in an optimum combination of accuracy and time required for testing. When applying recorded signals (for procedures see Appendix D), it is very important to reproduce the signal exactly. Optimum equalizer settings for this type of testing are not presented in this report, as the capabilities of the equalizer will be expanded.

The HP-9825A program manual presented in Appendix D takes care of the complete data reduction. It will subtract the signal of the receiver microphone from the source noise spectrum and apply any necessary corrections. The number of points on the measured spectra that are analyzed by the computer (200) has been chosen to minimize the data reduction time and at the same time, to maximize the accuracy of the results. In the future the program will be expanded to compute and plot pertinent theoretical predictions.

Following the procedures recommended in Appendix D will not automatically result in a flawless completion of the research program. To prevent any mistakes or delays, an orderly bookkeeping system appears to be crucial, as many specimens will be tested and analyzed. From previous experience, it was found that the following system worked satisfactorily (i.e., it is not overly complicated):

1. Every (new) specimen was numbered.
2. Specimen number and specifications were written down on the specimen log sheet (an example is shown in Appendix D).
3. After testing a specimen, specimen number, the date and a brief description of the panel and all test conditions were specified on the test log sheet. (Appendix D includes an example.)
4. It is recommended to test sets of approximately ten specimens, and to keep test results and a copy of the test log together. The original of the test log will be stored separately.
5. It is also recommended to store the digitized panel transmission loss curves on (HP-9825A) computer tape for any additional plotting or comparisons with other results. The location of storage on the tape should be specified on the test log sheet.

It is expected that the adaption of all the procedures discussed above will minimize any unexpected or undesired results.

7.6 Future Expansions

At the time of writing this report, the basic test facility, including the depressurizing system, is completed and operational. Consequently, flat panels can be tested at an angle perpendicular to the direction of sound incidence, with and without a static pressure differential across them. The capabilities of this facility will be

expanded to allow for the testing of curved and slanted specimens, and panels with static in-plane stresses.

To allow for the testing of panels at various angles to the direction of sound propagation, test sections will be constructed that will be placed between the two existing sections (i.e., speaker enclosure and termination). These sections will be constructed so as to allow for testing of curved as well as flat panels. At the time of this writing, the sections are in the design stage. It is expected that the construction can be started in early September and finalized in early October. A conceptual design of such a special section is shown in Figure 7.8.

A special frame will be constructed to induce in-plane stresses in the test specimens. The design of this frame will be started after the completion of the sections for curved and slanted panels. An example of what this frame may look like is shown in Figure 7.9

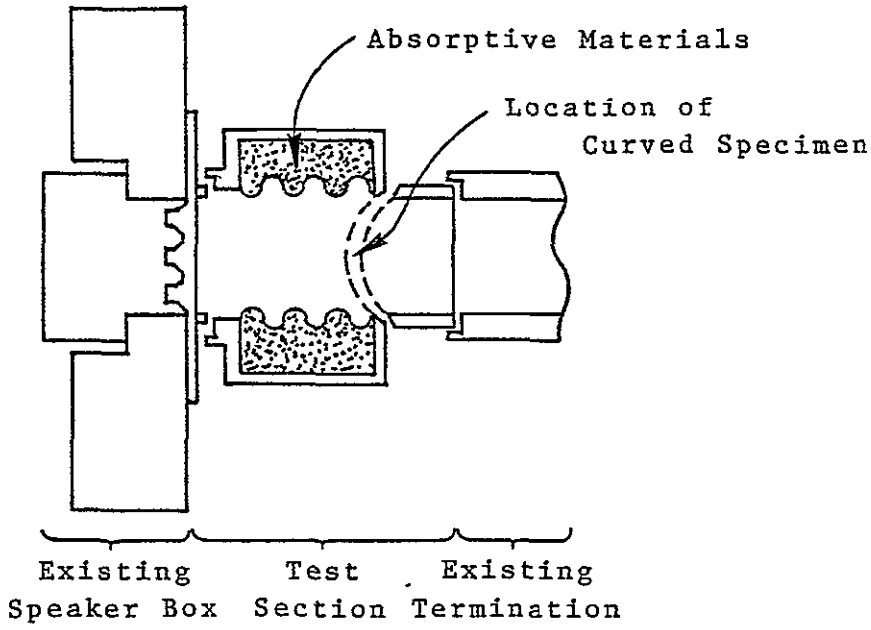

Figure 7.8. Conceptual Design of a Section for Testing of Curved Panels.

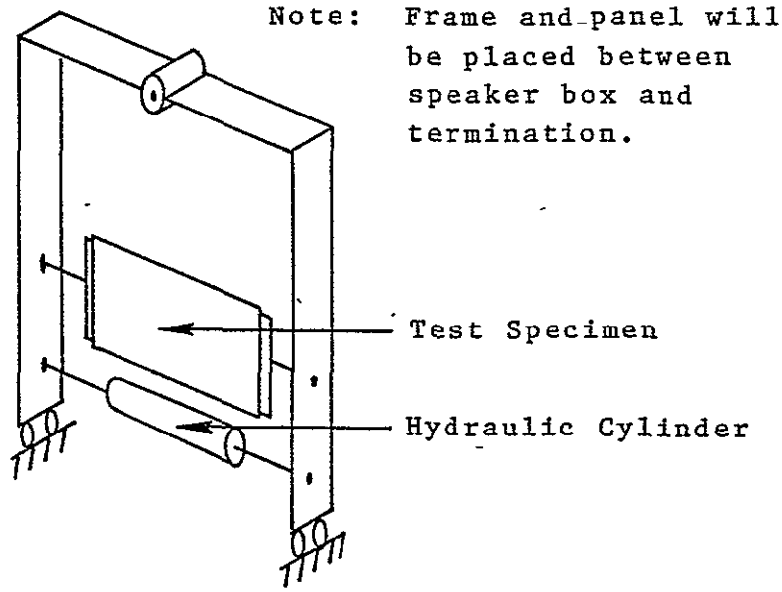

Figure 7.9. Conceptual Design of a Frame for Applying In-plane Forces to Panels.

CHAPTER 8

TEST SPECIMENS AND CONDITIONS

In the March 1977 proposal to NASA (Reference 2) a preliminary list was presented of test specimens and test conditions. Since then, some revisions have been made and these are included in Table 8.1. This table is a result of the objective to vary parameters describing specimens and conditions systematically and to provide functional relationships between these variables and the behavior of panels. The frame within which parameters can be changed will cover the complete range of conditions and specimens currently present in the area of general aviation and possibly present in the future. Consequently, specimens will include aluminum sheet from the fuselage sidewalls and doors, steel sheet from the fire wall and plexiglass from the windows. In addition, panels of fiberglass sheet and composite sandwich materials will also be examined since these types of materials are finding increased usage in aircraft. A number of materials will be treated with stiffeners and sound proofing material and retested to study the sound transmission loss characteristics of the combinations.

The aluminum, steel, honeycomb, and plexiglass materials are being supplied by the general aviation manufacturers at no cost to the project. At the present time, two manufacturers have submitted materials including many thicknesses and stiffening patterns. These materials are listed in Table 8.2. Two other aviation manufacturers have been contacted about providing additional specimens, including fibrous composites.

The sound proofing materials that will be applied to the test panels are being supplied by commercial vendors, again at no cost to the project. A list of vendors was obtained from Reference 25. These

Table 8.1 Summary of Panels and Materials to be Tested in KU-FRL Test Facility

Test Specimens ↓ / Test Conditions →	Number of specimen thicknesses	Number of damping materials to be tested	Number of damping material patterns to be tested	Number of stiffening patterns on test specimen	Number of angles specimen will be tested at	Number of radii of curvature for test specimen (other than ∞)	Number of types of excitation	Number of pressure differentials across test specimen (other than 0)	Number of in-plane stresses (other than 0)
Unstiffened Aluminum Panels	5	6	4		5	3	3	3	3
Stiffened Aluminum Panels	1	2	2	2	1		1	3	
Fibrous Composites	3			3 (ply orientations)	1		1		3
Plexiglass	3			2	5	3	3	3	3
Honeycomb Panels (i.e., PCV-foam)	3				1		1	3	3
Typical Fire Wall Panels (i.e., stainless steel)	3	6	4	2	5	3	3	3	3

Table 8.2 Aircraft-type Base Materials
Received by August 1977

Company	Test Specimen
Cessna Aircraft Co.	.016" Aluminum Sheet
	.020" Aluminum Sheet
	.025" Aluminum Sheet
	.032" Aluminum Sheet
	.040" Aluminum Sheet
	.025" Stiffened Aluminum Sheet
	.025" Stiffened Aluminum Sheet
	.032" Al Sheet w/full coverage LD400*
	.032" Al Sheet w/18" x 18" LD400
	.032" Al Sheet w/14.2" x 14.2" LD400
	.032" Al Sheet w/3" edge of LD400
	.016" Steel (19" x 20")
	.020" Steel
	.032" Steel
	1/8" Plexiglass
	3/16" Plexiglass
	1/4" Plexiglass
Grumman American Aviation Corp. P. O. Box 2205 Savannah, Georgia 31402	Honeycomb panels

*LD400 is a vibration damping material supplied by Lord Corporation and used on most Cessna Aircraft.

manufacturers were contacted with requests for materials suitable for aircraft use. An example of the letter(s) used, is presented in Appendix E. The manufacturers that have submitted samples to date are listed in Table 8.3. All materials and treatments received are suitable for "flat-panel" tests with an angle of sound incidence of 90° relative to the surface of the specimens. For testing of slanted and curved panels, additional materials need to be obtained.

The order in which specimens will be tested depends on the available capabilities of the test facility. At the time of this writing, flat specimens can and will be tested at an angle of sound incidence of 90°. The test conditions will include the presence of a pressure differential across the panels. Testing of curved and slanted panels is expected to start in the end of October, after the construction and calibration of the necessary test sections has been completed. Testing of panels with in-plane stresses will be initiated as soon as the construction of the frame required for applying the necessary forces is completed.

Table 8.3 Acoustic Treatment Materials
Received by August 1977

Company	Test Specimen
Carney & Assoc., Inc. P. O. Box 1237 Mankato, Minn. 56001	Fiberglass - 1" thick
Chemprene, Inc. Div. of the Richardson Co. 570 Fishkill Ave. Beacon, N.Y. 12508	Foam - 1/4" thick with backing
Foamade Industries 1220 Morse Street Royal Oak, Michigan 48068	Foam - 1" thick (2 & 4 lb/ft.^{3})
Forty-Eight Insulations, Inc. Aurora, Illinois 60504	Fiberglass - 1" thick (8, 6, & 3.5 lb/ft^3)
Insul-Coustic Corp. Jernee Mill Rd. Sayreville, N. J. 08872	Visco-elastic paste used to bond secondary damping panel to primary sheet
Singer Partitions, Inc. 444 North Lake Shore Drive Chicago, Illinois 60611	Visco-elastic paste
Specialty Composites Corp. Delaware Industrial Park Newark, Delaware 19711	1) Antiphon - 13^{TM} vibration damping pads 2) Antiphon - 13/foam sandwich 3) High density foam pads 4) Multi-density foam sandwich 5) "Deadened Steel" (steel sheet sandwich with visco-elastic core
Duracate Corp. 350 North Diamond St. Ravenna, Ohio 44266	Miscellaneous foam and plastic samples

CHAPTER 9

CONCLUSIONS AND RECOMMENDATIONS

9.1 Conclusions

The interior noise state-of-the-art in general aviation aircraft is a topic of concern. This has been explained in Chapter 3 with a comparison of typical in-cabin noise levels with several criteria. Considering the support of NASA and general aviation industry to the project, this conclusion has been verified.

The in-cabin noise levels are affected by the characteristics of the noise sources, transmission paths and receiving space (cabin). In Chapters 4 and 5 an attempt has been made to prove that every one of these factors can have a significant influence on the interior acoustic environment. Of these, the control of the transmission of sound is generally considered as a potentially effective and possibly efficient means of improving the exposure of passengers to noise. That this opinion is shared by both NASA and general aviation industry may be deduced from their willingness to help the project.

Realizing the importance of the control of transmission of sound, the KU-FRL noise research team has engaged in a research program focusing on this phenomenon. The project objectives necessitate theoretical as well as experimental work. The combination of both approaches will yield results that can augment NASA's goal to investigate structural transmission phenomena and prediction. By focusing the research on materials and structures that are potentially applicable in light aircraft, the results can also be of direct use to general aviation industry.

The resulting support provided by NASA and industry is sufficient to achieve the project goals, outlined in Reference 2, but insufficient to allow for any excursions. Consequently, attention needs to be paid to the financial management of the project. At this writing, barring any unforeseen events, it is anticipated that the project goals will be met within the financial limits (Chapter 2).

In addition to financial constraints, time limitations have a definite influence on project planning. At this writing the actual research progress has kept up with the projections required to meet the project deadline. It is expected that this trend will continue, as (1) a competent research team will succeed the current research personnel, and (2) the time consuming preparation phase is in its final stage (Chapter 2).

The achievements to date include the completion of a test facility (described in Chapter 7) and a basis for the development of theoretical analysis procedures (Chapter 6). Preliminary research has indicated that (1) this theoretical basis is well understood, and (2) this test facility yields comparable results. Differences between test conditions in the KU-FRL plane wave tube, ASTM-type reverberant facilities and actual flight conditions are indicated in Table 9.1.

Thus, based on the state-of-the-art of the KU-FRL noise research project, it is expected that the project goals will be met.

9.2 Recommendations

9.2.1 General Project Activities

Testing of flat specimens at an angle of ninety degrees relative to the direction of sound incidence should continue through 1977. Concurrently, pertinent sound transmission phenomena should be investigated

Table 9.1 Comparison of Test Environments with Actual Flight Conditions.

	KU/FRL	ASTM	AIRCRAFT
Direction of sound propagation	one (predetermined) angle at a time	random	probably random with one predominant angle
Excitation spectrum	any	any (but stationary)	position and flight condition dependent
Frequency range	20-5000 Hz (narrow band)	125-4000 Hz (1/3 octave bands)	≈50-2000 Hz (narrow band)
Specimen size	18" x 18"	8' x 8'	≈8" x 8"
Receiver location	near field (9") (1 position)	far field (several positions)	near field
Test variables	pressurization source characteristics angle of sound incidence initially stressed	?	pressurization source characteristics angle of sound incidence initially stressed flow of air temperature

theoretically. Specifically, the effects of the following parameters should be studied during this period of time:

- Testing and analysis of the influence of pressurization on the transmission of sound through panels should be finalized.
- Analysis of the effect of stiffeners on the transmission loss of a panel should be continued, and more stiffened specimens should be used to experimentally validate theoretical results.
- It is recommended to measure sound at different locations on the receiving side of the panel to evaluate the current microphone location and results.
- The effect of specimen dimensions and edge conditions should be experimentally evaluated by measuring a) the transmission loss of a small panel positioned over a hole in a massive steel plate which is clamped in the test facility as a normal (18" x 18") specimen, and b) the transmission loss of a (similarly sized) subpanel of a stiffened specimen, the other subpanels of which are treated to obtain a high transmission loss.
- It is advised to continue testing and analysis of specimens treated with sound proofing materials. Included in the collection of treatments should be tuned dampers, and damping and absorptive materials. The transmission loss of panels made of fibrous composites and of double walled configurations should also be studied.
- The increase in sound transmission of a panel due to the presence of holes should be measured.

All flat specimens have been acquired, except for some panels made of fibrous and honeycomb materials. It should be attempted to obtain

these at no cost to the project. The collection of sound proofing materials is considerable but not inexhaustive. Care should be taken not to run out of these materials. Items that have not been acquired yet are tuned dampers. Commercial vendors manufacturing these should be contacted. After completion of the special test sections, the transmission loss of curved and slanted specimens will be measured. Completion of the construction and calibration of these sections is expected by the end of October, 1977. Concurrently with the testing of curved and slanted panels (which will possibly be continued through early spring, 1978), attention should be paid to the evaluation or development of theoretical prediction procedures. It is recommended to order specimens early, as a considerable period of lead time may be required.

Before any testing, attention should be paid to the clamping of the specimen. It has been found that high and uniform clamping forces along the panel edges are mandatory if reliable results are to be obtained. A tool recommended for this purpose is a torque-wrench.

When testing with a static pressure differential across a specimen, care should also be taken not to over-pressurize, as it has been found that permanent panel deformations can result.

Before the testing of curved and slanted specimens is started, it is recommended to repeat some measurements on panels positioned in the special test sections at an angle of ninety degrees relative to the direction of sound incidence. By comparing the results with previous data, any changes in the acoustic properties of the facility due to the presence of the additional section may be detected. The uniformity of the excitation field in the sections should be verified by measuring

sound levels at different locations relative to the surface of the specimen.

A frame will be constructed to apply in-plane forces to specimens. For financial reasons, it appears that a device will be constructed capable of inducing a uni-axial stress state only. However, the possibilities of constructing a low cost frame that is able to handle bi-axial stress states should be explored. Completion of the final frame is expected near the end of 1977. Consequently, measurement and analysis of sound transmission through initially stressed specimens cound be done during the early spring of 1978.

To maximize the time available for any theoretical work, it is recommended to develop a computer program that will take care of time consuming analysis work that should be repeated for every specimen. This program should be developed in the fall of 1977.

Finally, some time should be dedicated to the preparation of additional or follow-up research work. At this writing, it is believed that the noise research areas listed below may need attention.

1. Preliminary acoustic tests with pressure differentials across the surface of specimens have indicated that a small over-pressure inside a cabin may result in a significant interior noise reduction. Verification of these laboratory results in-flight appears desirable.
2. The influence on the interior noise of every single panel in the structure of the fuselage depends on the location of the panel. It seems worthwhile to determine the importance of every panel by consecutively exciting single panels while measuring the distribution of sound inside the cabin.

3. In flight, there are differences between the excitations of the fuselage panels. These differences may be determined by measuring mode shapes and accelerations of single panels.
4. It is possible that engine vibrations have a significant influence on in-cabin noise levels (see Chapter 4). To verify this it is necessary to measure the fluctuating forces transmitted through the engine mountings in flight.

9.2.2 Theoretical Activities

In Appendices B and C theoretical procedures are presented to analyze the effects of stiffness and pressurization on the transmission of sound through panels. In the future part of the on-going noise research project, other parameters that could influence the acoustic panel behavior will be tested extensively but should also be analyzed theoretically. It is recommended to focus this theoretical work on the vibrational characteristics of panels, as these can be directly related to its sound transmission (except in cases where sound absorption occurs). The influence of many parameters on the static and dynamic deflections of panels has been discussed in numerous publications. The following is a summary of theoretical considerations and publications recommended for the analysis of pertinent phenomena.

Effect of (base) material properties. The influence of the properties of the (base) panel on its vibrations can be determined from Equation 7.2. The flexural rigidity primarily affects the stiffness controlled oscillations while panel mass affects the mass controlled vibrations. Equations like 6.2 and 6.5 may be used to evaluate base materials, including stiffened and honeycomb panels. When analyzing the transmission of sound through stiffened panels, discussions of the

effects of non-rigid stiffeners and sub-panel resonances may be useful (References 19 and 24). The effect of material damping properties on the transmission of sound should be determined experimentally in the KU-FRL facility by observing resonant transmission loss amplitudes. Due to the complexity of equations of damped panel motion, it is not recommended to attempt to derive basic material damping properties (e.g. loss factor) from sound or plate deflection measurements.

Effect of damping treatments. Explanations of the effect of damping treatments on the total damping of a panel (e.g. laminates containing a viscoelastic layer) are presented in References 3, 13, 19, and 22. These publications give design procedures to optimize the treatment for a given panel and damping material properties. It is advised to use these methods for evaluating treatments presently used in general aviation aircraft.

Influence of absorptive materials. It is intended to measure the sound transmission loss of panels treated with absorptive blankets. Detailed theoretical discussions as presented in References 19 and 26 may be helpful for optimization of this type of treatments.

Effect of panel curvature. The effect of curvature on (finite) panel vibrations can be derived from the governing differential equations of motion as presented in Reference 24. A helpful discussion on the influence of curvature on the effective panel rigidity and stiffness controlled transmission loss can be found in Reference 20. Reference 27 gives a useful discussion on the sound transmissivity of infinite curved shells.

Influence of in-plane stresses. To analyze the effect of in-plane stresses on the sound transmission loss of panels, a theoretical approach

similar to the one presented in Appendix C (for the influence of pressurization) may be useful.

Effect of angle of sound incidence. The decrease in transmission loss of infinite plates due to a decrease in the angle of sound incidence is discussed in References 13 and 19. The vibrational behavior of finite panels may best be analyzed by solving the governing differential equation of panel motion (Equation 7.2) for the appropriate loading conditions.

Effect of holes and slits in the panel. When attempting to analyze the transmission of sound through a hole, discussions on the effects of changes in the cross-sectional areas of pipes may be useful (Reference 19). The total transmission loss of non-homogeneous panels can be derived from equations as presented in References 13 and 19.

REFERENCES

1. "Proposal to NASA for: A Research Program to Reduce Interior Noise in General Aviation Airplanes," The University of Kansas Center for Research, Inc., submitted Feburary 1976.

2. "Proposal to NASA for the continuation of: A Research Program to Reduce Interior Noise in General Aviation Airplanes," The University of Kansas Center for Research, Inc., submitted March 1977.

3. Faulkner, L. L., Handbook of Industrial Noise Control, Industrial Press, Inc., 1976.

4. Radrapatna, A. N., and I. D. Jacobson, "The Impact of Interior Cabin Noise on Passenger Acceptance," SAE Paper 760466, 1976.

5. Catherines, J. J., and W. H. Mayes, "Interior Noise Levels of Two Propeller-driven Light Aircraft," NASA TM X-72716, July 1975.

6. Catherines, J. J., and S. K. Jha, "Sources and Characteristics of Interior Noise in General Aviation Aircraft," NASA TM X-72839, April, 1976.

7. Brown D., et al., "Propeller Noise at Low Tipspeeds," AFAPL-TR 71-55, 1971.

8. Anonymous, "Hamilton Standard Generalized Propeller Noise Estimating Procedure," Revision D, 1971.

9. Rathgeber, R. K., and D. E. Sipes, "The Influence of Design Parameters on Light Propeller Aircraft Noise," SAE Paper 770444, 1977.

10. The Institution of Mechanical Engineers, "Vibration and Noise in Motor Vehicles," 1972.

11. Jha, S. K., and J. C. Catherines, "Interior Noise of a General Aviation Aircraft - Its Sources and Transmission Paths," NASA Paper, not published, 1976.

12. Ganesan, N., "Evaluation of Aircraft Internal Noise," SAE 740360, 1974.

13. Richards, E. J., and D. J. Mead, Noise and Acoustic Fatigue in Aeronautics, John Wiley & Sons Ltd., 1968.

14. Franken, P. A., et al., "Methods of Flight Vehicle Noise Prediction," WADC Technical Report 58-343, 1958.

15. Beranek, L. L., "Principles of Sound Control in Airplanes," OSRD No. 1543, 1944.

16. Wilby, J. F., "An Approach to the Prediction of Airplane Interior Noise," AIAA Paper No. 76-548, 1976.

17. Peschier, T. D., et al., "Progress Report for a Research Program to Reduce Interior Noise in General Aviation Airplanes," KU-FRL-317-2, June 1977.

18. Wolf, J. A. Jr., et al., "Structural-Acoustic Finite Element Analysis of the Automobile Passenger Compartment," General Motors Corp., Report GMR-2029R, 1975.

19. Beranek, L. L., Noise and Vibration Control, McGraw-Hill Book Co., 1971.

20. Getline, G. L., "Low Frequency Noise Reduction of Lightweight Airframe Structures," NASA CR-145104, 1976.

21. Crocker, M. J., "Noise and Vibration Control Engineering," Purdue University, 1972.

22. Ganesan, N., "Composites for Noise Control," SAE Paper 730339, 1973.

23. Henderson, T. D., "Design of an Acoustic Panel Test Facility," University of Kansas, M. E. project report, 1977.

24. Szilard, R., Theory and Analysis of Plates: Classical and Numerical Methods, Prentice-Hall, Inc., 1974.

25. Anonymous, "Compendium of Materials for Noise Control," HEW Publication No. (NIOSH) 75-165, 1975.

26. Beranek, L. L. and G. A. Work, "Sound Transmission through Multiple Structures Containing Flexible Blankets," J. Acous. Soc. Am., Vol. 21, No. 4, July, 1949.

APPENDIX A

PREDICTION OF THE FLEXURAL RIGIDITY AND RESONANCES OF A PANEL

APPENDIX A

PREDICTION OF THE FLEXURAL RIGIDITY AND RESONANCES OF A PANEL

The resonance frequencies of plates can be computed by solving the governing differential equations of motion. The equation shown below is based on the dynamic equilibrium principle (Reference A.1):

$$D\nabla^2\nabla^2 w(x,y,t) = p_z(x,y,t) - \bar{m}\frac{\partial^2 w(x,y,t)}{\partial t^2} \qquad (A.1)$$

The dynamic parameters of this system are shown in Figure A.1.

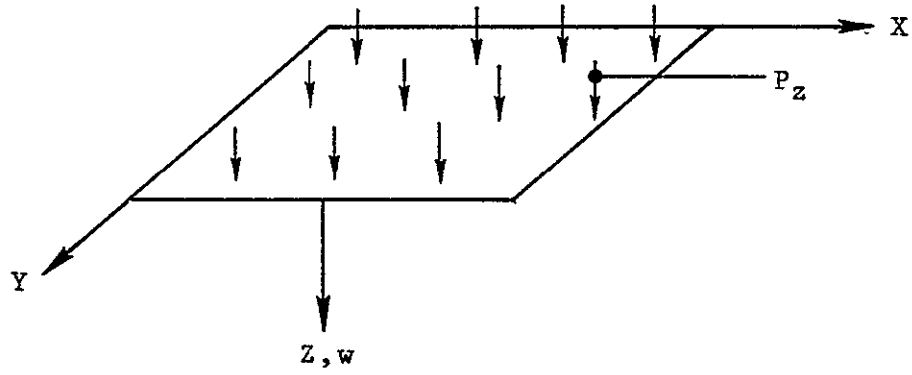

Figure A.1 Dynamic Parameters of a Vibrating Plate.

Equation A.1 describes the undamped motion of plates. Damping effects are not included, because they have usually little or no effect on the natural frequencies (Reference A.1). To find the undamped natural frequencies, the homogeneous differential equation (i.e. $p_z = 0$) needs to be solved. This solution depends on the boundary conditions. References A.1 and A.2 present solutions for many different cases (note: also derived from energy methods). Some of the results, that are useful for the KU-FRL noise research team, are presented in Table A-1. Equations for the calculation of the flexural rigidity (D) are presented in Table A.2.

Table A.1 Summary of Methods to Compute Resonance Frequencies of Rectangular Panels

Note: 1. for definition and calculation of D, D_x, . . . (flexural rigidities) see Table A.2.

2. ρ = mass density per unit area.

1) Isotropic Panels

Configuration and Boundary Conditions	Equations and Constants	Notes
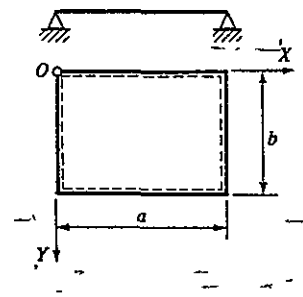	$\omega_{mn} = \pi^2\left(\frac{m^2}{a^2} + \frac{n^2}{b^2}\right)\sqrt{\frac{D}{\rho}}$ m,n = 1,2,3, . . .	First mode is ω_{11}; second ω_{12}, etc. From Ref. A.1.
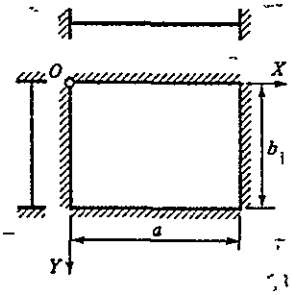	$\omega_i = \frac{\lambda_i}{b^2}\sqrt{\frac{D}{\rho}}$ b/a | λ_1 | λ_2 | λ_3 1.00 | 36.0 | 73.8 | 109.0 1.50 | 27.0 | 67.6 | 81.6 2.00 | 24.5 | 65.4 | 72.7 3.00 | 23.2 | 64.0 | 67.0	i = 1,2,3, . . . represents 1st, 2nd, 3rd, etc. modes. From Ref. A.1.
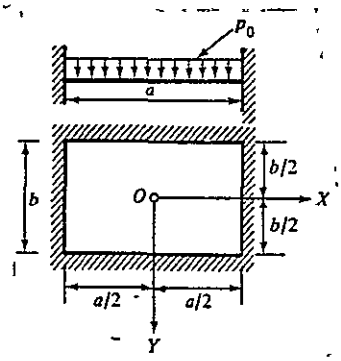	$\lambda/\pi^2 = \omega a^2/\pi^2\left(\sqrt{\rho/D}\right)$ 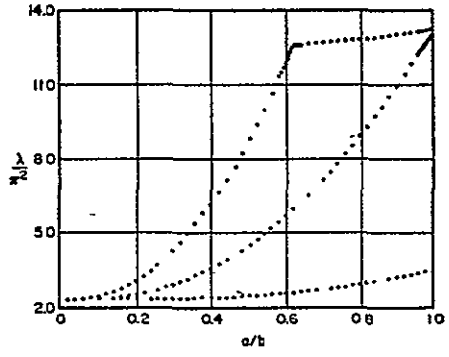	Modes symmetric about both x- and y- axes From Ref. A.2.

Table A.1 (Continued)

Configuration and Boundary Conditions	Equations and Constants	Notes
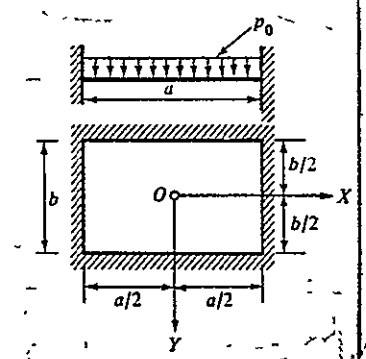	$\lambda/\pi = \omega a^2/\pi^2\left(\sqrt{\rho/D}\right)$ 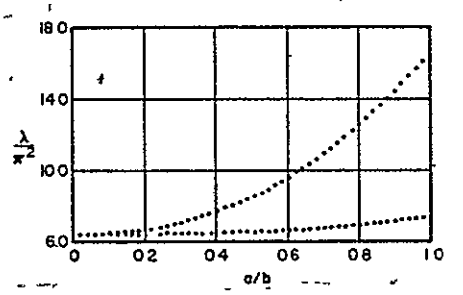	Modes antisymmetric about $\bar{x} = 0$ and symmetric about $\bar{y} = 0$. From Ref. A.2.
	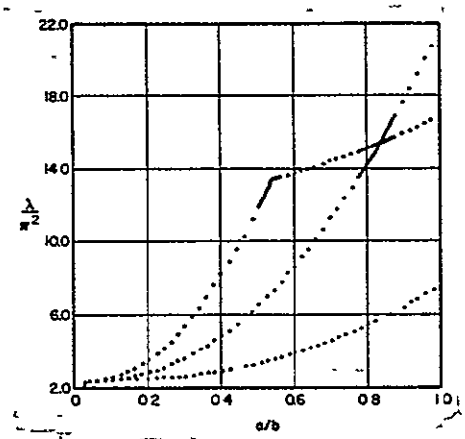	Modes symmetric about $\bar{x} = 0$ and antisymmetric about $\bar{y} = 0$. From Ref. A.2.
	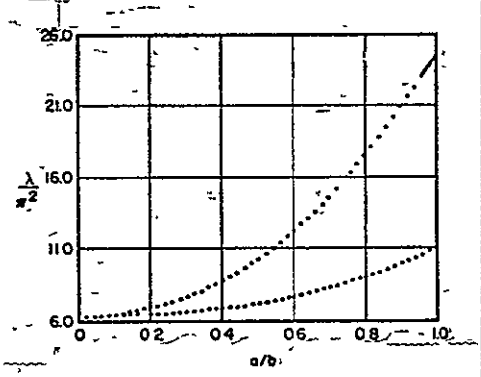	Modes antisymmetric about both x- and y-axes. From Ref. A.2.
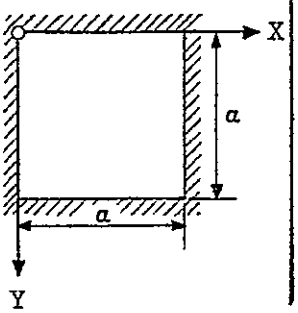	$\omega a^2\sqrt{\rho/D}$ Mean Value / Max. Error % / Mode Symmetry 36.0384 — 0.19 — Symmetric about both x and y 132.38 — 0.63 132.9 — 0.87 224.5 — 2.98 73.790 — 0.59 — Symmetric about x, antisymmetric about y 167.89 — 2.13 213.00 — 1.43 109.027 — 0.84 — Antisymmetric about both x and y 244.021 — 0.87 246.552 — 1.85	From Ref. A.2.

Table A.1 (Continued)

Configuration and Boundary Conditions	Equations and Constants	Notes
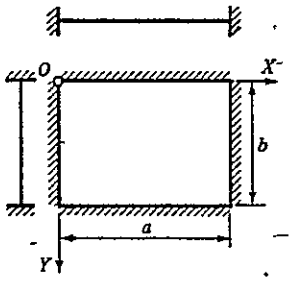	$\lambda/\pi^2 = \omega a^2/\pi^2 \left(\sqrt{\rho/D}\right)$ 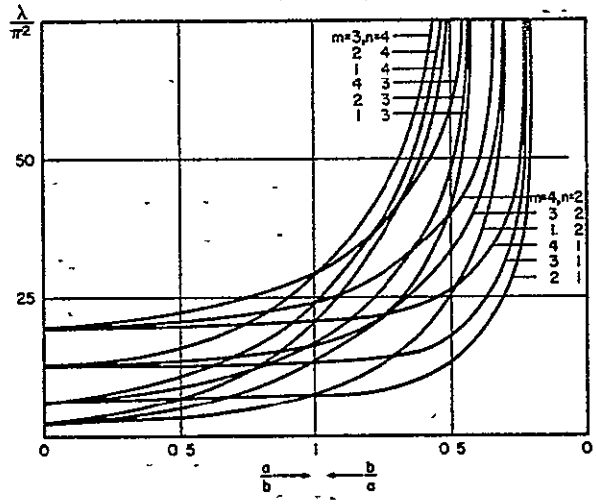	From Ref. A.2.

2) Orthotropic Panels

Configuration and Boundary Conditions	Equations and Constants
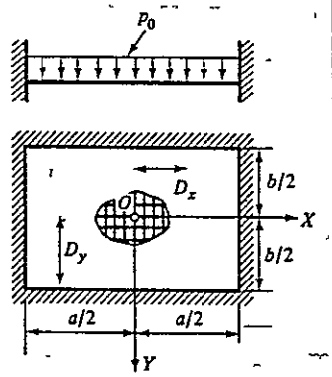	$\omega^2 = \frac{1}{\rho}\left(\frac{A^4 D_x}{a^4} + \frac{B^4 D_y}{b^4} + \frac{2C}{a^2}\frac{D_{xy}}{b^2}\right)$ Approximate

A	B	C	m	n
4.730	4.730	151.3	1	1
4.730	ε_2	$12.30\varepsilon_2(\varepsilon_2-2)$	1	1
γ_2	4.730	$12.30\gamma_2(\gamma_2-2)$	2,3,4	2,3,4
γ_2	ε_2	$\gamma_2\varepsilon_2(\gamma_2-2)(\varepsilon_2-2)$	2,3,4	2,3,4

where: $\gamma_0 = m\pi$ $\quad \varepsilon_0 = n\pi$

$\gamma_1 = \left(m + \frac{1}{4}\right)\pi$ $\quad \varepsilon_1 = \left(n + \frac{1}{4}\right)\pi$

$\gamma_2 = \left(m + \frac{1}{2}\right)\pi$ $\quad \varepsilon_2 = \left(n + \frac{1}{2}\right)\pi$

From Ref. A.2.

Table A.1 (Continued)

Configuration and Boundary Conditions	Equations and Constants	Notes
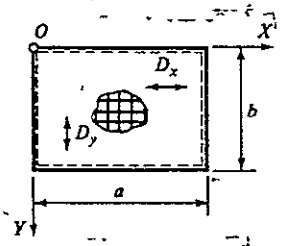	$\omega^2 = \frac{1}{\rho}\left(\frac{A^4 D_x}{a^4} + \frac{B^4 D_y}{b^4} + \frac{2C\ D_{xy}}{a^2\ b^2}\right)$ where: A: γ_0; B: ε_0; C: $\gamma_0^2 \varepsilon_0^2$; m: 1,2,3; n: 1,2,3 $\gamma_0 = m\pi$ $\quad \varepsilon_0 = n\pi$ $\gamma_1 = \left(m + \frac{1}{4}\right)\pi$ $\quad \varepsilon_1 = \left(n + \frac{1}{4}\right)\pi$ $\gamma_2 = \left(m + \frac{1}{2}\right)\pi$ $\quad \varepsilon_2 = \left(n + \frac{1}{2}\right)\pi$	Approximate From Ref. A.2.
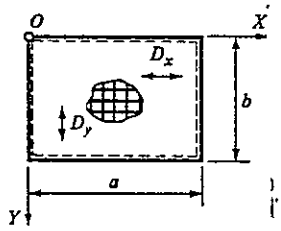	$\omega_{mn} = \frac{\pi^2}{b^2}\sqrt{\frac{D^*_{mn}}{\bar{\rho}}}$ where: $D^*_{mn} = D_x\left(\frac{mb}{a}\right)^4 + 2Bn^2\left(\frac{mb}{a}\right)^2 + D_y n^4$	Exact From Ref. A.1.

3) Stiffened Panels

Configuration and Boundary Conditions	Equations and Constants	Notes
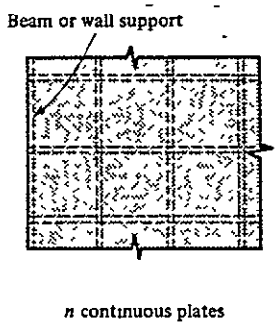	Use isotropic plate theory for plate, and beam theory for beams, including twisting. Apply continuity conditions across stiffeners (see Ref.A.1).	From Ref. A.1.

Table A.1 (Continued)

Configuration and Boundary Conditions	Equations and Constants	Notes
Beam or wall support 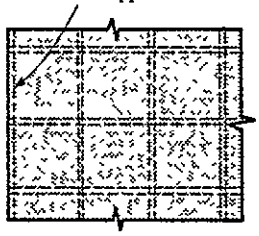 *n* continuous plates	Use orthotropic theory, even for large stiffener spacing (fairly accurate for 3 stiffeners or more- Ref. A.2.).	From Ref. A.2.
Beam or wall support 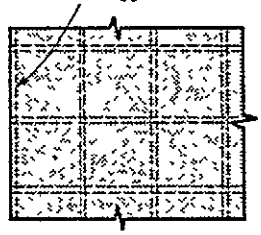 *n* continuous plates	$\omega_1 = \pi \left(\sqrt[4]{\frac{n}{\sum_{i=1}^{n} \frac{1}{f_{1i}^4}}} + \sqrt[4]{\frac{\sum_{i=1}^{n} (f_{1i}^*)^4}{n}} \right)$ For Estimating Only n = number of panels f_{1i} = first natural frequency of the ith panel assuming simple supported boundary conditions f_{1i}^* = same as above but with fixed boundaries	From Ref. A.1.

4) Panels With In-Plane Forces

Configuration and Boundary Conditions	Equations and Constants	Notes
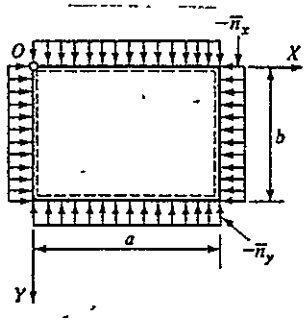	$\omega_{mn}^2 = \frac{D}{\rho}\left[\left(\frac{m\pi}{a}\right)^2 + \left(\frac{n\pi}{b}\right)^2\right]^2 + \frac{N_x}{\rho}\left(\frac{m\pi}{a}\right)^2 + \frac{N_y}{\rho}\left(\frac{n\pi}{b}\right)^2$	From Ref. A.2.

Table A.1 (Continued)

Configuration and Boundary Conditions	Equations and Constants

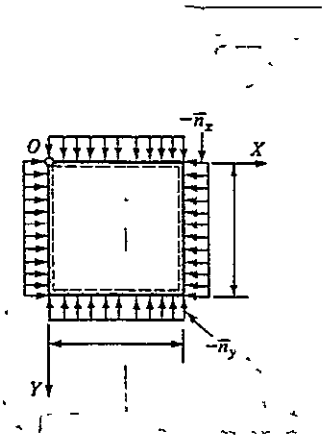

$\frac{Na^2}{\pi^2 D}$	Frequency parameters for simply supported plate		Frequency parameter $\omega a^2\sqrt{\rho/D}$ for clamped plate	
	$\omega_{11}a^2\sqrt{\rho/D}$	$\omega_{12}a^2\sqrt{\rho/D}$	Lower Bound	Upper Bound
5	36.928	69.788	49.580	49.847
10	48.350	85.473	59.922	60.392
15	57.549	98.696	68.580	69.271
20	65.467	110.340	76.124	77.088
30	78.960	130.560	89.268	90.656
50	100.650	163.670	110.600	112.900
100	140.960	226.140	148.260	154.980
200	198.380	315.980	207.790	215.690

From Ref. A.2.

5) Curved Panels

Configuration and Boundary Conditions	Equations and Constants	Notes

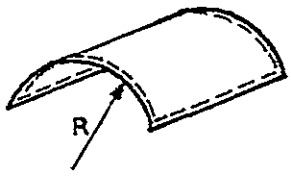

$$f_{mn}^2 = \frac{Em^4}{4\pi^2\rho R^2\left[m^2 + n^2(a/b)^2\right]^2} + f_{mn_{flat}}^2$$

From Ref. A.3.

Table A.1 (Continued)

6) Multi-layered Panels

Configuration and Boundary Conditions	Equations and Constants	Notes
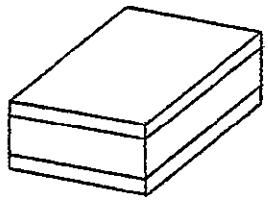	Calculate D or D_x, D_y, ...	From Ref. A.1.
	Then: use equations for isotropic or orthotropic panels (Table A.1: 1 & 2).	If core is compressible dilational resonances will occur. For calculation of these: see Ref. A.3.

Table A.2 Summary of Methods to Compute Panel Flexural Rigidity

1. Isotropic Materials (Reference A.1)

$$D = \frac{Eh^3}{12(1 - \nu^2)} \quad (Nm)$$

where: E = Young's modulus (N/m^2)

h = plate thickness (m)

ν = Poisson's ratio

2. Orthotropic Materials (References A.1 and A.2)

$$D_x = \frac{E_x h^3}{12(1 - \nu_x \nu_y)} \quad (Nm)$$

$$D_y = \frac{E_y h^3}{12(1 - \nu_x \nu_y)} \quad (Nm)$$

$$D_{xy} = D_x \nu_y + 2D_t \quad (Nm)$$

$$D_t = \frac{G_{xy} h^3}{12} \quad (Nm)$$

where: indices x and y denote properties with respect to x and y axis respectively

G_{xy} = shear modulus (N/m^2)

3. Stiffened Plates - Stiffeners in Y-direction (Reference A.3)

$$D_x = D_{plate} \quad (Nm)$$

$$D_y = D_{plate} + \frac{EI_y}{b} \quad (Nm)$$

where: I_y/b = running moment of inertia of stiffeners along Y-axis (m^3)

4. Multi-layered Materials (Reference A.1)

$$D = \frac{AC - B^2}{A} \quad (Nm)$$

Table A.2 (Continued)

where: $A = \sum_k \frac{E_k}{1 - \nu_k^2} (z_k - z_{k-1})$

$$B = \sum_k \frac{E_k}{1 - \nu_k^2} \frac{(z_k - z_{k-1})^2}{2}$$

$$C = \sum_k \frac{E_k}{1 - \nu_k^2} \frac{z_k^3 - z_{k-1}^3}{3}$$

z_k = distance between k^{th} layer and surface of laminate (m)

5. Three Ply Laminates (Reference A.1)

$$D = \frac{Eh_f h^2}{2(1 - \nu^2)} \text{ (Nm)}$$

where: E = Young's modulus of faces (N/m^2)

ν = Poisson's ratio of faces

h_f = thickness of faces (m)

h = thickness of laminate (m)

REFERENCES

A.1 Szilard, R., Theory and Analysis of Plates: Classical and Numerical Methods, Prentice-Hall, Inc., 1974.

A.2 Leissa, A. W., "Vibration of Plates," NASA SP-160, 1969.

A.3 Getline, G. L., "Low-Frequency Noise Reduction of Lightweight Airframe Structures," NASA CR-145104, 1976.

APPENDIX B

AN EQUATION FOR THE PREDICTION OF TRANSMISSION LOSS IN THE STIFFNESS CONTROLLED FREQUENCY REGION

APPENDIX B

AN EQUATION FOR THE PREDICTION OF TRANSMISSION LOSS IN THE STIFFNESS CONTROLLED FREQUENCY REGION

Existing equations for the prediction of the transmission of sound through panels in their stiffness controlled frequency region (i.e., below the fundamental frequency) do not yield satisfactory results. The results of an equation given in Reference B.1 are shown in Figure B.1 together with measured data. Therefore, this Appendix will present a more accurate relationship based on three assumptions:

1. The fundamental mode shape of the panel completely determines the deflection of the panel below its fundamental frequency. Consequently, this deflection can be written as follows (Reference B.2):

$$w(x, y, t) = W_{11} \sin \frac{\pi x}{a} \sin \frac{\pi y}{b} \sin \omega t \quad (m) \tag{B.1}$$

where: $$W_{11} = \frac{16\, p_{max}/\pi^2}{\overline{m}(\omega_{11}^2 - \omega^2)} \quad (m)$$

p_{max} = amplitude of forcing sound pressure (N/m^2)

2. The sound radiation mechanism of this oscillating plate is similar to the one of a piston (i.e., all points of the surface vibrate in-phase). As a result, the sound power is proportional to the plate area and the mean-square velocity of its center.

$$W_A \doteq V^2_{rms_{\text{plate center}}} \; S \quad \text{(Watt)} \tag{B.2}$$

3. A plane wave is radiated by the panel. Consequently, the sound pressure behind the panel can be expressed as follows:

$$p_{rms}^2 \doteq W_A/S \qquad (N^2/m^4) \qquad (B.3)$$

Combining equations B.1, B.2 and B.3 yields:

$$p_{rms} \doteq \frac{\omega}{\sqrt{2}} \frac{4\, p_{max}}{\overline{m}(\omega_{11}^2 - \omega^2)\pi^2} \qquad (N/m^2) \qquad (B.4)$$

This equation can be substituted into equation 7.3. The result will be:

$$TL = 20 \log \frac{\overline{m}|(f_{11}^2 - f^2)|}{f} + K \qquad (dB) \qquad (B.5)$$

The constant K accounts for the following inaccuracies: 1) the actual panel deflection will not be identical to the fundamental mode shape, 2) the radiated sound power is proportional to a panel surface velocity smaller than the maximum velocity, and 3) the sound wave radiated by the panel is not exactly plane.

The magnitude of K can be determined from experimental results. From preliminary KU-FRL data, it was found that K = -39 is a close approximation.

The accuracy of this prediction method is illustrated in Figure B.1. Shown are measured data, the predictions of Reference B.1, and the results of Equation B.5. Included is a region of frequencies slightly higher than the fundamental resonance frequency of the panel. It is believed that Equation B.5 can yield reasonably accurate results at these frequencies,

as the deflection shape of the panel still closely resembles its fundamental mode shape.

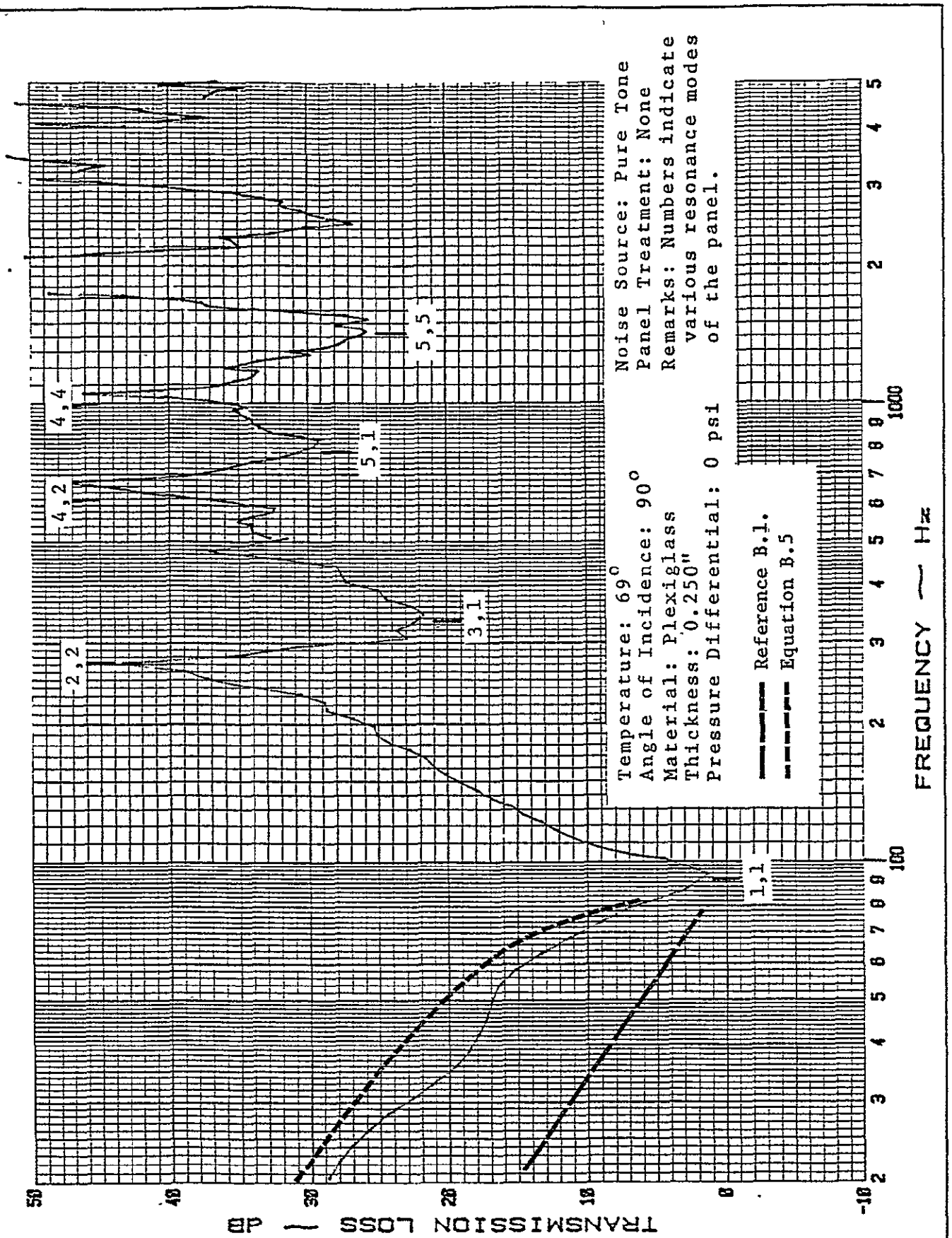

CALC			REVISED	DATE
CHECK				
APPD				
APPD				

Figure B.1. Sound Transmission Loss Characteristics of a 0.250" Thick Plexiglass Panel of 18" x 18" under Standard Conditions.

UNIVERSITY OF KANSAS

REFERENCES

B.1 Franken, P. A., et al., "Methods of Flight Vehicle Noise Prediction," WADC Technical Report 58-343, 1958.

B.2 Szilard, R., Theory and Analysis of Plates: Classical and Numerical Methods, Prentice-Hall, Inc., 1974.

APPENDIX C

THE INFLUENCE OF PRESSURIZATION ON PANEL VIBRATIONS AND SOUND TRANSMISSION

APPENDIX C

THE INFLUENCE OF PRESSURIZATION ON PANEL VIBRATIONS AND SOUND TRANSMISSION

Several methods are available to compute the vibrations of a panel subjected to an acoustic excitation. To include the effect of a pressure differential across the panel appears to be harder. The plate theory is based on the assumption that plates have flexural rigidity only. It predicts a static plate deflection due to the pressure differential across the panel plus an unchanged vibrational motion (i.e., equal to unpressurized case). Consequently, it does not predict an increase in the effective stiffness of the panel.

The equation that is being used in this Appendix is the one for simultaneous bending and stretching of a panel. It is assumed that the pressure differential across the panel will result in an internal membrane stress (σ), which is constant throughout the plate. This assumption is not exact. Reference C.1 shows that σ is a function of the location on the plate. The maximum value of σ is:

$$\sigma_{max} = C\left[E\left(\frac{\Delta p\ a}{t}\right)^2\right]^{1/3} \quad (N/m^2) \qquad (C.1)$$

where

C = constant given in Reference C.1

Δp = pressure differential (N/m^2)

a = longest dimension of the panel (m)

t = thickness of the panel (m)

E = Young's modulus (N/m^2)

Assuming a constant normal stress throughout the panel, the equation of motion becomes (Reference C.2):

$$D\nabla^4 w = p_z + N\nabla^2 w - \bar{m}\frac{\partial^2 w}{\partial t^2} \qquad (C.2)$$

where

$w = w(x, y, t)$ = deflection of panel (m)

$p_z = p_z(x, y, t)$ = acoustic excitation = $p_{max} \sin\omega t$ (N/m^2)

N = internal membrane force per unit length = $\sigma x t$ (N/m)

The solution of equation C.2 for a panel with simply supported edges can be found using Fourier series expansions. The result is:

$$w(x, y, t) = \sin\omega t \sum_{mn}\sum W_{mn} \sin\frac{m\pi x}{a} \sin\frac{n\pi y}{b} \quad (m) \qquad (C.3)$$

where

$$W_{mn} = \frac{16\ p_{max}/\pi^2 mn}{D\left[\left(\frac{m\pi}{a}\right)^2 + \left(\frac{n\pi}{b}\right)^2\right]^2 - \bar{m}\,\omega^2 + N\left[\left(\frac{m\pi}{a}\right)^2 + \left(\frac{n\pi}{b}\right)^2\right]} \quad (m)$$

$m, n = 1, 3, 5, \ldots\ldots$

By assuming $p_z = 0$ in equation C.2, the resonance frequencies of the panel can be found:

$$\omega_{m,n} = \pi\sqrt{\frac{D}{\bar{m}}}\sqrt{\pi^2\left\{\left(\frac{m}{a}\right)^2 + \left(\frac{n}{b}\right)^2\right\}^2 + \frac{N}{D}\left\{\left(\frac{m}{a}\right)^2 + \left(\frac{n}{b}\right)^2\right\}} \quad (rad/sec) \qquad (C.4)$$

Combining equations C.3 and C.4 yields:

$$W_{mn} = \frac{16\ p_{max}/\pi^2 mn}{\bar{m}(\omega_{mn}^2 - \omega^2)} \quad (m) \qquad (C.5)$$

This expression is identical to the one for the unpressurized case. However, the values of ω_{mn} are higher in the pressurized case (equation C.4).

Consequently, the equation derived in Appendix B for the computation of the sound transmission loss below the fundamental frequency of the panel should also be valid in the cases where pressurization is applied. That this is true can be seen from Figure C.1. Equation B.5 and the measured fundamental frequency (Figure C.1) have been used to predict the transmission loss in the stiffness controlled region. The proximity of the measured and predicted curves, seems to indicate the validity of Equation C.5.

The relationship between N and Δp has to be derived from experiments. An expression similar to Equation C.1 is suggested:

$$N = K \times t \times \left[E\left(\frac{\Delta p \times a}{t}\right)^2\right]^{1/3} \quad (N/m) \qquad (C.1\text{-}b)$$

At the moment of writing this report, not enough test data were available to evaluate this expression.

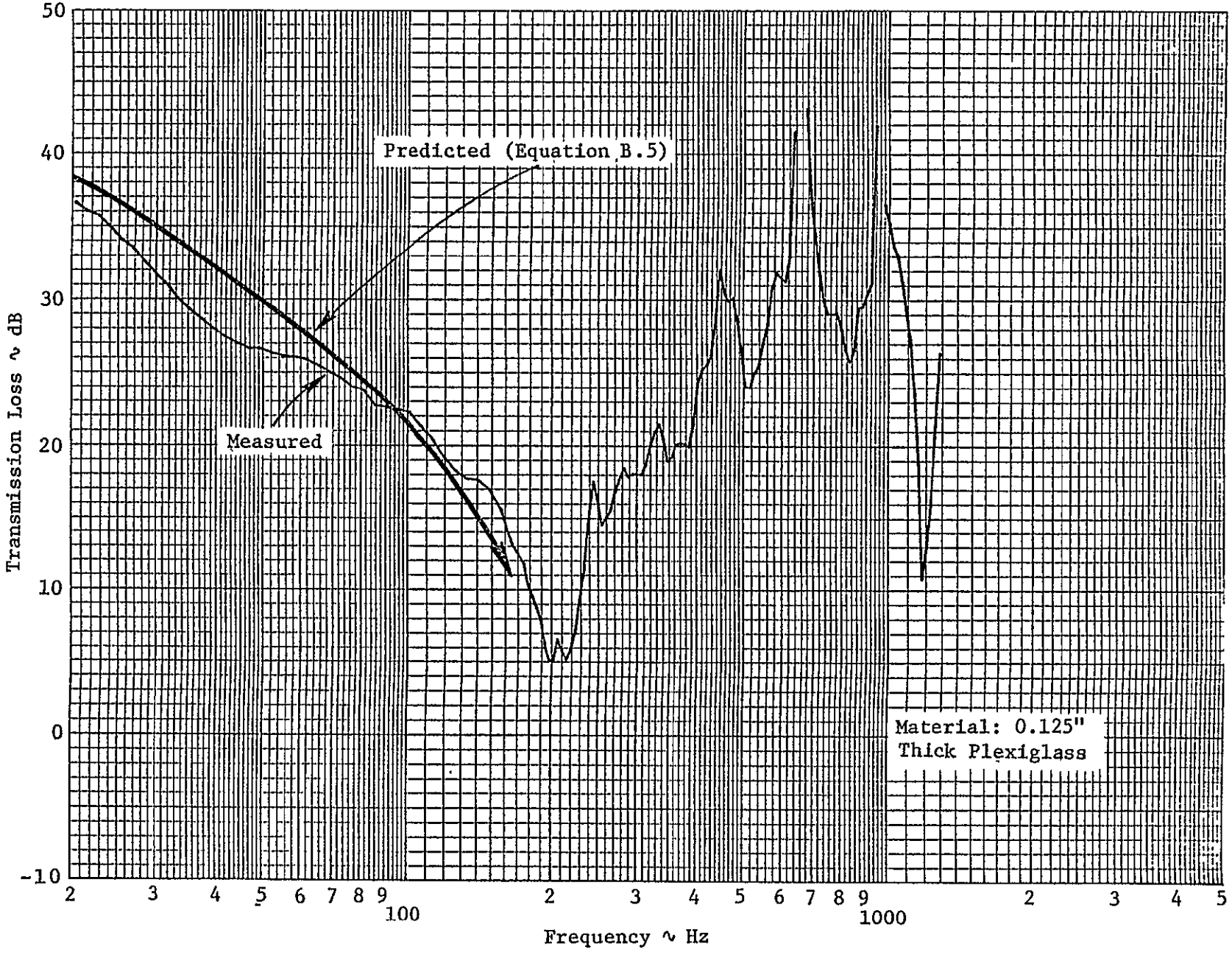

Figure C.1. Comparison between Measured and Predicted Sound Transmission Characteristics for a Pressurized Panel.

	CALC	CHECK	APPD	DATE
				REVISED

UNIVERSITY OF KANSAS

REFERENCES

C.1 Bruhn, E. F., Analysis and Design of Flight Vehicle Structures, Tri-State Offset Co., 1973.

C.2 Szilard, R., Theory and Analysis of Plates: Classicial and Numerical Methods, Prentice-Hall, Inc., 1974.

APPENDIX D

COMPILATION OF RECOMMENDED CALIBRATION, TEST AND DATA REDUCTION PROCEDURES

APPENDIX D

COMPILATION OF RECOMMENDED CALIBRATION, TEST AND DATA REDUCTION PROCEDURES

This Appendix presents recommended calibration, test and data reduction procedures, intended to (1) facilitate research work, (2) assure reliable experimental results and (3) prevent possible damage to electronic equipment. The procedures outlined here are based on equipment handbooks, conversations with electronic experts and experiences of the noise research team. The recommendations concern research work being conducted at the time of this writing (August 1977). Any changes or additions to the current scope will require new or modified recommendations.

The following procedures are included:

1. Calibration of the SD-335 Analyzer Scope
   X-axis
   Y-axis
2. Analyzer, Sweep Oscillator and X-Y Plotter Scaling and Calibration
3. Panel Test Procedures
   A. Using Sweep Oscillator
   B. Using White Noise
   C. Using Recorded Actual Aircraft Noise
4. Manual of HP-9825A Computer Program for Reducing Test Data

Also included are the following items:

5. Example of a Specimen Log Sheet
6. Example of a Test Log Sheet

1. Calibration of the SD-335 Analyzer Scope

X-Axis Calibration

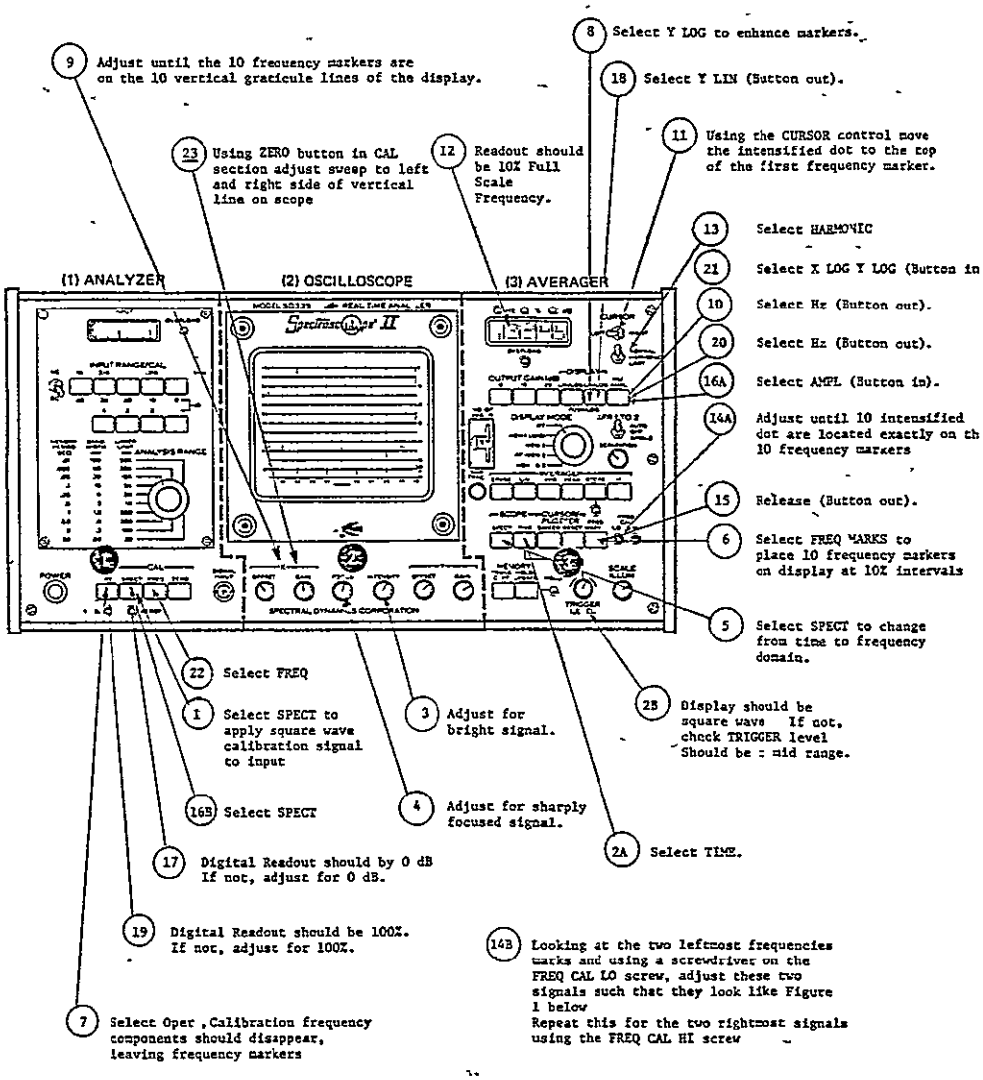

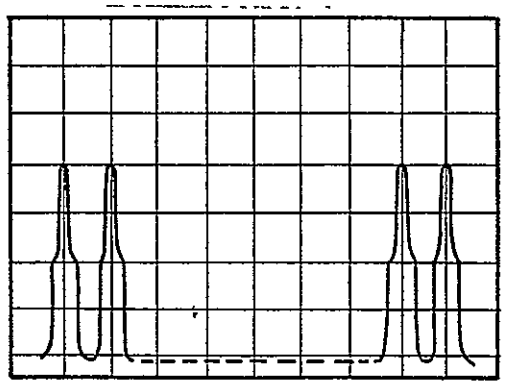

Figure D.1 Frequency marks after adjustment.

Y-Axis Calibration

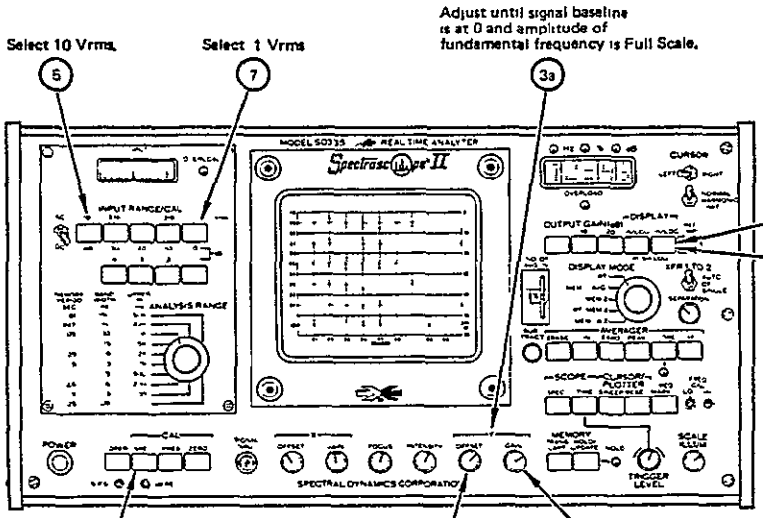

3b * Lin Scale

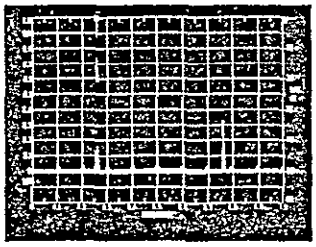

Repeat steps 5, 6, 7 AND 8 until the fundamental is at −40 dB and 0 dB, and there is no interaction between steps

9a

9b † Log Scale.

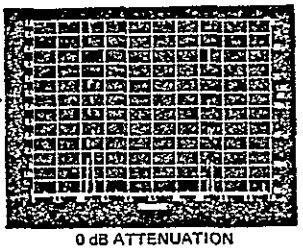

0 dB ATTENUATION

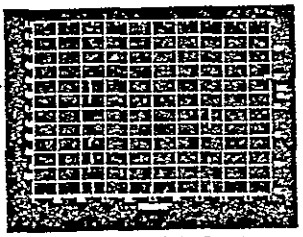

20 dB ATTENUATION

10

Select 0, 10, 20, 30 dB
Fundamental should drop 2 divisions each time the calibration signal is attenuated by an additional 10 dB

* Check this full scale to zero calibration by momentarily pushing in and releasing the CAL ZERO button When the ZERO button is pressed, only a baseline should be visible on the scope When the ZERO button is out, the calibration signal should be full scale

† The voltage of the input calibration signal is adjusted so that the amplitude of the fundamental frequency of the square wave is 100 mVrms The third harmonic (viewed at 76 8% of full scale) is always approximately 10 dB down from the fundamental when viewing the Y-axis data on a log scale

2. Analyzer, Sweep Oscillator and X-Y Recorder Scaling and Calibration

First: Turn on all equipment (except Crown power amplifier) and let it warm up for approximately 1 minute.

Setting Up

1. Attach clean sheet lin-log paper, left edge against black post, using "Chart Hold" switch. Freq. axis should be horizontal (left to right).

2. Real Time Analyzer settings should be:

Input Range	.1 V_{RMS}
Analysis Range	5K
"CAL" Group	"OPER" button in
Switch under Cursor Switch	Normal
Output Gain	0 dB
Display	X log (in), Y log (in)
Hz/AMPL	Hz (button out)
Display Mode	RT
XFR 1 to 2	Off
Averager	(setting not important here)
"Scope"	"SPECT" button in
Cursor/Plotter	(All buttons out)

3. Sweep Oscillator Settings:

Multiplier (A)	1
Multiplier (B)	10
Sweep Rate	(setting not important here)
Sweep Control	"LINEAR SWEEP", "SINGLE"
Function	Sine Wave (~)
Sweep Buttons	push "RESET DOWN" button

4. X-Y Recorder Settings:

	X	Y
Polarity	+ RT	+ UP
Response	SLOW	SLOW
Range	.5 V/IN	.5 V/IN
Line	ON	
Chart	HOLD	
Servo	STAND BY	
Pen	LIFT	

5. Connect Output of Sweep Oscillator (coaxial cable, shield grounded) to "SIGNAL INPUT" of Analyzer.

6. Press "FREQ" button ("CAL" section).

7. Adjust "X-OFFSET" and "X-GAIN" until beginning of green line on scope coincides with "0" on frequency scale, and end of line with "1.0".

8. Press "SPECT" button ("CAL" section).

9. Adjust "Y-OFFSET" and "Y-GAIN" until top of vertical line on scope coincides with "1.0" on vertical scale, and bottom (horizontal line) with "0".

10. Press "OPER" button.

Adjustment of Sweep Oscillator Limits

11. Set Analyzer cursor to 10 Hz (digital readout).

12. Press X Lin (button out) (Analyzer).

13. Adjust "LOWER SWEEP LIMIT" on Sweep Oscillator (using screw driver) until test signal (10 Hz) peak on Analyzer scope coincides with cursor dot.

14. Press X Log (Button in) (Analyzer).

15. Set Analyzer cursor to 5000 Hz (digital readout).

16. Press "RESET UP" button on Sweep Oscillator.

17. Adjust "UPPER SWEEP LIMIT" on Sweep Oscillator until test signal peak on Analyzer scope coincides with cursor dot.

18. Press "RESET DOWN" button on Sweep Oscillator.

Frequency Adjustment X-Y Plotter

19. Set cursor to 500 Hz.

20. Be sure plotter pen in inserted; remove cap from pen.

21. Turn X-Y Plotter servo switch "ON".

22. Move Sweep Oscillator control knob from "LINEAR SWEEP, SINGLE" to "MAN".

23. Adjust "FREQ ADJ" control on Sweep Oscillator until test signal peak on analyzer scope coincides with cursor dot. This will move X-Y plotter pen into grid area of graph paper.

24. Adjust "ZERO" knob in "X" section of plotter controls until pen makes a dot on the 500 Hz line of lin-log graph paper. To check dot location, move "PEN" switch on plotter to "RECORD", then return switch to "LIFT" position. Turn servo switch off.

25. Set Analyzer cursor to 5000 Hz.

26. Turn X-Y plotter servo switch "ON".

27. Pen should now make a dot on the 5000 Hz line on graph paper when "PEN" switch is momentarily moved to "RECORD". If necessary, adjust pen position with the "CAL" knob on Recorder's X "RANGE" control.

28. Move cursor (on Analyzer) to 500 Hz. Recorder pen should move to 500 Hz line. Check pen's exact position by switching pen control to "RECORD". If necessary, adjust pen position with X "ZERO" knob (located on the recorder).

29. Repeat steps 21 and 27 until pen position is correct at both 500 and 5000 Hz.

Amplitude Adjustment of X-Y Plotter

30. Connect microphone power supply output with analyzer input.

31. Determine sound pressure level of piston phone by subtracting atmospheric correction (gauge) from specified reference value (= 124 dB).

32. Connect piston phone to source or receiver microphone.

33. Move the intensified dot in the scope, using the "CURSOR", to the peak of the calibration signal.

34. Energize plotter servo. Plotter pen will move to peak of calibration signal.

35. Adjust Plotter Y - "GAIN" knob such that pen moves to cal. level on a predetermined vertical scale.

36. Press 20 dB "INPUT RANGE/CAL" button on Analyzer.

37. Adjust Plotter Y - "ZERO" knob such that pen moves to cal. level - 20 dB on predetermined vertical scale.

38. Press 0 dB "INPUT RANGE/CAL" button on Analyzer.

39. Repeat steps 34 thru 37 until pen position is correct at both cal. level and cal. level - 20 dB.

3. Panel Test Procedures

A) Using Sweep Oscillator

1. Switch equipment on (except Crown amplifier) and let it warm up for approximately 1 minute. Check equalizer setting.

2. Calibrate Analyzer, set limits of Sweep Oscillator (10-5000 Hz) and scale X-Y Plotter as described in sections 1 and 2.

3. Install panel. Adjust clamps.

4. Connect output Microphone Power Supply with input Anlayzer, and output Sweep Oscillator with input Equalizer.

5. Set equalizer gain to 0 dB, Sweep Oscillator level to 4-5.

6. Set "SWEEP RATE" (Sweep Oscillator) to 30 Hz/sec.

7. Set "ANALYSIS RANGE" knob (Analyzer) to 5K.

8. If small panel TL values are expected: press 0 dB "INPUT RANGE/CAL" knob (Analyzer). For high TL values: use 10 dB attenuation.

9. Set knob on Microphone Power Supply such that source microphone will be analyzed.

10. Switch on Crown amplifier. Set level knob half way.

11. Increase output level of Sweep Oscillator such that VU-meter of Equalizer will not indicate an overload at any frequency. Use "RESET-UP" and "RESET-DOWN" buttons (Sweep Oscillator) to check complete frequency range.

13. Press "RESET-DOWN" button (Sweep Oscillator).

14. Turn "DISPLAY MODE" knob to: "MEM 1".

15. Press consecutively: "STORE"

"ERASE"
"PEAK"

(Analyzer)

16. Press "SWEEP-UP" (Sweep Oscillator).

17. When sweep is completed: Press consecutively:

"STORE"	(Analyzer)
"RESET"	(Analyzer)
"SPECT" ("SCOPE")	(Analyzer)

18. Using "CURSOR", move intensified dot to 500 Hz (Analyzer).

19. Energize plotter servo, and press: "SWEEP" (Analyzer).

20. When plot is completed: de-energize plotter servo.

21. Change Microphone Power Supply knob to analyze receiver microphone.

22. Press 0 dB "INPUT RANGE/CAL" knob (Analyzer).

23. If moderate panel TL values are expected: press 0 dB "OUTPUT GAIN" button (Analyzer). For high values use 10 dB gain. For very high values use 20 dB gain. (Be sure not to overload Analyzer).

24. Press consecutively: "STORE"
"ERASE"
"PEAK"

(Analyzer)

25. Press "SWEEP-UP" (Sweep Oscillator).

26. When sweep is completed: Press consecutively:

"STORE"	(Analyzer)
"RESET"	(Analyzer)
"SPECT ("SCOPE")	(Analyzer)

27. Using "CURSOR", move intensified dot to 500 Hz (Analyzer).

28. Press 0 dB "OUTPUT GAIN" button (Analyzer).

29. Repeat steps 19 and 20.

30. Set "ANALYSIS RANGE" button (Analyzer) to 500.

31. Change "SWEEP RATE" to 5 Hz/sec. (Sweep Oscillator).

32. Press consecutively: "STORE"
"ERASE"
"PEAK"
(Analyzer)

33. Press "SWEEP-UP" (Sweep Oscillator).

34. When sweep is completed: Press consecutively:

"STORE"	(Analyzer)
"RESET"	(Analyzer)
"SPECT" ("SCOPE")	(Analyzer)

35. Using "CURSOR", move intensified dot to 50 Hz.

36. Energize plotter servo and using the "ZERO" knob in the "X" section of the recorder controls adjust until the pen makes a dot on the 50 Hz line of the lin-log graph paper. To check dot location, move "PEN" switch on plotter to "RECORD", then return switch to "LIFT" position. Move "CURSOR" to 20 Hz.

37. Energize plotter servo, and press: "SWEEP" (Analyzer).

38. When plot is completed: de-energize plotter servo.

39. Change Microphone Power Supply knob to analyze source microphone.

40. Press "INPUT RANGE/CAL" button to the setting used for the 500-5000 range analysis.

41. Press consecutively: "STORE"
"ERASE"
"PEAK"

(Analyzer)

42. Press "SWEEP-UP" (Sweep Oscillator).

43. When sweep is completed: Press consecutively:

"STORE"	(Analyzer)
"RESET"	(Analyzer)
"SPECT"(SCOPE")	(Analyzer)

44. Using "CURSOR", move intensified dot to 20 Hz.

45. Press 0 dB "OUTPUT GAIN" button (Analyzer).

46. Energize plotter servo, and press: "SWEEP" (Analyzer).

47. When plot is completed: de-energize plotter servo.

48. Using "CURSOR", move intensified dot to 500 Hz.

49. Energize plotter servo and using "ZERO" knob in the "X" section of the plotter controls adjust until pen makes a dot on the 500 Hz line of the lin-log graph paper. To check dot location, move "PEN" switch on plotter to "RECORD", then return switch to "LIFT" position.

50. Change "SWEEP RATE" to 30 Hz/sec. (Sweep Oscillator)

51. To test another panel repeat steps 7-49.

B) Using White Noise

1. Switch equipment on (except Crown amplifier) and let it warm up for approximately 1 minute.

2. Calibrate Analyzer and Scale X-Y plotter as described in sections 1 and 2.

3. Install panel. Adjust clamps.

4. Connect output of White Noise generator to the input of the equalizer and output of Microphone Power Supply to the input of the Analyzer.

5. Set equalizer gain to 0 dB, White Noise generator to 1 volt.

6. Set knob on Microphone Power Supply such that the source microphone will be analyzed.

7. Set "ANALYSIS RANGE" knob (Analyzer) to 5K.

8. Switch on Crown amplifier. Increase level to get a high signal (but no overload) on the Analyzer's scope.

   If greater signal strength is needed : increase, in order, the controls up to the stated values.

   a) Increase White Noise generator up to 2 volts,

   b) Increase equalizer gain up to +15 dB,

   c) Increase White Noise generator up to 3 volts.

9. Turn "DISPLAY MODE" knob to "MEM 1" (Analyzer).

10. Select the number of averages to be taken (normally 256).

11. Press consecutively: "STORE"
    "ERASE"
    "LIN"
    (Analyzer).

12. When red light below "STORE" button lights analysis is complete: press consecutively:

"STORE"	(Analyzer)
"RESET"	(Analyzer)
"SPECT"	(Analyzer)

13. Using "CURSOR", move intensified dot to 20 Hz.

14. Energize plotter servo, and press: "SWEEP" (Analyzer).

15. When plot is completed: de-energize plotter servo.

16. Change Microphone Power Supply knob to analyze receiver microphone.

17. If moderate TL values are expected: press 0 dB "OUTPUT GAIN" button (Analyzer). For higher values use 10 dB gain. For very high values use 20 dB gain. (Be sure not to overload Analyzer).

18. Repeat steps 9-13.

19. Press 0 dB "OUTPUT GAIN" (Analyzer).

20. Energize plotter servo, and press: "SWEEP" (Analyzer).

21. When plot is completed: de-energize plotter servo.

22. To test another panel repeat steps 6-21.

C) Using Recorded Actual Aircraft Noise

C.1 Use of Nagra Recorder

1. Check batteries of Recorder

2. Load tape onto Recorder

3. Select proper speed (usually 7.5 ips)

4. Settings for playback:

   "LINE&PHONES" on: TAPE

   "◁◁◁ ▷▷▷" switch in: middle

   Channel selector on: 1

   Pinch-wheel controlling level: backwards (see Figure D.2 below)

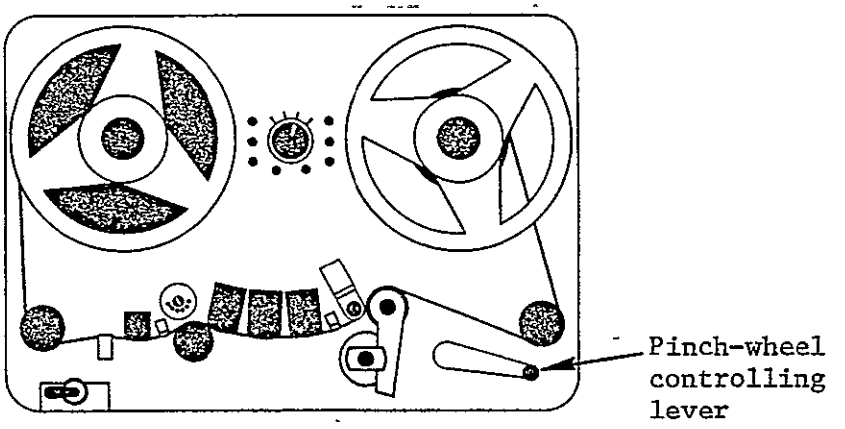

Figure D.2 Top View of Nagra IV Recorder

   Tape head cover: closed

   Function selector knob on: "PLAYBACK"

5. Settings for (fast) rewind:

   "◁◁◁ ▷▷▷" switch to: left

   Pinch-wheel controlling lever: forward

   Tape head cover: open

   Function selector knob on: "PLAYBACK"

C.2 Calibration of Equipment

1. Switch on Analyzer, Microphone Power Supply, Equalizer.

2. Connect output of channel 1 (Recorder) to input of Analyzer.

3. Play back the recording of actual noise and write down the Recorder input attenuation specified in the explanation recorded on tape just before the noise recording.

4. Check for Analyzer overloads and adjust Analyzer input attenuation accordingly.

5. Rewind tape.

6. Play back recorded signal and analyze and (linearly) average signal with Analyzer.

7. Transfer analyzed signal to "MEM-2."

8. Connect output of channel 1 (Recorder) with input of Equalizer.

9. Connect output of Microphone Power Supply with input of Analyzer.

10. Set Power Supply switch so as to analyze source microphone.

11. Install a panel and close tube.

12. Switch on Power Amplifier (volume half way).

13. Rewind tape.

14. Play back recorded signal and analyze and (linearly) average signal with analyzer.

15. Compare signals in "MEM 1 & 2."

16. Adjust Equalizer settings to minimize differences between signals in "MEM 1 & 2."

17. Repeat steps 13 through 16 till differences between the two signals have been minimized.

18. Rewind tape to its beginning, where calibration signal is recorded.

19. Play back explanation on tape just before calibration signal and write down the specified Recorder input attenuation setting (during calibration signal).

20. Compute difference between Recorder input attenuations during calibration and actual noise signals.

21. Play back calibration signal and analyze and average (linearly) signal with analyzer.

22. Energize plotter and adjust "Y-ZERO" knob so that pen moves to a level on the graph paper equal to the calibration level corrected for the difference computed in step 20.

C.3 Testing of Panels

1. Rewind tape.

2. Play back noise recording and analyze and (linearly) average signal with Analyzer.

3. Plot result on graph paper using X-Y Plotter.

4. Rewind tape.

5. Change setting of Microphone Power Supply knob to analyze receiver microphone signal.

6. Repeat steps 2 and 3.

4. Manual of HP-9825A Computer Program for Reducing Test Data

1. Turn on calculator and plotter. Switches are located on right and front sides respectively.

2. Insert tape cartridge, label side towards rear of calculator.

3. Type in: trk1;ldf240 and press 'EXECUTE' button. The program, contained on file 240 of track one, is now loaded in calculator memory. The cartridge may be removed.

4. Press 'CHART LOAD' button on plotter. Plotter arm will move to upper right hand corner.

5. Press '4' button on plotter. The arm will pick up the number 4 pen and return to upper right hand corner.

6. If number 4 "pen" is not the sight glass (cursor), then carefully remove the pen from the plotter arm and install the sight glass in the arm. Cap the pen removed.

7. Place raw data plot of source and receiver sound levels in lower left corner of plotter. Press 'CHART HOLD' button and smooth paper. If edges of graph are not parallel to horizontal motion of sight glass/plotter arm (check this by operating the ↑, ↓, →, ← buttons), press 'CHART LOAD,' straighten paper and press 'CHART HOLD' again.

8. Press 'P1' button on plotter. Plotter arm will move to lower left corner.

9. Use the 4-direction buttons (those labeled ↑, →, ↓, ←) to center the sight glass on the intersection point of the botton horizontal grid line (usually 70 dB) and the 20 Hz line. When sight glass is centered hold down the 'ENTER' button while pressing 'P1.' (Both these buttons are on the plotter.)

10. Use the 4-direction buttons to center the sight glass on the intersection of the top grid line (usually 140 dB) and the 500 Hz line. When sight glass is centered, hold down the 'ENTER' button and press 'P2.'

11. Press 'RUN' on calculator.

12. "graph number" will appear on calculator display. Type in the appropriate digit(s) (no letters, e.g. in 12a, are permitted), and press 'CONTINUE.'

13. Display will now read "pressure difference in psi." (Such messages are termed prompts.) Find the correct value on the Data Log sheet (furnished with raw data plots) and type it in. Press 'CONTINUE.'

14. The next prompt requests "source input atten[uation]: 20 - 500 Hz." Find this information in the Data Log, type it in, and press 'CONTINUE.' If no frequency range is stated in the Data Log, the value given applies to both low and high frequency ranges (20 - 500 and 500 - 5000 Hz).

15. Five more prompts will appear, one after another, requesting gain and attenuation data. These prompts are:

    "source output gain: 20 - 500 Hz"
    "receiver output gain: 20 - 500 Hz"
    "source input atten: 500 - 5 KHz"
    "source output gain: 500 - 5 KHz"
    "receiver output gain: 500 - 5 KHz"

    In each case, the appropriate value must be found in the Data Log and typed in on the calculator keyboard, after which 'CONTINUE' must be pressed. Only one value can be entered at a time.

16. For the next prompt, "min[inum] readable level," type in the dB level of the lowest point on the receiver curve of the raw data plot. The lowest level is usually a flat line between 2000 and 5000 Hz. To avoid uncertainty in digitizing, pad the lowest level by .2 or .3 dB. Thus, if the lowest level is 75.4 dB, type in 75.7. Press 'CONTINUE.'

17. The calculator will now ask, "Is [the] vert[ical] scale 70 - 140 dB? 1 = Yes." To answer in the affirmative, press '1,' then press 'CONTINUE.' To answer in the negative, press any other number, and 'CONTINUE.'

18. If the answer was negative, the calculator will ask "What is the level of the bottom line?" Type in the correct value and press 'CONTINUE.' "Level of top line?" will be requested next. Type in the value and press 'CONTINUE.'

19. Regardless of the answer in step 17, "Source curve: 20 - 500 Hz" will now appear on the display, and the sight glass will move to the 20 Hz line.

20. Using only the plotter buttons for <u>vertical</u> movement (i.e., '↑' and '↓'), position the sight glass center dot exactly on the <u>source</u> curve. Then press 'ENTER' button plotter.

21. The sight glass cursor will automatically move a predetermined distance to the right. Again move the cursor <u>vertically</u> until it is on the curve, and press 'ENTER.' This is called digitizing.

22. Repeat step 21 until calculator beeps (this will happen at about the 500 Hz location). Plotter will then move back to the 20 Hz line and calculator will display "Receiver curve 20 - 500 Hz."

23. Digitize the low frequency (20 - 500 Hz) part of the <u>receiver</u> curve. After last point is digitized, calculator will beep.

24. Similarily, the high frequency (500 - 5000 Hz) source and receiver curves need to be digitized. In response to the "Reenter P1 & P2 for 500 - 5 KHz" prompt, repeat steps 9 and 10 for 500 and 5000 Hz, respectively; then press 'CONTINUE.' Digitize the high frequency durves by the methods of steps 19 - 23.

25. In case of error in digitizing (cursor not on curve when 'ENTER' pressed), press 'STOP,' then 'CONTINUE' on calculator. Cursor should back up to incorrectly digitized location, permitting correct redigitization.

    Occasionally the plotter 'ENTER' button may bounce, causing calculator to read two points instead of one, as cursor moves two steps. If this happens the incorrect second point can be redigitized as if it were a digitizing error.

26. After last point, calculator will beep and display "Ready to plot TL: reenter P1 & P2." Press 'CHART LOAD,' remove raw data plot, and place blank graph paper on plotter table. Locate and hold paper down as described in step 7.

27. Reset P1 and P2 (at lower left and upper right corners) as described in steps 8 to 10.

28. Press 'CONTINUE' on calculator. Plotter will draw the TL curves, label the axes, and number the graph.

29. Press 'CHART LOAD' and remove graph.

30. Calculator will display "To store TL curve on tape, type 1." If you don't want to, type a different number. Then type 'CONTINUE.' Program will end.

31. If you elected to store the curve, the calculator will instruct, "Insert marked, [write-]enabled tape." Do so, and press 'CONTINUE.'. Prompts for tape track number (only 0 and 1 are permitted) and file number will then appear. Type each and press 'CONTINUE.' The curve is now stored on tape.

32. Whether you stored the curve or not, the plotter will exchange the pen for the sight glass, in preparation for more data reduction. To reduce more data, press 'RUN' and return to step 4 of this procedure.

    If, however, you would like another plot of the TL curve, load a fresh sheet of semilog paper and reset P1 and P2, as described in steps 26 and 27. Then type: cont76 and press 'EXECUTE.' The plotter will redraw the curve as in step 28, and the calculator will ask about tape storage again.

33. To recall a TL curve from tape storage:

    A) Perform steps 2 and 3, if program is not already present in calculator memory.

B) Type: erase v and press 'EXECUTE.' (This step is only necessary if data, e.g. a TL curve, is already present in calculator memory.)

C) Insert the tape cartridge containing the desired TL curve.

D) Type: cont63 and press 'EXECUTE.'

E) Three prompts will appear successively:

"RECALLING GRAPH No..?"
"TRACK No."
"FILE No."

Respond to each prompt by typing the appropriate digit(s), and pressing 'CONTINUE.'

F) The prompt "Ready to plot TL: reenter P1 and P2" will appear. Respond as in steps 26 - 30.

5. Example of a Specimen Log Sheet

SPECIMEN LOG SHEET

Page No. _____

Company	Date Contacted	Date of Reply	Specimens		Remarks
			No.	Type	

6. Example of a Test Log Sheet

TEST LOG

PAGE NO. ____

Date	Graph Number	Panel Number	Panel Type	Panel Treatment	Noise Source	Angle of Incidence	Temperature	Pressure Differential	Source Input Attenuation	Output Gain	Color Coding (Graphs)		Remarks	Operator
											Source	Receiver		

APPENDIX E

EXAMPLE OF INVITATION FOR COMMERCIAL VENDORS TO SEND SPECIMENS

Telephone: 913/864-3173/3043

Gentlemen:

The University of Kansas Flight Research Lab, in conjunction with NASA and the General Aviation Aircraft Industry, is developing an acoustic material testing facility to examine and compare sound reduction characteristics of the latest in vibration damping materials.

The testing program, which is slated to begin in May 1977, will consist of systematically mounting vibration damping materials onto various types of aluminum and fiberglass aircraft structural samples and determining the sound transmission loss characteristics of the combinations. The results of the testing will be made available to aircraft manufacturers through a published NASA report. Two general aviation aircraft manufacturers have already voiced interest in the anticipated results.

Your company was listed in "Compendium of Materials for Noise Control" (HEW Publication No. NIOSH 75-165) as a supplier of noise control material. If you would like to participate in the testing program and feel you have vibration damping materials suitable for use in light aircraft, you are invited to send sample specimens, along with related acoustical data, to the University of Kansas at the addresses listed below.

The following data describes the specimens we're looking for:

Material Type: Anything bondable to aluminum or fiberglass sheet (i.e. foams, fiberglass batts, etc.) that provides damping for unsupported surfaces up to 20" x 20".

Weight:	The materials are to be used in flight, so the primary concern is for light weight. Typically, materials with a specific weight of less than 5 lb/ft^3 are considered suitable for aircraft use.
Dimensions:	20" x 20" x 1" maximum thickness. Of course, thinner materials may also be used.
Number Desired:	4 specimens of each thickness to be tested, if possible, otherwise one specimen will do.

If you have any questions, please feel free to contact myself or Mr. Ton Peschier at (913) 864-3173/3043.

Sincerely,

Doug Andrews
Flight Research Lab

DA:pc

Memo No.: 77-05-02*

SEND MATERIALS TO: K. U. Center for Research, Inc.
Project 3170
2291 Irving Hill Drive-Campus West
Lawrence, Kansas 66045

CRINC LABORATORIES

Chemical Engineering Low Temperature Laboratory

Remote Sensing Laboratory

Flight Research Laboratory

Chemical Engineering Heat Transfer Laboratory

Nuclear Engineering Laboratory

Environmental Health Engineering Laboratory

Information Processing Laboratory

Water Resources Institute

Technical Transfer Laboratory

Air Pollution Laboratory

Satellite Applications Laboratory

CRINC